

BRUNEL UNIVERSITY

**EXPLOITING PHASOR  
MEASUREMENT UNITS FOR  
ENHANCED TRANSMISSION  
NETWORK OPERATION AND  
CONTROL**

A thesis submitted for the degree of Doctor of Engineering

This research programme was carried out in  
collaboration with National Grid

by

Phillip Michael Ashton

Supervised by Prof. Gareth Taylor

Brunel Institute of Power Systems  
Department of Electronic and Computer Engineering  
Brunel University, UK

# *Abstract*

In order to achieve binding Government targets towards the decarbonisation of the electricity network, the GB power system is undergoing an unprecedented amount of change. A series of new technologies designed to integrate massive volumes of renewable generation, predominantly in the form of offshore wind, asynchronously connecting to the periphery of the transmission system, are transforming the requirements of the network. This displacement of traditional thermal generation is leading to a significant reduction in system inertia, thus making the task of system operation more challenging. It is therefore deemed necessary to develop tools and technologies that provide far greater insight into the state of the power system in real-time and give rise to methods for improving offline modelling practices through an enhanced understanding of the systems performance.

To that extent PMUs are seen as one of the key enablers of the Smart Grid, providing accurate time-synchronised measurements on the state of the power system, allowing the true dynamics of the power system to be captured and analysed.

This thesis provides an analysis of the existing PMU deployment on the GB transmission system with a view to the future system monitoring requirements. A critical evaluation and comparison is also provided on the suitability of a University based Low Voltage PMU network to further enhance the visibility of the GB system. In addition a novel event detection algorithm based on Detrended Fluctuation Analysis is developed and demonstrated, designed to determine the exact start time of a transmission event, as well as the suitability of such an event for additional transmission system analysis, namely inertia estimation. Finally, a reliable method for the estimation of total system inertia is proposed that includes an estimate of the contribution from residual sources, of which there is currently no visibility. The proposed method identifies the importance of regional inertia and its impact to the operation of the GB transmission system.

# *Acknowledgements*

Firstly I would like to express my gratitude to Prof Gareth A. Taylor for providing the opportunity to undertake this research project and for his guidance and encouragement throughout the past 4 years. I would also like to thank Dr Alex Carter and Dr Martin Bradley for their help and support during my time at National Grid.

In addition I would like to thank Prof Malcolm Irving, Dr Ioana Pisica and Dr Christopher Saunders from the Brunel Institute of Power Systems for their valuable help and guidance, and Dr Ronan Jamieson and Dr Bernie Dolan from the Electricity National Control Centre at National Grid for all their insights, help, suggestions and of course the doughnuts!

I gratefully acknowledge the full sponsorship and financial support from both the Engineering and Physical Sciences Research Council (EPSRC) and National Grid.

Finally, I would like to give thanks to all my friends and family.

# Declaration of Authorship

The work detailed in this thesis has not been previously submitted for a degree in this University or at any other and unless otherwise referenced it is the authors own work.

# Contents

<b>Abstract</b>	<b>i</b>
<b>Acknowledgements</b>	<b>ii</b>
<b>Declaration of Authorship</b>	<b>iii</b>
<b>Table of Contents</b>	<b>iv</b>
<b>List of Tables</b>	<b>viii</b>
<b>List of Figures</b>	<b>ix</b>
<b>Abbreviations</b>	<b>xii</b>
<b>1 Introduction</b>	<b>1</b>
1.1 Environmental Legislation . . . . .	1
1.2 The GB Transmission System 2020-2050 . . . . .	2
1.2.1 The Evolving Generation Pattern . . . . .	4
1.2.2 Network Design . . . . .	6
1.3 Wide Area Monitoring Systems . . . . .	8
1.4 Power System Inertia . . . . .	10
1.5 Research Objectives . . . . .	11
1.6 Principle Contributions to Knowledge . . . . .	13
1.7 Background to the Engineering Doctorate . . . . .	14
1.8 List of Publications Arising from the EngD . . . . .	15
1.8.1 Journal Publications . . . . .	15
1.8.2 Technical Reports . . . . .	16
1.8.3 Conference Publications . . . . .	16
1.8.3.1 First Author . . . . .	16
1.8.3.2 Co-Author . . . . .	17
1.8.4 Invited Presentation . . . . .	17
1.9 Organisation of the Thesis . . . . .	18
<b>2 Synchronised Phasor Measurement Technology</b>	<b>21</b>

2.1	Introduction . . . . .	22
2.2	The History of Synchronised Phasor Measurement Technology . . . . .	23
2.2.1	Phasor Measurement Units . . . . .	24
2.2.2	Phasor Data Concentrator . . . . .	26
2.3	Development and Evolution of the Synchrophasor Standard . . . . .	28
2.4	Phasor Measurement Applications . . . . .	30
2.4.1	Offline Applications . . . . .	30
2.4.1.1	Post-event analysis . . . . .	31
2.4.1.2	Network Model Validation . . . . .	32
2.4.2	Online Applications . . . . .	33
2.4.2.1	Wide Area Monitoring . . . . .	33
2.4.2.2	Monitoring of Inter-Area Oscillations . . . . .	34
2.4.2.3	Dynamic Line Ratings . . . . .	35
2.4.2.4	Improved State Estimation . . . . .	36
2.5	Global PMU Deployment and Initiatives . . . . .	37
2.5.1	North America . . . . .	37
2.5.2	China . . . . .	40
2.5.3	The Central European System . . . . .	41
2.5.4	The Nordic region . . . . .	43
2.6	Concluding Remarks . . . . .	45
<b>3</b>	<b>System Monitoring and Control at National Grid</b>	<b>48</b>
3.1	Introduction . . . . .	49
3.2	Supervisory Control and Data Acquisition (SCADA) systems . . . . .	51
3.2.1	Frequency and Time Error (FATE) . . . . .	53
3.2.2	Settlement Metering . . . . .	54
3.2.2.1	Operational Metering . . . . .	55
3.2.3	Ancillary Services Business Monitoring (ASBMON) . . . . .	55
3.2.4	Power Quality . . . . .	57
3.2.5	Fault Recording and Dynamic System Monitoring . . . . .	58
3.2.6	Protection Systems . . . . .	59
3.3	The IEMS and the State Estimator . . . . .	60
3.4	Remote Asset Management and Monitoring . . . . .	63
3.5	Power System Dynamics Monitoring . . . . .	64
3.5.1	Power System Oscillation Detection Procedure . . . . .	68
3.6	Concluding Remarks . . . . .	71
<b>4</b>	<b>Wide Area Monitoring on the GB System</b>	<b>74</b>
4.1	Introduction . . . . .	74
4.2	National Grid WAMS Implementation . . . . .	75
4.2.1	Data Accuracy and Availability . . . . .	76
4.2.2	Communications Infrastructure Latency . . . . .	79
4.2.2.1	PMU Internal Measurement Delay . . . . .	82
4.3	State Estimator Comparisons . . . . .	86

4.3.1	Voltage Magnitude Comparisons . . . . .	88
4.3.2	Phase Angle Comparisons . . . . .	89
4.4	Domestic Supply Based WAMS . . . . .	92
4.4.1	ELPROS - University based WAMS deployment . . . . .	93
4.4.2	FNET . . . . .	97
4.5	Future WAMS Requirements . . . . .	98
4.5.1	Data Storage Requirements to 2050 . . . . .	100
4.6	Concluding Remarks . . . . .	104
<b>5</b>	<b>Event Detection and Big Data Analytics</b>	<b>106</b>
5.1	Introduction . . . . .	106
5.2	Detrended Fluctuation Analysis . . . . .	107
5.2.1	The DFA Algorithm . . . . .	108
5.2.2	DFA Exact Start of Event and Baseline Analysis . . . . .	112
5.2.3	Instantaneous Generation Loss Determination . . . . .	115
5.3	Overview of HPC and Big Data Analytics . . . . .	117
5.3.1	Parallel Processing Methods . . . . .	118
5.3.2	MapReduce Programming Model . . . . .	119
5.3.3	MapReduce Implementation with Hadoop . . . . .	120
5.4	The Design of PDFA . . . . .	123
5.4.1	PDFA Implementation . . . . .	124
5.5	Evaluation and Results . . . . .	127
5.5.1	Experimental Setup . . . . .	127
5.5.2	Results . . . . .	128
5.5.3	Speedup Analysis . . . . .	131
5.6	Concluding Remarks . . . . .	134
<b>6</b>	<b>Inertia Estimation of the GB Power System</b>	<b>135</b>
6.1	Introduction . . . . .	135
6.2	Frequency Response Requirements . . . . .	136
6.2.1	Inertia Contribution . . . . .	139
6.3	Power System Inertia Constant . . . . .	139
6.4	Inertial Frequency Response Estimation . . . . .	140
6.4.1	Factors Affecting Inertia Estimation . . . . .	143
6.4.2	Frequency Calculation . . . . .	144
6.4.3	RoCoF Calculation . . . . .	145
6.5	Results and Analysis . . . . .	148
6.6	Regional Inertia Estimation . . . . .	150
6.6.1	Modelled Examples . . . . .	152
6.6.2	Results from Genuine GB System Events . . . . .	157
6.7	Concluding Remarks . . . . .	161
<b>7</b>	<b>Conclusions and Further Work</b>	<b>162</b>
7.1	Thesis Summary and Conclusions . . . . .	162
7.1.1	Thesis Contributions . . . . .	168

---

7.2	Further Work . . . . .	170
7.2.1	Modelling and Analysis of WAMS Information and Communication Technology Infrastructures . . . . .	170
7.2.2	Development of an Ambient Inertia Estimation Methodology	172
7.2.2.1	System Studies . . . . .	174
7.2.2.2	Inter-Area Oscillation Analysis . . . . .	175
7.2.2.3	System Impedance Analysis . . . . .	175
<b>Appendix A</b>	<b>Generation Boundaries and Location of PMUs</b>	<b>178</b>
<b>Appendix B</b>	<b>Location of DSM Units in England and Wales</b>	<b>181</b>
<b>References</b>		<b>183</b>



# List of Tables

4.1	Individual PMU substation latency statistics . . . . .	82
5.1	DFA on 10 generation loss events as identified by 3 PMUs from the GB transmission system . . . . .	115
5.2	Experimental configuration of the Hadoop cluster . . . . .	128
6.1	22 generation loss events captured from the GB transmission system	148
6.2	Variation in measured $df/dt$ from 3 PMUs . . . . .	150
6.3	Loss estimation on a modelled example from 41 monitoring nodes .	154
6.4	Inertia estimation on modelled example 1 based on 3 monitoring nodes . . . . .	157
6.5	Inertia estimation on modelled example 1 based on 7 monitoring nodes . . . . .	157
6.6	Inertia estimation accuracy based on 7 modelled examples . . . . .	158
6.7	Inertia estimation based on 22 generation loss events from the GB transmission system with 3 monitoring nodes . . . . .	159
6.8	Inertia estimation based on 3 generation loss events from the GB transmission system with 7 monitoring nodes . . . . .	160
7.1	Network latencies for variable background traffic . . . . .	172

# List of Figures

1.1	Demand and generation background, Gone Green scenario. . . . .	5
2.1	Phasor representation of a sinusoidal signal. . . . .	23
2.2	Major elements of a typical PMU . . . . .	25
2.3	Hierarchy of a Wide Area Monitoring System . . . . .	26
2.4	Evolution of the synchrophasor standard . . . . .	29
2.5	GB system frequency following a generation loss of 1170MW . . . . .	31
2.6	Hybrid State Estimation approaches . . . . .	37
2.7	PMU deployment in North America. . . . .	38
2.8	Inter-area modes of the Central European System . . . . .	42
3.1	Wide Area Monitoring Protection and Control (WAMPAC) appli- cations . . . . .	50
3.2	Monitoring and Protection systems at National Grid . . . . .	52
3.3	State Estimation process and application at NG . . . . .	62
3.4	All the equipment connected through the RAMM system . . . . .	64
3.5	Example of unstable 0.5Hz oscillations in the Scotland-England transfer, 1982 . . . . .	65
3.6	PMU placement - Dynamic Stability Monitoring of the Anglo-Scottish interconnection . . . . .	67
3.7	Psymetrix PhasorPoint oscillatory analysis Locus plot . . . . .	69
4.1	Initial WAMS network infrastructure within NG's internal Busi- ness LAN . . . . .	77
4.2	PMU data availability statistics October 2013 . . . . .	79
4.3	PMU configuration, NG Business LAN . . . . .	80
4.4	Network latency for 6 BLAN connected PMUs . . . . .	81
4.5	Arbiter PMU phasor measurement window . . . . .	82
4.6	Arbiter PMU data acquisition delay . . . . .	83
4.7	Network latency for 6 BLAN connected PMUs excluding internal PMU measurement delay . . . . .	85
4.8	Smoothed network latency accounting for internal PMU latency . . . . .	85
4.9	PU voltage magnitude from 7 PMUs over a 10-second window . . . . .	87
4.10	PU voltage magnitude comparison between BLYTH PMU and equiv- alent SE Bus over a 4-hour period . . . . .	89
4.11	PU voltage magnitude difference between 7 PMUs and equivalent SE Bus over a 4-hour period . . . . .	90

4.12	Phase angle difference between LAGA and HARK, and equivalent SE buses over a 10-second period . . . . .	91
4.13	Phase angle difference between LAGA and HARK, and equivalent SE buses over a 4-hour period . . . . .	91
4.14	Phase angle difference for all PMUs, and equivalent SE buses over a 4-hour period . . . . .	92
4.15	Location of Low Voltage PMUs on the GB system . . . . .	94
4.16	Generation loss of 1000MW on the GB transmission system as measured by 7 PMUs from the transmission and domestic supply level . . . . .	95
4.17	Phasor plot showing angle difference for NG, SPT and ELPROS PMUs with Harker as the reference . . . . .	96
4.18	Angle difference minus DC offset for NG, SPT and ELPROS PMUs with Harker as the reference . . . . .	97
4.19	Anticipated number of installed PMUs with linear progression out to 2050. . . . .	101
4.20	Data storage requirements for increasing volumes of PMUs linear progression . . . . .	101
4.21	Potential number of installed PMUs by 2050 based on 4 scenarios. . . . .	103
4.22	Data storage requirements for increasing volumes of PMUs with all circuits monitored by 2050 . . . . .	103
5.1	Integrated PMU signal and the corresponding “trend” . . . . .	109
5.2	DFA on 10 seconds of PMU voltage magnitude data . . . . .	110
5.3	DFA on phase angle difference from NG, SPT and ELPROS PMUs . . . . .	112
5.4	DFA on voltage magnitude and phase angle difference for a localised event at Staythorpe . . . . .	112
5.5	Frequency trace following a 1000MW generation loss - local monitoring node . . . . .	113
5.6	Frequency trace following a 1000MW generation loss - distant monitoring node . . . . .	114
5.7	DFA on frequency data following an instantaneous generation loss . . . . .	116
5.8	DFA on frequency data following a staggered generation loss . . . . .	117
5.9	The MapReduce model. . . . .	120
5.10	The Hadoop framework. . . . .	121
5.11	Architecture of PDFFA implementation. . . . .	124
5.12	Analysis of PDFFA efficiency. . . . .	128
5.13	The relative accuracy of PDFFA compared to DFA. . . . .	129
5.14	The scalability of PDFFA, execution time against number of Mapper nodes (VMs). . . . .	130
5.15	Speedup analysis of the PDFFA algorithm. . . . .	131
5.16	Computational overhead of PDFFA against data block size. . . . .	133
5.17	The speedup of PDFFA against data block size. . . . .	133
6.1	Frequency response requirements on the GB transmission system. . . . .	138
6.2	Frequency resolution from voltage phase angle compared with DFR . . . . .	145

---

6.3	Frequency trace and calculated $df/dt$ following a 1000MW in-feed loss of generation in the South of the Network. . . . .	146
6.4	FFT on measured frequency transients following 1000MW generation loss . . . . .	147
6.5	Low pass filter applied to measured frequency transient. . . . .	147
6.6	Variation in residual inertia estimation from 3 separate PMUs . . .	151
6.7	Location of monitoring nodes, installed PMUs and simulated events	155
6.8	Generator groupings relative to PMU monitoring nodes . . . . .	156
6.9	Known inertia from generation compared with total GB system demand for 22 separate generation loss events . . . . .	158
7.1	Network latencies for 6 modelled PMUs using the OPNET model .	171
7.2	Total system demand with contribution from synchronous generation.	173
7.3	Total inertia from generation (H · MVA), including a split between Scotland and the network of England & Wales. . . . .	174
7.4	Analysis of the inter-area oscillation frequency using Prony's method.	175
7.5	Frequency of inter-area mode plotted against inertia from generation, with all tie line circuits in service. . . . .	176
7.6	Frequency of inter-area mode plotted against inertia from generation, with one of the tie line circuits out of service. . . . .	176
A.1	Location of installed PMUs used in this thesis . . . . .	179
A.2	Generation boundaries of the GB transmission system . . . . .	180
B.1	Location of DSM units on the transmission system of England and Wales . . . . .	182

# Abbreviations

ADC	Analogue to Digital Converter
AGC	Automatic Generation Control
BLAN	National Grid Internal Business LAN
CCGT	Combined Cycle Gas Turbine
CCS	Carbon Capture and Storage
CESA	Continental European Synchronous Area
CSC	Current Source Converter
CT	Current Transformer
DFT	Discrete Fourier Transform
DFR	Digital Fault Recorder
DG	Distributed Generation
DLR	Dynamic Line Rating
EMR	Electricity Market Reform
EMS	Energy Management System
ENTSO-E	European Network of Transmission System Operators for Electricity
EU	European Union
FNET	Wide Area Frequency Monitoring Network
GB	Great Britain
GPS	Global Positioning System
HVDC	High Voltage Direct Current
ICT	Information and Communications Technology
IEC	International Electrotechnical Committee
IED	Intelligent Electronic Device
IEEE	Institute of Electrical and Electronic Engineers

---

IT	Instrument Transformer
LAN	Local Area Network
LCPD	Large Combustible Plant Directive
MSC	Mechanically Switched Capacitors
NASPI	North American Synchrophasor Initiative
NERC	North American Electricity Reliability Corporation
NETSO	National Electricity Transmission System Operator
NG	National Grid
NGET	National Grid Electricity Transmission
NETSO	National Electricity Transmission System Operator
NIST	National Institute for Standards and Technology
OCGT	Open Cycle Gas Turbine
OFGEM	Office For Gas and Electricity Markets
OpTel	Operational Telecomms
PDC	Phasor Data Concentrator
PMU	Phasor Measurement Unit
POD	Power Oscillation Damping
PPP	Psymetrix PhasorPoint
PSS	Power System Stabilizer
PSTN	Public Switch Telephone Network
RAMM	Remote Access for Monitoring and Metering
RIIO	Revenue = Incentives + Innovation + Outputs
RMS	Route Mean Squared
RoCoF	Rate of Change of Frequency
RSVC	Robust Static Variable Compensator
RTU	Remote Terminal Units
SCADA	Supervisory Control And Data Acquisition
SCDR	Symmetrical Components Distance Relay
SCDFT	Symmetrical Components Discrete Fourier Transform
SE	State Estimation
SHETL	Scottish Hydro Electric Transmission Limited

---

SIPS	Special Integrated Protection Scheme
SO	System Operator
SPDC	Super Phasor Data Concentrator
SPTL	Scottish Power Transmission Limited
SVC	Static Variable Compensator
TCSC	Thyristor Controlled Series Compensation
TO	Transmission Owner
TSO	Transmission System Operator
TSC	Transmission System Operator Security Cooperation
TVE	Total Vector Error
TYDP	Ten-Year Development Plan
UCTE	Union for the Co-ordination of Transmission of Electricity
VSC	Voltage Source Converter
VT	Voltage Transformer
WAMPAC	Wide Area Monitoring Protection And Control
WAMS	Wide Area Monitoring System
WAN	Wide Area Network
WAPOD	Wide Area Power Oscillation Damping
UK	United Kingdom

# Chapter 1

## Introduction

The following sections will outline the motivations and objectives behind the research presented in this thesis. An account is provided of relevant background information including an outline of wide area monitoring and the applications to the electric power system. The overall objectives of this research project are presented within the context of improving the operation of the GB transmission system whilst increasing the penetration of renewable generation to the grid.

### 1.1 Environmental Legislation

In order to achieve the UK Governments and European Parliaments ambitious targets for the decarbonisation of greenhouse gas emissions, the power sector, seen as the largest single contributor in Great Britain (GB), is undergoing some drastic changes. Legally binding targets are in place, designed to reduce the UKs total CO<sub>2</sub> emissions by 34% by 2020 and 80-95% by 2050 relative to the baseline levels of 1990 [1–3].

Based on these targets the Electricity Networks Strategy Group (ENSG), working in collaboration with the Government, the Office for Gas and Electricity Markets (Ofgem) and the Transmission Owners (TO) of GB, have developed a vision for the future electricity networks in the UK. The report [4] originally published in



2009 and amended in 2012 [5], details the requirements for transmission network reinforcements deemed necessary to achieve the Government's 2020 renewable energy commitments [6, 7]. In addition to these reports the vision is echoed in a number of National Grid's (NG) own documents, the most recent of which [8], provides a detailed analysis of credible future energy scenarios out to 2035 and 2050, outlining the necessary developments in generation and demand patterns, anticipated technologies and market arrangements required to secure the future electricity supply.

## 1.2 The GB Transmission System 2020-2050

The electricity transmission networks in GB are owned by National Grid Electricity Transmission plc (NGET) in England and Wales, Scottish Power Transmission Limited (SPTL) in south and central Scotland and Scottish Hydro Electric Transmission Limited (SHETL) in the north of Scotland. These three networks form the onshore transmission system.

In addition to its role as the TO in England and Wales, following the implementation of British Electricity Transmission and Trading Arrangements (BETTA), NGET became the Great Britain System Operator (GBSO) on 1<sup>st</sup> April 2005. On 24<sup>th</sup> June 2009, following the "Go Active" of offshore transmission, National Grid then became the National Electricity Transmission System Operator (NETSO), which extended its GBSO operation to include the offshore transmission system.

The NGET transmission network is connected to the SPTL transmission network to the North, through two double 400kV AC circuits. There are Current Source Converter (CSC) HVDC interconnections to France (IFA 2000MW), The Netherlands (BritNed 1200MW) and Northern Ireland (Moyle 500MW). The network's first Voltage Source Converter (VSC) HVDC link to Ireland (EWIC 500MW) was commissioned in April 2013. The Transmission System comprises approximately 8000kms of overhead lines and underground cables, with around 350 substations at 240 sites. At present, the network supplies electricity from over 150 individual

large power stations to 12 distribution networks and a small number of directly connected customers such as steelworks.

The GB transmission network is considered to be a highly meshed system, which operates at 3 voltage levels. The Scottish transmission network is predominantly made up of 132kV and 275kV circuits, with some 400kV circuits connecting the network with the North of England. The network of England and Wales consists of 275KV urban rings connected through a 400kV Supergrid, originally installed in the 1960's to accommodate the transfer of bulk generation based around the coalfields. In the late 1980's this was supplemented by gas fired generation plants supplied from the North Sea

The system can be summarized as having the majority of its generation towards the North with the largest demand centre in the South East, this has allowed for a relatively consistent direction of power flow that stems from predominantly thermal generation plants, of which the generating output is largely controllable.

Within this system NG has to accommodate a winter peak of around 56GW with a forecast mid winter generation capacity for 2013/2014 of 74.7GW [9] from a total installed generation capacity of 93GW. However, due to the increasing penetration of renewable generation, the main cause for concern when managing the network is now the summer minimum. The Summer Outlook report for 2014 [10] advises an anticipated minimum demand of 19GW, this figure poses a growing risk to the network in terms of security of supply; when considering the existing capacity of non-synchronous generation, this demand could be met through generation sources of which over 50% contribute zero inertia to the system.

Currently the network has to cater for a maximum infrequent infeed loss of 1320MW however, subsequent reviews of the this criteria relating to the whole GB system [11], have resulted in an increase to this infeed loss risk, rising to 1800MW from 14<sup>th</sup> April 2014. A consequence of these changes is that the offshore network criteria has also been modified, such that offshore generation with a capacity up to 1800MW can be radially connected via a single cable. This change has prompted the review of existing generator response and reserve requirements in line with

reducing system inertia, as a means to cope with the potential increased in-feed loss risk [12].

The main area of concern in terms of network stability at present is the Anglo-Scottish constraint boundary (B6), as an inter-area mode, previously identified [13] at around 0.5Hz, exists between the generators in Scotland and those of England & Wales, involving the entire GB system. With increasing volumes of renewable generation scheduled to be connected in Scotland, the ability to effectively manage this boundary is becoming increasingly important.

With the majority of transmission infrastructure and generation plant having been installed some 50 years ago, when greenhouse gas emissions were not engineering design considerations, there is now a requirement for heavy investment in this area. Ofgems Project Discovery consultation [14] in 2009, found that the GB energy industry faces an unprecedented challenge to secure supplies to consumers, as a result of the global financial crisis, tough environmental targets, increasing gas import dependency and the closure of ageing power stations. It identified the issue of tightening capacity margins, due to power station closures from the Large Combustion Plant Directive (LCPD) [15], as early as 2014/2015. Around £200 billion of investment needs to be found by 2020 to secure sustainable energy supplies and keep costs as low as possible for consumers. The Government is addressing the problem of attracting £100 billion of private investment to build new forms of generation through its Electricity Market Reform (EMR) however, there still remains £32 billion of network investment which falls within Ofgems remit, representing an increase of over 75% in the value of Britains energy networks, effectively doubling the rate of investment on the last 20 years [16].

### 1.2.1 The Evolving Generation Pattern

Taking into account the Governments renewable energy commitments [6, 7], understanding that by 2020 around 30% of the UKs electricity demand will have to

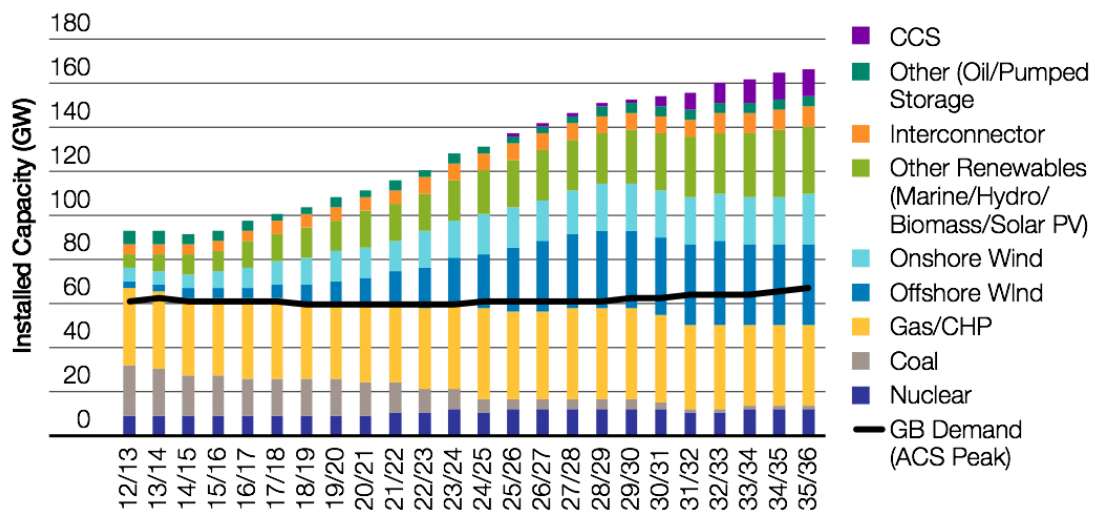


FIGURE 1.1: Demand and generation background, Gone Green scenario [8].

be met by renewable sources, NG, working with their customers and key stakeholders, have developed a “Gone Green” scenario designed to meet the nations environmental targets [8].

The impact of this scenario on the generation mix, looking out to 2035 can be seen in Figure 1.1. The key impacts are summarised below:

- Onshore wind shows an increase to 21GW in 2035, with offshore wind showing a higher increase post-2015 to a level of 12.1GW in 2020. Post-2020 there is a further increase in the deployment of offshore wind reaching 28.6GW in 2025 and an installed capacity of 37.5GW in 2035, resulting in a total wind capacity figure of 59.2GW by 2035. A ten-fold increase.
- The first new Nuclear plant is assumed to connect towards the beginning of the 2020s, with an overall net increase in capacity of 2.4GW.
- Gas-fired capacity is seen to rise by a total of 1.9GW, with closures of existing plant roughly matched by the installation of new plant. The amount of new gas plant is heavily dependant on the level of renewables, especially onshore and offshore wind, as they are assumed to be quite high in this scenario.
- The majority of the existing unabated coal plant is assumed to be closed by the mid-2020s resulting in a total unabated coal installed capacity in 2030 of

around 2GW. It is assumed some Carbon Capture and Storage (CCS) plant is installed in the late 2020s and 2030s with a total CCS capacity reaching over 6GW by 2035.

In addition the existing installation of micro generation is understood to be around 1.5GW [8], made up of predominantly Solar PV with a small amount of Wind and some Hydro. Under Gone Green, this is projected to rise to a total of nearly 20GW of which 17GW is Solar PV by 2035. Traditionally the system power flow has been directed logically from generation through to the consumer however, as a result of reduced unit costs, improvements in technology, reduction in installation costs and economic recovery [8], the system is starting to see two-way power flows from a growing amount of Distributed Generation (DG). This poses a serious issue for NG as they have minimal if any direct visibility of this, in terms of the exact location and quantity of the supply.

### 1.2.2 Network Design

The GB transmission system has predominately been in its present form since the 1960's. In order to accommodate the massive volumes of renewable generation set to connect to the system by 2020 and onwards, a large programme of upgrading and network expansion is required [5, 8].

With a large volume of renewable generation being installed in Scotland, a program of necessary reinforcements was identified [5] to reduce the constraint on the existing Anglo-Scottish connection. The power transfer across this boundary is currently stability-limited to approximately 2500MW, thus heavily restricting the connection of any additional renewable generation in the Scottish network. The installation of Thyristor Controlled Series Compensation (TCSC) and Mechanically Switched Capacitors (MSCs), are set to raise the boundary up to its thermal limit of approximately 4400MW. The connection of the first intra-network CSC HVDC cable link along the West coast is set to further increase the boundary to

6600MW by 2016. An additional link proposed down the East coast of GB will see the B6 boundary reach a potential total capacity of 8800MW by 2018/19 [11].

The level of interconnection with Europe is expected to double by 2030, with the continued development of European energy markets. Additional links are expected to Norway, Belgium, and France, increasing the projected total link capacity to 8.6GW. In line with the growing volumes of interconnection the European Network of Transmission System Operators for Electricity (ENTSO-E) has published its latest Ten-Year Development Plan (TYDP) [17]. The report outlines anticipated investments into the member states' electricity networks required to support a stepwise evolution to a pan-European supergrid and acts as the starting point for the e-Highways 2050 project [18], which aims to deliver a top-down methodology to support the planning of the pan-European transmission network.

A need for efficient management of the expanding electricity network in Europe requires unified coordination between the TSOs involved. National Grid has therefore entered into a commercial arrangement with TSOs from France (RTE), Belgium (Elia), North and East Germany (50Hertz) and Italy (Terna), managed by a regional coordinated service centre, Coreso, set up to improve the security of supply in western Europe by monitoring the power flows on the interconnections between member transmission systems [19]. In addition, TSO Security Cooperation (TSC) [20], another regional coordinated service comprising of thirteen TSOs in central Europe, is receiving operational forecasting data from its members to provide grid wide security calculations to maximise security of supply for the supporting countries.

The complexity of the transmission networks is now growing on a European wide scale. The displacement of traditional thermal generation, through large amounts of electrically decoupled renewable generation and growing volumes of interconnection with Europe is leading to a significant reduction in system inertia, thus making the systems increasingly vulnerable in terms of small-signal stability from a security of supply point of view. In addition, NG, now operating under the new price control structure RIIO (revenue = incentives + innovation + outputs) [21], is

now offered real incentives for driving innovation, and so is becoming increasingly focused towards system performance, harnessing the optimum operating range from existing network assets.

Transmission networks are now being pushed closer towards their designed limits and are required to be more flexible and smarter. It is therefore necessary to develop tools and technologies that provide greater information on the state of the power system in real-time and give rise to methods for improving offline modelling practices through an enhanced understanding of the systems performance. Importance is therefore heavily placed on the availability of high-resolution time-synchronised measurements of power system quantities deemed vital to facilitating such detailed analysis.

### **1.3 Wide Area Monitoring Systems**

Phasor Measurement Units (PMU) measure three phase voltages and currents (magnitude and phase) and, depending on their configuration, calculate time synchronised positive-sequence values at rates equivalent to the power systems fundamental frequency, 50Hz on the GB system. These high-resolution measurements make it possible to track dynamic changes on the grid and monitor the wide area snap-shot of the power system in real-time.

PMUs are typically installed at distributed locations around the power network, transmitting data over a specified communications network back to a Phasor Data Concentrator (PDC). The devices are realising the possibilities of Wide Area Monitoring Systems (WAMS), providing key information to enable a number of applications deemed vital to operating power systems of increasing complexity going forward. One clear advantage of the technology over traditional Supervisory Control and Data Acquisition (SCADA) systems being post-event analysis, through the ability to very quickly and conveniently collate all of the time synchronised data together, thus facilitating investigation into the cause and impact of system incidents as they can be seen to “ripple” through transmission networks. This can

lead to identifying areas of weakness in the networks and point out key areas for reinforcements.

The positive-sequence measurements are considered to represent the state vector of the power system, fundamental in all analysis [22] and so it is preferable to use these directly obtained results to exclusively monitor the state of the power system [23] over the non-linear algorithms typically employed in the State Estimation (SE) process of Energy Management Systems (EMS). The existing SE process being more prone to errors and typically only run every 5-10 minutes, making the assumption that the network is static over this period. Utilising PMUs for this application can lead towards a process of state determination over estimation, but it is estimated that to achieve the required level of observability, PMUs would need to be installed at approximately 1/3 of all system buses [24], this does not take into account the redundancy requirements and at present the numbers of installed PMUs are some way from this. The majority of practical applications in this area are therefore focused on combining the synchrophasor information with that of existing SCADA data, to improve the accuracy of the SE process, shortening the computation time and increasing precision.

Recognising wide area monitoring as one of the key aspects of the Smart Grid, power utilities globally are using PMUs to improve situational awareness through online stability monitoring, in the analysis of the inter-area modes of the power system, and real time data visualisations. Predominantly the application of the technology has focused around offline analysis of colated datasets, looking at post-event analysis. It is expected that the increased use of WAMS will result in a more efficient and reliable use of corrective actions for system-wide disturbances [25].

The long term goal of the technology is that of Wide Area Monitoring Protection and Control (WAMPAC), with the growing complexities of power networks requiring applications to seek a network wide perspective to ensure that decisions secure the optimum outcome for the overall system, as opposed to just solving a localised problem. This is heavily dependant on robust communications infrastructures with very low network latencies and fast acting algorithms.



In the interim WAMS can be seen to bridge the gap between the network wide SCADA monitoring solutions and more localised systems such as those of protection applications or dedicated control systems. WAMS has the potential to provide a new platform, to combine a number of existing applications together, offering improvements to operational and planning systems. The subject of PMUs and WAMS is discussed in greater detail in Chapter 2

## 1.4 Power System Inertia

Large synchronous generators provide the majority of the inertia to the GB system, the remaining system inertia, referred to in this thesis as the residual contribution and currently assumed to contribute around 20% to the total, is provided by small and micro generation, which is embedded in the distribution network and by industrial, commercial and domestic demand, for which there is very limited information available [12].

The existing assumption is that system inertia varies linearly with demand, as will be shown in this thesis, this assumption is becoming increasingly invalid, with growing volumes of the demand being met by electronically decoupled generation such as HVDC interconnectors and wind farms. An accurate knowledge of system inertia is crucial to determining the frequency behaviour of the power system and with a large number of changes due to impact the power network, this is becoming increasingly important.

The inertia is defined as the rotational energy stored in the rotating masses of the power system and serves to arrest the initial drop in frequency following a generation infeed loss event. It is important to understand the difference in post-event frequency behaviour around the power system, as an instantaneous loss of generation will impact various parts of the power network in different ways, this impact is determined by the location of the loss in terms of electrical connectivity and the localised inertial contribution.

Generation loss events are a rare occurrence on the GB system, but at present provide the only reliable source of information on system frequency behaviour, and with it the only opportunity to calculate estimates of total system inertia. The ability to accurately capture frequency data surrounding such events is now vital.

Existing inertia estimation methods in the literature [26–28] examine the post-event frequency behaviour of the power system with a view to determining an average value of the inertia of a specific system, based on an individual monitoring point. The work presented in this thesis takes into account the variations in frequency behaviour around the network, as a result of an event and proposes an accurate method based on the summation of inertia estimates on a regional level to provide an estimate for the total inertia of the power system [29].

Provision of accurate synchronized frequency information pertaining to such events becomes vital when attempting to perform these estimates. Additionally, an understanding of the measurement algorithms employed and any limitations of a devices transient performance is now also necessary [29, 30].

The subject of power system inertia and its estimation is covered in greater detail in Chapter 6.

## 1.5 Research Objectives

To decarbonise the UK electricity supply an unprecedented amount of change is required to the GB transmission system. Large volumes of variable renewable generation are due to impact on the transmission network before 2020, predominantly in the form of offshore wind connecting to the periphery of the transmission system. To that extent technologies currently unfamiliar to the GB system are being planned, including offshore embedded HVDC links and TCSC on the circuits of the prominent constraint boundary. In addition, the closure of a significant number of existing large-scale coal fired and nuclear power stations is also planned

to occur before the end of the decade meaning not only a huge displacement of system inertia from the system, but also the potential deactivation of a number of power system stabilisers (PSS), thus heavily impacting the small-signal stability of the network.

Significant changes will also be required with regard to operational control procedures in order to secure such future transmission networks, especially with regard to stability and frequency constraints. All of these changes are becoming heavily reliant on increased information pertaining to the state of the power system.

In order to provide possible improvements to the observation and control of the transmission system PMUs are being deployed across the GB transmission network to provide improved resolution and data accuracy with regard to wide area monitoring and control. Therefore it is considered extremely beneficial to both NG and the GB electricity industry in general, to conduct a rigorous investigation into the potential to exploit novel PMU-based techniques as a means to improve the operation of the GB transmission system as operated by NG.

Therefore the main objectives of this research project presented in this thesis are to review the existing PMU deployment and WAMS implementation at NG, looking at all aspects of the deployment from communications infrastructure to data accuracy and reliability. The focus being to develop the future system monitoring requirements for the GB network, working towards the ultimate goal of WAMPAC, deemed necessary to operate the future electricity network.

This review will be performed on the wider understanding of existing monitoring and planning procedures, seeking to exploit the use of PMUs to improve the operation of as many existing procedures as possible. Global use of applications of PMU based technologies will be reviewed focusing on the applicability to the GB system with the aim of developing a range of algorithms and applications.

In addition to the transmission level deployment of PMUs an analysis of a University based PMU network will also be provided, with a view to how such a system could benefit the GBSO, either through furthering the visibility of the network

from a greater number of monitoring devices or by providing an additional level of redundancy for the main WAMS network.

The main initial objectives of this research project can be summarised as follows:

- To carry out a review of the existing PMU deployment on the GB transmission system.
- Review the existing applications of PMU technologies available, through an analyses of the global PMU deployment schemes, with a view towards the applicability to the GB system.
- Investigate the potential for PMU networks based at the domestic supply to further the visibility of the GB transmission system.
- Develop suitable algorithms and applications to improve the operation of the GB transmission system.

## 1.6 Principle Contributions to Knowledge

The principle contributions to knowledge, as presented in this thesis, can be summarised as follows

- A comprehensive review of the following has been provided:
  - the existing system monitoring applications and requirements for the GB transmission system, with proposals for future adoption from PMUs or similar devices.
  - the existing PMU based network in place on the GB transmission system with proposed requirements for the future WAMS.
- Investigation into the suitability of a GB Low Voltage University based PMU network to further the visibility of the GB transmission system.

- A novel event detection algorithm based on Detrended Fluctuation Analysis has been developed and demonstrated, designed to determine the exact start time of a transmission event, as well as the suitability of such an event for additional transmission system analysis, namely inertia estimation. The algorithm has also been parallelized in the Hadoop MapReduce framework, to work on massive volumes of PMU data.
- The development of a reliable method for the estimation of total system inertia is presented that includes an estimate of the contribution from residual sources, of which there is currently no visibility. The proposed method identifies the importance of regional inertia and its impact to the operation of the GB transmission system.

## 1.7 Background to the Engineering Doctorate

The Engineering Doctorate (EngD) in Environmental Technology provided by Brunel University, is a four year advanced degree focused around industry relevant research. The scheme, funded by the Engineering and Physical Sciences Research Council (EPSRC) and a sponsoring organisation, presents the opportunity to design and research practical techniques for solving an industry led research problem, with a focus on environmental significance. The vast majority of the research is therefore carried out with the sponsoring organisation providing the researcher with valuable industrial experience. The research outcomes from an EngD need to satisfy, at least, the same requirements as a traditional PhD. In addition the candidate has to undertake an extensive program of professional development courses, which are designed to prepare the candidate for an industrial career [31].

This EngD project was supported by National Grid and the majority of the work was conducted at the ENCC (Electricity National Control Centre) near Wokingham in Berkshire.

## 1.8 List of Publications Arising from the EngD

The work detailed in this thesis has resulted in number of refereed publications, as follows:

### 1.8.1 Journal Publications

P. M. Ashton, G. A. Taylor, M. R. Irving, I. Pisica, A. M. Carter and M. E. Bradley, “Novel Application of Detrended Fluctuation Analysis for State Estimation using Synchrophasor Measurements”, *IEEE Transactions on Power Systems*, vol. 28, No. 2 May 2013, pp. 1930-1938.

P. M. Ashton, C. S. Saunders, G. A. Taylor and A. M. Carter, “Inertia Estimation of the GB Power System Using Synchrophasor Measurements”, *IEEE Transactions on Power Systems* 2014.

M. Khan, P. M. Ashton, M. Li, G. A. Taylor and J. Liu, “Parallel Detrended Fluctuation Analysis for Fast Event Detection on Massive PMU Data”. *IEEE Transactions on Smart Grid* 2014.

M. Golshani, P. M. Ashton, I. Pisica, G. A. Taylor and A. M. Carter, “Novel Performance Evaluation of Communications Infrastructure to Enable Wide Area Monitoring System Deployment”. (Submitted *IEEE Transactions on Power Delivery* June 2014).

J. Turunen, H. Renner, W. Hung, A. M. Carter, P. M. Ashton and L. C. Haarla, “Simulated and Measured Inter-Area Mode Shapes and Frequencies in the Electrical Power System of Great Britain”. (Submitted *IEEE Transactions on Power Systems* June 2014).

## 1.8.2 Technical Reports

A. H. Alikhanzadeh, I. Pisica, C. S. Saunders, P. M. Ashton and G. A. Taylor. e-Highways 2050 Modular Development Plan of the Pan-European Transmission System 2050, WP3 - Technology portfolio to meet the 2050 scenarios, Sub-Task 3.2.8, “Impacts of ICT on the pan-European Power Systems up to the 2050 Time Horizon”, July 2014.

P. M. Ashton, M. Cousins, P. Dagger, J. Dagle, A. Kizer and B. Coffey. International Electricity Infrastructure Assurance (IEIA) Forum - Technology Maturity and Applications of Transmission/Distribution Systems, Paper 1: Synchrophasors, July 2014.

## 1.8.3 Conference Publications

### 1.8.3.1 First Author

P. M. Ashton, G. A. Taylor and A. M. Carter, “Transient Event Detection and Analysis of the GB Transmission System using Synchrophasor Measurements”, in Proc. UPEC 2013, 2-5 September 2013, Dublin, Ireland.

P. M. Ashton, G. A. Taylor, A. M. Carter and W. Hung, “Application of Phasor Measurement Units to Estimate Power System Inertial Frequency Response”, in Proc. IEEE Power Engineering Society General Meeting Conf July 2013.

P. M. Ashton, G. A. Taylor and A. M. Carter, “Future Wide Area Monitoring Requirements for the GB Transmission System”, in Proc. The IET ACDC. 4-6 December 2012, Birmingham UK.

P. M. Ashton, G. A. Taylor, A. M. Carter and I. Pisica, “Critical Evaluation of Wide Area Monitoring Systems from a GB Transmission System Operator Perspective”, in Proc. UPEC 2012, 4-7 September 2012, London, UK.

P. M. Ashton, G. A. Taylor, M. R. Irving, A. M. Carter and M. E. Bradley, “Prospective Wide Area Monitoring of the Great Britain Transmission System

using Phasor Measurement Units”, in Proc. IEEE Power Engineering Society General Meeting, July 2012.

P. M. Ashton, G. A. Taylor, A. M. Carter, H. Renner, “Opportunities to Exploit Phasor Measurement Units (PMUs) and Synchrophasor Measurements on the GB Transmission Network”, in Proc. UPEC 2011, 5-8 September 2011, Soest, Germany.

### **1.8.3.2 Co-Author**

A. H. Alikhanzadeh, I. Pisica, C. S. Saunders, P. M. Ashton and G. A. Taylor, ”Impacts of ICT on the pan-European Power System up to the 2050 Time Horizon”, in Proc. UPEC 2014, Cluj-Napoca, Romania.

M. Golshani, G. A. Taylor, I. Pisica, P. M. Ashton, “Implementation of Wide Area Monitoring Systems and Laboratory-Based Deployment of PMUs”, in Proc. UPEC 2013, 2-5 September 2013, Dublin, Ireland.

M. Golshani, G. A. Taylor, I. Pisica, P. M. Ashton, “Laboratory-Based Deployment and Investigation of PMU and OpenPDC Capabilities”, in Proc. The IET ACDC. 4-6 December 2012, Birmingham UK.

M. Golshani, G. A. Taylor, I. Pisica, P. M. Ashton, “Investigation of Open Standards to Enable Interoperable Wide Area Monitoring for Transmission Systems”, in Proc. UPEC 2012, 4-7 September 2012, London, UK.

### **1.8.4 Invited Presentation**

IEEE PES General Meeting, 21-25 July 2013, Vancouver, British Columbia, Canada. Panel Session “The use of CIM Standards in Smart Grid Applications” G. A. Taylor, N. Hargreaves, P. M. Ashton, M. E. Bradley and A. M. Carter, “Potential integration of Phasor Measurement Units and Wide Area Monitoring Systems based upon National Grid Enterprise Level CIM”.



## 1.9 Organisation of the Thesis

### **Chapter 1 - Introduction**

This chapter outlines the motivations behind the research presented in this thesis, in the massive amount of changes due to impact the GB electricity system as a result of climate change targets. An account is provided of the relevant background information including an outline of phasor measurement technology and the applications to the electric power system, as well as a brief description of power systems inertia. The overall objectives of this research project are presented within the context of improving the operation of the GB transmission system whilst increasing the penetration of renewable generation to the grid.

### **Chapter 2 - Synchronised Phasor Measurement Technology**

This chapter details the history of WAMS and PMUs and the concepts behind the applications in power systems today. A brief account is also provided of existing global applications of the technology and their applicability to the operation of the GB system. The aim being to develop the future system monitoring requirements for the GB network, working towards the ultimate goal of a wide area monitoring protection and control (WAMPAC) system, that is deemed necessary to operate the future electricity network.

### **Chapter 3 - System Monitoring and Control at National Grid**

In this chapter the existing monitoring and control systems in operation at National Grid are reviewed, with a focus on which systems or applications could be further improved or adopted by PMUs. Details are provided on the Power System Dynamics (PSD) monitoring system that first introduced PMUs to the GB transmission system, specific information pertaining to GB WAMS deployment is provided in Chapter 4.

### **Chapter 4 - Future GB Wide Area Monitoring Systems**

The existing WAMS deployment on the GB transmission system is analysed in this chapter, in terms of the historic availability and accuracy of the data from PMUs. Information is also provided on a University based WAMS initiative comprising

PMUs installed at a low voltage level. The future requirements for PMU deployment and WAMS implementation looking out to 2050 is then discussed, looking at the anticipated number of devices and the realistic applications for the GB system, based on the system experience of other TSOs and the growing requirements and motivation for system monitoring at NG.

### **Chapter 5 - Event Detection and Big Data Analytics**

In this chapter a novel event detection methodology based on Detrended Fluctuation Analysis (DFA) is described, the method is demonstrated as a basic means of event source location through identifying the closest PMU to an event, and also the determination of the exact event start time ( $t = t_0$ ), deemed vital to inertia estimation methodologies. The method also determines the suitability of a transmission system event to provide an estimate on the total inertia of the power system, the key requirement on this being the instantaneous nature of the loss. The approach is then further expanded to be parallellised for the use on massive volumes of PMU data. With this an introduction to Big Data analytics is provided and the implementation of the Parallel DFA (PDFA) approach is presented in the Hadoop MapReduce programming model.

### **Chapter 6 - Inertia Estimation**

In this chapter a method is proposed for estimating the total inertia of the GB power system, by dividing the network into groups or regions of generation based around the constraint boundaries of the GB network. The inertia is first estimated at a regional level before it is combined to provide a total estimate for the whole network. This estimate is then compared with the known contribution to inertia from generation, to provide an estimate for the currently unknown contribution to inertia from residual sources; namely synchronously connected demand and embedded generation. The approach is first demonstrated on the full dynamic model of the GB power system before results are presented from analysing the impact of a number of instantaneous transmission in-feed loss events, using phase-angle data provided by the 3 PMUs from the GB transmission network and also the devices installed at the domestic supply at 4 GB Universities.

**Chapter 7 - Conclusions and Further Work**

In this final chapter a summary is provided on the work presented in this thesis outlining the specific contributions. In addition an outline of proposed future work is presented before some preliminary results are presented.

## Chapter 2

# Synchronised Phasor

# Measurement Technology

The research presented in this thesis is heavily reliant on the provision of synchronised measurements of power system quantities. The quality and accuracy of that data is of increasing importance to NG and TSOs globally, as power systems become increasingly complicated to operate. The time-synchronised high accuracy data allows, for the first time, exact snap-shots of the power system to be captured.

This chapter details the history of synchronised phasor measurement technology and the concepts behind its application in power systems today. A brief account is also provided of existing global applications of the technology and their applicability to the GB system, with the goal of developing the future system monitoring requirements for the GB network, working towards the ultimate goal of wide area monitoring protection and control (WAMPAC), deemed necessary to operate the future electricity network. A detailed account of which, is provided in Chapter 4.

## 2.1 Introduction

The voltage phase angles between two buses in an electrical power system are of great interest to Power System Engineers. The majority of applications involving the operation and planning of the power system are predominantly concerned with power flow and it is well known that active power flow over a transmission line is nearly proportional to the sine of the voltage angle difference between the respective terminals of the line [22].

$$P = \frac{E_1 \cdot E_2}{X_L} \sin(\delta_1 - \delta_2) \quad (2.1)$$

The key to measuring phase angles lies in the ability to estimate phasors of power system quantities. A phasor is essentially a vector representation of a pure sinusoidal waveform, shown in Figure 2.1, as:

$$x(t) = X_m \sin(\omega t + \delta) \quad (2.2)$$

Where  $X_m$  is the magnitude of the signal,  $\omega = 2\pi f$  is the angular frequency of the signal and  $\delta$  is the phase angle. The phase angle,  $\delta$  of the signal needs to be defined relative to a reference at  $t = 0$ . The analogue signal can then be digitally represented as a phasor, taking into account the angular position of the signal and its magnitude, which is converted to its root mean squared (RMS) value by:

$$X = \frac{X_m}{\sqrt{2}} e^{j\delta} \quad (2.3)$$

However, in order for these phasor quantities to be useful and directly comparable with others measured at dispersed locations around a network, there needs to be a unified reference signal of significant accuracy from which the relative phase angles can be determined. This was the major factor in enabling the deployment of the technology.

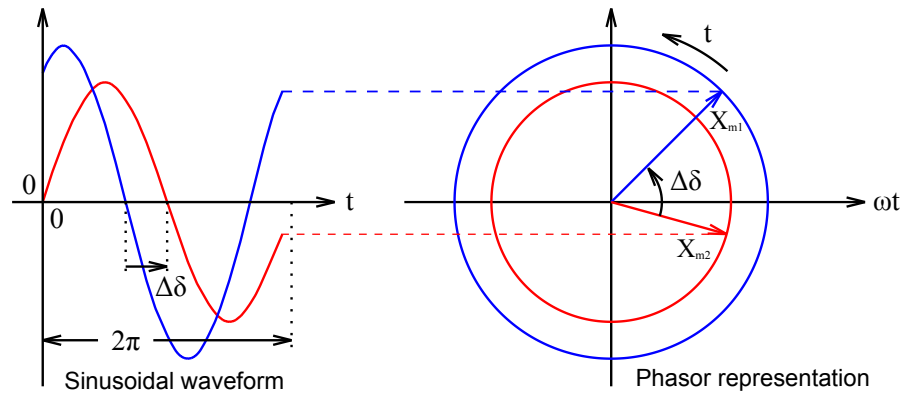


FIGURE 2.1: Phasor representation of a sinusoidal signal [32].

## 2.2 The History of Synchronised Phasor Measurement Technology

The 1965 blackout in the North East of America triggered a large amount of research into the provision of real time data on the state of the power system. It was recognised that due to the technological limitations of the period, high resolution synchronised data rates were not an option. For this reason wide area measurements were originally introduced as inputs for static state estimators, designed to assess system security from the point of view of the next network contingency [33]. The measurement systems had to be designed to provide the best “quasi-steady state” approximation to the state of the power system.

An understanding of the computational challenges led to the development of the Symmetrical Components Distance Relay (SCDR) [22, 33]. This used an advanced relaying algorithm that was based on the measurement of positive-sequence, negative-sequence and zero-sequence voltages and currents at the transmission line terminals. The clear advantage of this algorithm was that it required the processing of only one equation to determine the location of all possible fault types. This led to the development of the recursive algorithm for calculating symmetrical components of voltages and currents, the Symmetrical Components Discrete Fourier Transform SCDFT [33, 34]. This work in turn identified the positive sequence component of the measurements to be of great significance. The positive sequence

voltage constitutes the state vector of the power system and is therefore of great importance to all power systems analysis [22, 33].

The positive sequence phasor can be calculated from the three individual voltage phasors through the principles of symmetrical components [35]:

$$X_1 = \frac{1}{3}(X_a + aX_b + a^2X_c) \quad (2.4)$$

Where  $X_a$ ,  $X_b$  and  $X_c$  are the three respective voltage phasors and  $a$  is their angular separation of  $120^\circ$ .

The first paper to identify the importance of positive sequence phasor measurements was published in 1983 [36]. At around the same time the global positioning system was beginning to be fully deployed and it became apparent that this was the best method of time synchronising measurements from remote locations within the power system [22]. With the present systems capable of achieving synchronisation accuracies of greater than  $1\mu s$ , equivalent to  $0.018^\circ$  on a 50Hz system.

### 2.2.1 Phasor Measurement Units

Moving on from the SCDR, Virginia Tech then went on to develop the first prototype synchronised phasor measurement units (PMU) in 1988 [33]. Devices were then installed in a few substations along the East coast of America, before collaborating with Macrodyne in 1991 to produce the first commercial manufacture of PMUs [22].

A functional block diagram showing the main elements of a typical PMU is provided in Figure 2.2. Analogue measurements of voltages and currents are taken from the secondary side of instrument transformers (IT), the sampling clock of the analogue to digital converter (ADC) is phase-locked with a reference, provided by a GPS signal at 1 pulse-per-second (pps). This signal also provides a time tag made up of the number of seconds since the 6<sup>th</sup> January 1980. Positive sequence

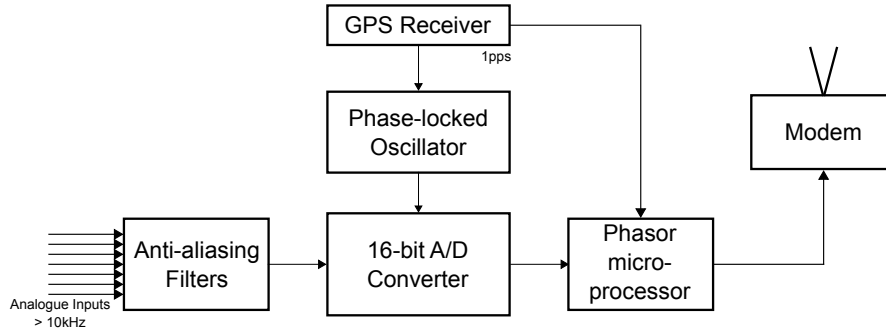


FIGURE 2.2: Major elements of a typical PMU [22].

phasor estimates of voltages and currents are then calculated, in addition to frequency and rate of change of frequency (RoCoF), at a rate typically equivalent to the fundamental frequency of the powers system, 50Hz on the GB system. The PMU is the most accurate device, to date, for calculating such positive sequence phasors and are the key input to any wide area monitoring system (WAMS).

The PMUs ability to measure the real-time system state can be attributed to the algorithms for phasor calculation from sampled data implemented in the units. The Discrete Fourier Transform (DFT) is the most commonly known method for the calculation of a phasor [37], a simplified phasor calculation can be obtained from the following equation:

$$X = \frac{\sqrt{2}}{N} \sum_{k=1}^N X_k e^{-j2k\pi/N} \quad (2.5)$$

Where  $N$  is the total number of samples and  $X_k$  is the  $k$ th sample of the analogue signal.

A computationally more efficient method is to recursively compute the phasors on a fixed sliding window, by adding in a new sample at the same time as discarding the oldest sample from the data set. With the recursive procedure, only two multiplications need to be executed with each new sample point [22]. This algorithm allows implementation within most digital devices currently used in power systems so long as time synchronization is included. PMUs can therefore either be considered as stand alone dedicated devices or as an integrated function of another unit, such as a digital fault recorder (DFR).



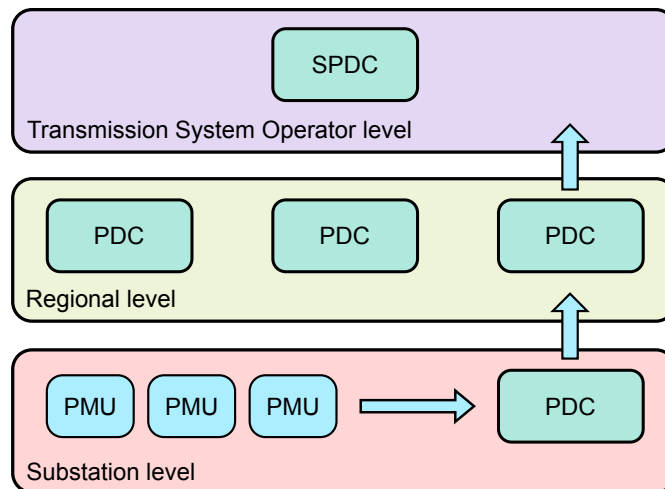


FIGURE 2.3: Hierarchy of a Wide Area Monitoring System

There are also two separate classes of PMU, M, intended for applications that do not require the fastest reporting speed, where M is used in reference to the accuracy of the measurement over the speed of the intended application and P, intended for applications requiring fast response such as protection [38]. A trade off is required between accuracy and speed, for example not all control applications require high speed response.

The time synchronised highly accurate measurements provide far greater detail over traditional SCADA based monitoring systems or state estimators. This allows, for the first time, both the dynamics and transient performance of the power system to be assessed in near to real-time.

## 2.2.2 Phasor Data Concentrator

The overall structure of any WAMS network will vary from utility to utility and is typically determined by the predominant phasor based application. The general hierarchy is as outlined in Figure 2.3.

The PMUs are generally installed in substations at the transmission level of the power grid, their main function is to make phasor data available as a steady stream transmitted over a secure wide area network (WAN), to remote locations containing phasor data concentrators (PDC). The role of the PDC is to collate

and time-align data from a number of PMUs and provide various quality checks to detect for the presence of bad data [39]. The PDC can also offer a longer term means of data storage and provide an interface with SCADA, energy management systems (EMS) or other PDCs through a number of specialised outputs, although this is not a requirement. An application layer is also possible to provide analysis and visualisation on the accumulated phasor data. The superPDC (SPDC), the top level in the hierarchical structure, plays a similar role to the PDCs in the lower levels, acting to collate and time-align data from the distributed PDCs of the WAMS network. Data from all of the PMUs in the network is not necessarily required at the SPDC.

The systems are designed based on application, with PDCs introducing additional levels of latency to the real time data through communication and data management processes, applications requiring fast responses will most likely not acquire data through a PDC and harness one of the output streams directly from the PMU itself [22].

A PMU or PDC can transmit its data as part of one or more separate data streams. Each stream may contain different information transmitted at different rates [39]. The destination of each stream may be a different device and location. For these reasons careful consideration needs to be taken when designing the communications infrastructure for WAMS, if PMUs are to become part of critical network infrastructure and more devices are to be installed, they will have to be integrated within a robust network, with proven reliability and accuracy of data. It is also necessary to consider the data resolution requirements for specific applications [40].

## 2.3 Development and Evolution of the Synchrophasor Standard

In order to account for synchrophasor measurement devices installed in the power system from different manufacturers and in numerous integrated forms, interoperability is of great significance so it is therefore essential that PMUs all conform to a common standard. The development of such a standard is as depicted in Figure 2.4.

The standard for synchrophasors was first introduced in 1995, as IEEE 1344-1995 [41]. However, after a series of interoperability tests it became apparent that the standard did not provide suitable performance for measurements of off-nominal system frequency [22, 42]. This led to revision of the standard in 2005 to IEEE C37.118-2005 [43], which noted a specific definition of phasors being estimated at off-nominal system frequencies, with the accuracy having to be maintained for system frequencies within  $\pm 5\text{Hz}$  of the nominal frequency. The new standard also introduced the concept of total vector error (TVE), as a means of verifying a measurements compliance with the standard. The standard however, did not address dynamic or transient performance requirements of the PMU, meaning that under such conditions devices from different manufacturers could produce very different results.

In 2009 the National Institute for Standards and Technology (NIST) joint task force, referred to as priority action plan 13 (PAP13) [44] was set up between the International Electrotechnical Committee (IEC) and the institute of Electrical and Electronic Engineers (IEEE), for the integration of synchrophasor data based on IEEE C37.118 into IEC 61850. The working group resolved to split the existing IEEE C37.118 standard into measurement C37.118.1 and communication C37.118.2 parts, which was consequently released in 2011.

In C37.118.1-2011 new requirements for measurements under dynamic conditions were added in addition to requirements for the measurement of frequency and

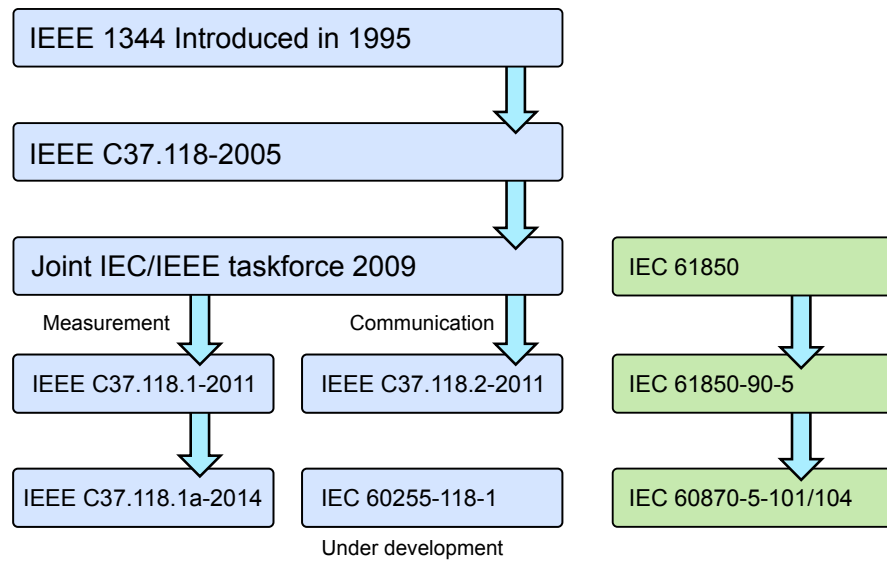


FIGURE 2.4: Evolution of the synchrophasor standard

RoCoF. The standard also provided complete mathematical definitions for synchrophasors and defined the 2 separate PMU performance classes, M and P [38, 45]. In C37.118.2-2011 a number of extensions of the 2005 standard were considered, but the working group resolved to limit changes to maintain backward compatibility. It was also assumed users would be migrating to the IEC 61850 protocol for communication needs and this already included many of these desirable features, consequently the data transfer part of the standard is predominantly unchanged from the 2005 version [45].

To resolve some issues with the synchrophasor measurement standard, where some of the requirements were seen as difficult to meet or required further clarification and interpretation [46], a revision was proposed in C37.118.1a that went to ballot in October 2013 [47] and was consequentially published in March 2014 [48]. The revision was designed to change some of the identified issues with RoCoF calculation, either by relaxing existing limits or suspending them altogether, and to simplify some of the other testing requirements.

The standard IEC 61850 has been substantially developed for substations and is seen as a key standard for all field equipment operating under both real-time and non-real time applications. Following on from the draft report IEC 61850-90-1 on the use of IEC 61850 for wide area communications, IEC 61850-90-5 was published

in May 2012 as a communication standard for the transmission of synchrophasor data according to C37.118.1. Work is to begin in early 2014 on IEC 60255-118-1 for the development of a synchrophasor measurement standard, expected to be very similar to the amended IEEE C37.118.1a standard [47].

Standard IEC 60870-5-101 is the proven standard used in the communication between the control centre SCADA system and the outstation or substation. The extension to IEC 60870-5-104 applies the additional benefit of changes in transport, network, link and physical layer services to provide complete network access. It should be noted that this is a generic protocol that has not been specifically designed for PMUs.

## **2.4 Phasor Measurement Applications**

Since the emergence of the technology in the early 1980s a growing number of phasor measurement applications have been utilised by power utilities globally; the following is a brief summary of those applications with an emphasis on their applicability to the GB transmission system.

### **2.4.1 Offline Applications**

When the first commercial PMUs became available, offline monitoring applications were the only option due to the low availability and high cost of communications channels required for real-time monitoring, control, and protection applications [49]. To that extent all phasor based applications begin at the offline analysis stage, looking at what could be learnt from historical data. A true benefit in the installation of PMUs needs to be demonstrated to warrant the investment in the necessary infrastructures.

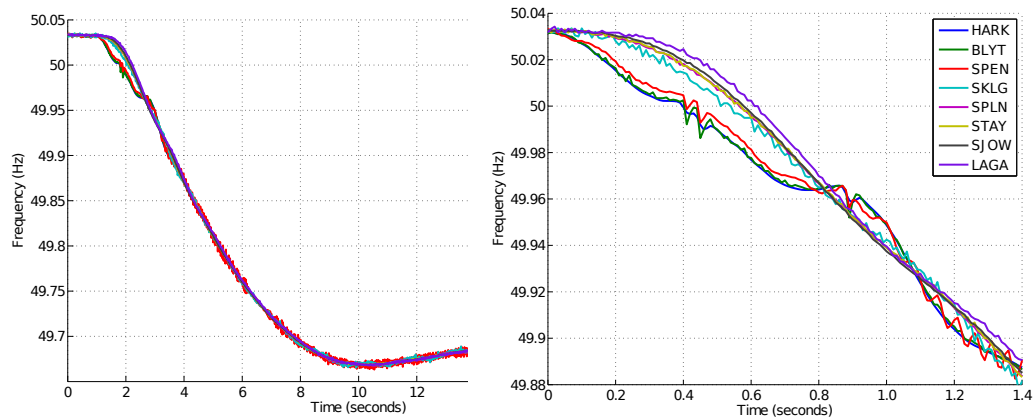


FIGURE 2.5: GB system frequency following a generation loss of 1170MW and zoomed (right) to show the events propagation through the transmission system

#### 2.4.1.1 Post-event analysis

Having identified an event in the power system a process of analysis is then desired to determine a number of factors; namely, route cause analysis, whether the event was isolated or as the result of a series of cascading incidents, control response and compliance and oscillation analysis, such as ringdown. A series of analysis can then be performed looking into detail at the system dynamics as a result of the event. Prior to the use of PMUs this was a very lengthy and time consuming process, as unsynchronised data would have to be assembled from various devices scattered amongst the network and then time aligned somehow for suitable comparisons along the same time axis. WAMS networks greatly simplify the analysis process, with time-aligned high resolution data being readily available in the PDCs of the network.

Figure 2.5 shows an example event from the GB transmission system in the loss of a generator exporting 1170MW in the Scottish part of the network. The corresponding PMU frequency measurements obtained from 8 locations around the network of England & Wales, show the initial impact of the event in varying magnitudes to different parts of the system. It can be clearly seen from the zoomed image on the right that the event is initially detected by the closest PMUs in the North of England at Harker and Blyth, before rippling through the network to the furthest monitoring point (electrically) from the event at Langage in the South

West of England. This type of information can help power system analysts and operators to understand the dynamic characteristics of the system by producing visualizations of the real data recorded during disturbances [22]. This can also inform event detection algorithms and power system inertial estimation techniques [30].

Attempts have been made to understand the propagation of transient events through transmission systems, with the phenomenon appearing to be related to the localised electrical inertias of the network [30, 50], the relative electrical strengths in terms of impedance, and the reactive power contributions of the generators causing the event [40].

This type of analysis has historically been focused on understanding the sequence of events that have led to large scale incidents or blackouts, so that weaknesses in the system can be identified and operational procedures improved for the future. However, growing concerns over reducing system inertia is increasing the importance of analysing all transmission level events, as they provide the only opportunity to assess the true response of the power system [30], leading to improvements in the accuracy of network models and consequentially the improvement of operational control procedures.

#### **2.4.1.2 Network Model Validation**

Validation of off-line system models is of vital importance, as inaccurate models can result in incorrect decisions being taken at the planning stage that filter through to live system operation. This can mean under utilisation of system assets leading to poor economical operation of the system or the over-stressing of systems, potentially resulting in large system issues or even blackouts. In the GB system, under the new RIIO operating model, the importance of accurate models of system behaviour is growing increasingly important, as the network is driven closer to its theoretical limits.

The only way to assess the true performance of the system is through actual measurements of system conditions [51]. Data captured around system events can then be used to actively tune network models. PMU data can also be used more directly to validate individual elements of the system model such as dynamic models of generators or transformers, by installing PMUs at the points in the network where the equipment of interest connects.

PMU data can be used in comparison with existing network models through comparisons during ambient [52, 53] or transient conditions [54], to verify or improve performance. Through the continued analysis of system performance during steady-state and from post-event analysis, in addition to gathered experience of analysed system incidents, a process of defining a system performance baseline can be undertaken.

## 2.4.2 Online Applications

The correct understanding of the applications from an offline perspective will go on to inform the processes or procedures for online applications.

### 2.4.2.1 Wide Area Monitoring

The ability to monitor, in real-time, synchronised power system parameters allows network operators a greater deal of visibility of evolving network conditions. However, this becomes a subject for appropriate visualisation tools [55], as just providing operators with graphs changing at high frequency would potentially just be a distraction or seen as information clutter.

The ability of WAMS to directly measure the phase angle differences around the power system, provides system operators with the ability to monitor the real time power transfer stress on various areas of the transmission system. This can help to build confidence when managing critical transmission corridors potentially allowing systems to be operated closer to their designed limits. This information



is particularly useful in large interconnected systems when the knowledge of a neighbouring interconnections system state is key to managing your own network. Following the blackout in the North East America and Canada in August 2003 it was deemed necessary to install a WAMS network for all regional transmission operators, to provide a more wide area view of emerging system conditions [56].

The practical application of wide area monitoring was first realised following data collected in Texas, America in July 1993 for the Comanche Peak load rejection test [50]. The frequency oscillations collected by PMUs revealed an electromechanical wave propagating through the system that was easily observed in the frequency measurements. This and similar measurements in other parts of America eventually led to the development of a frequency monitoring network, FNET [57], which through the installation of synchronised frequency disturbance recorders (FDR) throughout North America, provides a contour plot of frequency differences throughout North America. The system also uses a triangulation method based on the travelling wave of system events to determine the approximate source of an event or incident in the network.

On a large interconnected system like North America, with very long transmission distances, this sort of information is incredibly useful to network operators allowing them to forecast incipient system breakups and speed up remedial actions. The application to smaller heavily meshed systems such as that of GB is less apparent in real-time, as the system frequency is completely synchronised around the network during the steady-state. However, with increased integration with mainland Europe and the Nordic countries, pan-European integration of real-time frequency information may become vital.

#### **2.4.2.2 Monitoring of Inter-Area Oscillations**

In an interconnected power system inter-area oscillations typically exist across weak interconnections, where generators on one side of the interconnection swing against generators on the other side. The frequencies of such inter-area modes generally lie within the range 0.1 - 0.7 Hz [58], and so typical SCADA systems are

incapable of monitoring them, due to their network scan rates at around 4 - 10 seconds. The lack of synchronised data means an accurate picture of the shape of the modes cannot be established.

The addition of PMUs to the power system provides an enhanced level of monitoring for the oscillations in real-time, with accurate pictures of the mode shapes in terms of relative phase and percentage damping now able to be established online. Initial analysis takes place offline to establish the shape of a specific mode; the damping of the identified modes is then monitored closely in real-time as well as the amplitude and frequency.

Power system oscillations once observed can be damped through control systems however, it is through faults or excessive variations in generation or demand that cause this damping to break down. This needs to be monitored closely.

The GB system at present has as an inter-area mode at around 0.5Hz [13] that is typically well damped through installed PSS's, in addition to two other modes, which have been identified [59], with an unstable mode at around 0.83Hz and an inter-area mode at 0.7Hz that can be quite lightly damped. With huge changes due to impact the power system in terms of generation fleet, variability of supply and hence power flows, the damping of these modes is far less guaranteed. In addition, the drastic changes around the network could also give rise to additional modes previously unaccounted for. The increasing number of technologies on the system and competing control systems could mean that this phenomena will become increasingly complicated to predict and model.

#### **2.4.2.3 Dynamic Line Ratings**

The maximum power transfer capable along an overhead transmission line (amperacity) is defined ultimately by its thermal limit, defined by the performance of the lines conductor at increasing temperatures. This is not a constant value and depends on the weather conditions, namely ambient temperature, solar radiation

and wind velocity applicable to the line. It is understood that this is most often taken as a very conservative value implying under utilisation of system assets.

With a PMU installed at either end of a transmission line the synchronized phasor measurements facilitate the calculation of the lines true resistance. This information combined with knowledge of the type and length of the conductor allows the true rating of the line to be determined. The application is expected to increase asset utilization and operating efficiency.

#### **2.4.2.4 Improved State Estimation**

Wide area measurements were originally introduced as inputs for static state estimators, designed to assess system security from the point of view of the next contingency [22]. The measurement systems had to be designed to provide the best “quasi-steady state” approximation of the state of the power system.

Today State Estimation (SE) is seen one of the most important applications of the Energy Management System (EMS) providing operational security assessments and contingency analysis. The goal of SE is to provide the system state, in the positive sequence voltage values (magnitude and phase), for every bus of the system [22, 60]. This is achieved using the network model and typically a weighted least squares technique based on redundant data in the system [25]. This is a non-linear problem and it can take a relatively long time to converge a solution.

The inclusion of PMUs to the transmission system can greatly improve both the accuracy and speed of the SE solution, with the state of the network being directly measured as opposed to estimated [22]. Hybrid State Estimators, as shown in Figure 2.6 can either comprise a two-stage estimation approach, whereby the synchronised measurements are combined after the conventional SE or as a combined non-linear estimator at the start of the process [25, 61].

In addition, an advanced application dealing with the provision of synchronised phasor measurements to dynamic state estimation is explored in [62]; a Unscented Transformation combined with Kalman theory for the purposes of overcoming the

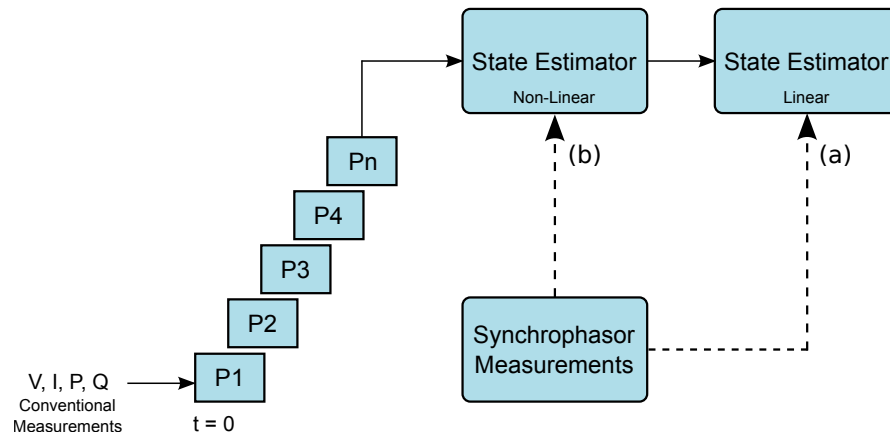


FIGURE 2.6: Hybrid State Estimation (a) two-stage estimation and (b) conventional non-linear estimator

challenges posed from highly non-linear mathematical models of network equations, usually approximated through a linearisation.

## 2.5 Global PMU Deployment and Initiatives

In order to develop a suitable deployment strategy for PMUs in the GB transmission system it is important to understand the global utility experience and the justification behind their PMU deployments. A large amount of technology that is new to the GB system has already been deployed in other areas of the world, such as TCSC and intra-network HVDC links. The addition of PMUs to monitor the challenges these devices bring are key to the future secure operation of the GB system. The following sections therefore summarise the funding initiatives and projects supporting the global deployment of PMUs.

### 2.5.1 North America

The 2003 blackout was seen as a major driver in improving the reliability of the North American grid. The US Department of Energy (DoE) report to congress emphasized several benefits of PMU technology, stating that the technology could be used to establish a real-time transmission monitoring system to improve the

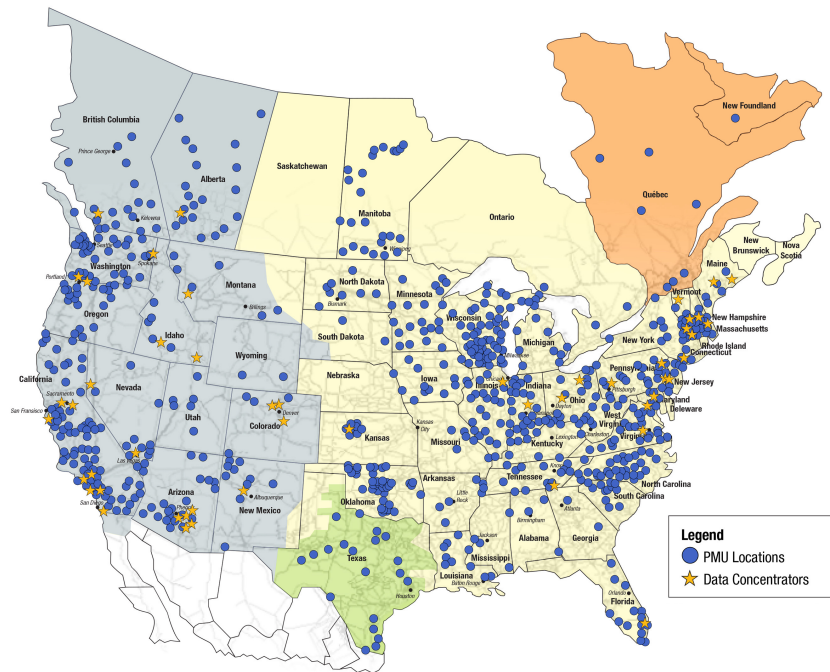


FIGURE 2.7: PMU deployment in North America [32].

reliability of the nations bulk power system. The use of enhanced situational awareness tools aiming to reduce the possibility of regional and inter-regional blackouts [63].

In 2007, the U.S. the DoE and the North American Electric Reliability Corporation (NERC), along with the involved electric utility companies and other organizations, formed the North American SynchroPhasor Initiative (NASPI). This effort combines the previous Eastern Interconnection Phasor Project (EIPP) and various activities associated with WAMS research, development and deployment activities as the primary focal point for continued DoE and NERC support and facilitation. The mission of the NASPI is to improve power system reliability and visibility through wide area measurement and control [32].

The US government, through the DoE has provided over \$150 million of grants to 58 utilities for ten projects for the deployment of nearly 850 PMUs throughout the USA, as can be seen form Figure 2.7 [32]. The entities also matched the US DoE grant resulting in over \$300 million investment in synchrophasor technology in the

span of three years from 2009-2012. Numerous utilities, transmission operators, universities and laboratories are involved [64].

The projects are focusing on the following key applications of PMU technology:

- Wide-area grid visualization and monitoring
- Angle and frequency monitoring across the grid
- Inter-area grid oscillation detection and analysis
- Proximity to grid voltage collapse
- Grid state estimation
- Dynamic grid model validation
- Fast grid frequency regulation

The DoE also awarded five three-year projects in 2011 worth a total of \$4.3 million. The projects are looking at:

- Adaptive relaying to make the grid respond to changing grid conditions most appropriately
- A three-phase tracking state estimator for unbalanced conditions and adaptive relaying
- Real-time implementation of a distributed dynamic state estimator
- Real-time visualization of frequency, voltage and current contours for security monitoring
- Examining power grid reliability and security through the analysis and simulation of a secure communication network.

## 2.5.2 China

The Chinese, following their soaring economy, are building one of the biggest and most complex power grids in the world. The first 1000kV AC transmission line and the  $\pm 800$ kV DC transmission line have already been put into operation with a  $\pm 1000$  kV DC based main transmission framework under construction [65].

The installation of PMUs began in the Chinese power grid in 1993, initially with the introduction of a Taiwanese made PMU, where around 40 devices were installed by 2002. The devices were capable capturing some of the low frequency oscillations present in the Chinese grid, this confirmed the value of PMU technology in assessing the dynamics of the power system [66].

By the end of 2002, Chinese manufacturers had began producing their own PMUs and over 400 devices were commissioned by 2007. By 2010 over 1000 PMUs had been installed in the network, with a requirement that all 500kV and above substations and all power plants over 100MW must have PMUs installed. Some of the phasor data is being stored at 100Hz resolution and with some PDCs containing over 10,000 phasors, high speed storage and data access is becoming a challenging task [63].

In order to tackle the challenges of processing the growing volumes of PMU data in a timely manner a high performance and scalable computing infrastructure is required. On this basis the work presented in [67] is looking at low frequency oscillation detection on data from 2000 PMUs, anticipating the scenario where potentially 120,000 evaluations of algorithms are required every second, assuming 2000 PMUs at 60Hz. The work explores the use of a cluster computer infrastructure to tackle the computation.

To date China is the clear leader in the deployment of PMUs with over 2500 PMUs active on their network. The WAMS network is primarily concerned with monitoring low frequency oscillations, as this is a severe issue in China due to long transmission lines running across relatively weak interconnections. The systems are also looking at model validation and wide-area data recording and playback,

with applications such as state estimation, and adaptive protection schemes also currently undergoing development [63, 66]

### 2.5.3 The Central European System

European TSOs began installing PMUs in 2003, with the main motivation being to improve situational awareness for the ever expanding system, with initial applications looking at voltage phase angle monitoring, line thermal monitoring and voltage stability [68].

However, system stability soon became a primary concern, following reconnection between the first and second UCTE (Union for the Co-ordination of Transmission of Electricity) synchronous zones in 2004 [69] and the connection of the Turkish power system in September 2010, the focus for PMU deployment then became the monitoring of poorly damped inter-area modes [68, 70].

Located central to the highly meshed system, Swissgrid is affected by cross power flows from all directions. Since 2004, Swissgrid has monitored the Swiss transmission grid using PMUs employing modal estimation tools for the monitoring of power oscillations. This was successively extended combining data from WAMS's from Austria and Croatia, enabling the real-time exchange of phasor data [63, 71]. The system was then further developed to include WAMS data from Denmark, Slovenia, Italy, Portugal, Greece and Turkey. With phasor data now being exchanged over a secure inter-TSO communication network, from over 20 PMUs with time resolution of 10Hz [68, 71].

The primary function of the inter-TSO WAMS is the monitoring of the known oscillatory modes, as shown in Figure 2.8, typically detected during normal, ambient, conditions [71].

- The East-West mode - involving coherent movement of generators in Portugal and Spain against those in Turkey. The mode is typically present between 0.13-0.15Hz and appeared following the connection of the Turkish network.



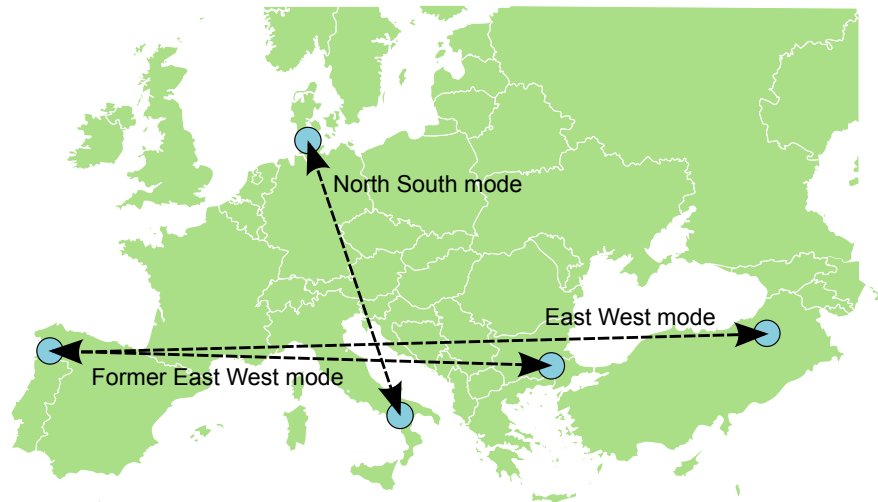


FIGURE 2.8: Inter-area modes of the Central European System [71].

Under normal operating conditions, this is the dominant mode with the most oscillatory energy.

- The Former East-West mode - involves coherent movement of generators in Portugal and Spain against those in Greece. This mode typically exhibits a frequency of around 0.17-0.2Hz and is most visible in frequency measurements from Greece and from Portugal.
- The North-South mode - involves coherent movement of generators in southern Italy against northern Germany and Denmark. This mode typically exhibits a frequency of around 0.23-0.27Hz.

The result of the live damping monitoring application correspond well with those achieved through system studies and engineering expectations regarding the dynamic characteristics of the ENTSO-E and Continental European Synchronous Area (CESA) system, and thus serves as an indirect and partial validation of the models used in those studies [71]. From the Swissgrid perspective, the next steps are to create a closer link between the WAMS and SCADA systems by setting up simple and comprehensive visualizations of system dynamics for the use by power system operators [71].

In addition, work package 13 (NETFLEX) of the Twenties project [72], was setup in 2010 to develop algorithms and tools to be integrated at CORESO. This aspect of the project was focusing on three main areas:

- The effects of controlling multiple power flow control (PFC) devices over a large area
- Wide-area advanced monitoring to detect large oscillations securing the system under extreme operational conditions.
- Dynamic line rating (DLR) tools.

The prime objective was to improve network flexibility, whilst not damaging the stability of the system. PMUs were used to help monitor the damping of the inter-area modes of the system, insuring that the use of PFCs and improved line ratings did not negatively impact system damping.

#### **2.5.4 The Nordic region**

The Nordic power system is a synchronously interconnected transmission grid comprising of systems in Finland, Sweden, Norway and Eastern Denmark. It should be noted that these networks also form a common electricity market. Transmission distances within the network can be very long, for example, in situations where power from Finland is flowing towards Sweden, the electrical transmission distance over the synchronous AC system is around 2000km. Under these circumstances, inadequate damping of post-fault power oscillations sets the limit for power transmission capability [73].

Research into the area of WAMS on the Nordic system began with Statnett, the Norwegian TSO, in 1999, working with ABB and Sintef on several R&D projects to test PMU technology and measurement processing algorithms to raise grid transfer limits [74]. Following on from this work, the project “Secure Transmission” was launched in 2005, with the main objective being to deploy a WAMS network in the

Norwegian 420kV system and demonstrate new concepts for secure operation of the power grid, focusing on solutions for the early detection of critical transmission operating conditions in the monitoring of critical inter-area modes. Initial work on computer simulations investigating the benefit from “global” PMU measurements to improve the efficiency of Static VAR Compensators (SVCs) to damp the critical modes, also began in this project [74].

PMUs have been installed in the Finnish transmission network for the application of low frequency oscillation analysis. The main mode for the low-frequency oscillation in the system is 0.3Hz, caused by generators in Southern Finland oscillating in phase against the generators in South Scandinavia [73]. For the application of inter-area low frequency oscillation analysis PMU data is down sampled from 50Hz to 10Hz, as this resolution is considered to adequately cover the frequencies of interest, whilst saving on data storage space [73]. In line with work taking place at Statnett, PMUs were also installed as an integral part of the SVC power oscillation damping controls, providing local frequency measurements and positive sequence voltage signals. To verify the performance of a damping controller, the 0.3Hz inter-area oscillations were excited by means of rapid changes in DC power flow [75].

Following expansions to the Finnish grid subsynchronous torsional damping has also been monitored using PMUs since 2006 [73]. However, data from these PMUs is collected using a separate PDC, which is applied to collect and store data at its maximum resolution of 50Hz, to enable coverage of the damping at the 5-20Hz range [73]. There are now 10 PMUs installed in Finlands power system, used to verify the performance of dynamic simulations, for component models and real-time estimation. The data is seen as vital in gaining knowledge of the dynamic behaviour of the network and tracking trends and directions over long periods of time [63].

Inter-area oscillations were also the focus for PMU deployment in the systems of Eastern Denmark and Sweden, with 2 PMUs commissioned independently to monitor the 0.7Hz mode between the two networks [76].

In June 2006 the Nordic TSO's, agreed to develop and implement a Nordic WAMS, to address growing concerns from increased renewables and inter-TSO power exchanges. In 2010 there were over 20 PMUs installed communicating to 3 separate PDCs.

Following the successful deployment of the initial WAMS network and computer simulations investigating wide area control [74], the implementation and testing of a Wide-Area Control Systems (WACS) for Wide-Area Power Oscillation Damping (WAPOD) [77], began in 2010. The initial testing showed the potential flexibility of the WAPOD approach, as it was capable of choosing from different PMU signals for those that have good observability of inter-area modes. This can be an advantage to the use of local feedback signals for damping control, which is the current practice today [77]. The system has been designed with a switch-over logic between the standard POD and the WAPOD, for instances when communication with the PDC or PMUs is lost for long intervals of time. When the local POD control is used the input signals to the SVC are line active power measurements, and when WAPOD control is used the input signals are bus voltage angle differences. With either local POD or WAPOD, the feedback signal is compared to a voltage set point to produce an error signal [77]

The end-to-end latency, due to communication and processing of the PMU data is vitally important in terms of the input signals to the WAPOD. This was typically noted to be negligible and normally within 30ms nevertheless, if the delay exceeds a pre-set threshold, an automatic switch-over to the local POD system is in place [77].

## 2.6 Concluding Remarks

This chapter provided an introduction to the concepts behind phasor measurement technology, from the history behind PMUs to their growing use in electric power systems today.

Having briefly summarised the global PMU deployment approaches, it is clear that a large amount of investment is being provided to utilities and system operators for the continued extension of WAMS networks, in a major effort to provide an increased awareness of the evolving power system conditions.

The motivations behind the PMU deployments stem from large challenges due to the integration of growing volumes of renewable generation and increased levels of interconnection with neighbouring TSOs. With power being transported over ever increasing distances at higher levels PMU data is being made available to improve situational awareness for system operators by furthering the wide area visibility of the power system.

The predominant application of the technology is the monitoring of intra-area oscillation damping, as growing transmission distances and increased power flow variances are exciting existing modes. There is also growing concern over the presence of new modes of oscillation as a result of the rapidly developing systems.

The key challenges in WAMS deployment are the supporting infrastructures in the communication systems and data storage requirements. Taking the example of the Chinese system where 10,000 phasors are already being stored at 100Hz in some PDCs, creating a phenomenal amount of data, importance is firmly placed around understanding the long term storage requirements of WAMS networks. An understanding is also required as to the application intention of the PMU deployment, taking the example of the Nordic system where PMUs have been installed primarily for inter-area damping estimation and the PMU data is actually downsampled to 10Hz saving hugely on the storage of data and the bandwidth requirements of the communications infrastructure. It is important to note however, that the downsampling of this data could reduce the accuracy for other applications, such as inertia estimation or the monitoring of Sub-Synchronous Resonance (SSR) [59].

The other TSOs also already have experience with a lot of the challenges set to face the GB system, with TCSC and intra-network HVDC already part of some networks. The progression of the Nordic system from WAMS to WACS over a 5-10 year period is particularly important, as it outlines the experience and

knowledge required from the monitoring applications to be able to progress to wide-area control. The coordination between the involved TSOs of the network is also vital.

## Chapter 3

# System Monitoring and Control at National Grid

The operation of the GB transmission system has proceeded relatively unchanged for the past 50 years. However, as a result of enforced climate change legislation an unprecedented amount of development is required and it is now necessary for both operations and control procedures to adapt accordingly. This is largely dependant on a more stringent approach to system monitoring (SM), as greater amounts of high-resolution time-synchronised data is now required.

However, until recently it has been difficult to justify changes to monitoring practices on the GB system, as it is a heavily meshed network with excellent reliability and has experienced very few issues with system stability in recent years [78]. Unlike the US, China or parts of the European system, no major blackouts or other severe incidents have occurred and so there are, at present, no major funding initiatives available for the deployment of PMUs or WAMS networks.

The existing installation of PMUs to the GB network have been in line with an uncoordinated bottom-up approach, through upgrades to existing equipment and “business as usual” type activities. It is anticipated that confidence and greater experience of the devices on the network will lead to more application specific

installations, although a benefit to system operation has to be demonstrated and quantified.

The next sections of this chapter reviews the existing monitoring and control systems at NG, with a focus on which systems or applications could be further improved or adopted by PMUs. Details are also provided on the Power System Dynamics (PSD) monitoring system that first introduced PMUs to the GB network, more specific information pertaining to the overall GB WAMS deployment is provided in Chapter 4.

## 3.1 Introduction

The monitoring and control of power systems can be broken down into 3 main areas, as show in Figure 3.1, depending on the specific application the data is required for, this is based on:

- The level of data coordination - whether it be localised to individual intelligent electronic devices (IEDs) and control systems or the application requires a network-wide view.
- The speed of response - from the millisecond range for fast acting systems such as protection, or in the order of seconds to minutes for applications such as steady-state estimation.

Wide area monitoring protection and control (WAMPAC) is the long term goal for power systems monitoring globally. The growing complexities of power networks are requiring applications to seek a network wide perspective to ensure decisions secure the optimum outcome for the overall system, as opposed to just solving a localised problem. This is heavily dependant on robust communications infrastructures with very low network latencies and fast acting algorithms.



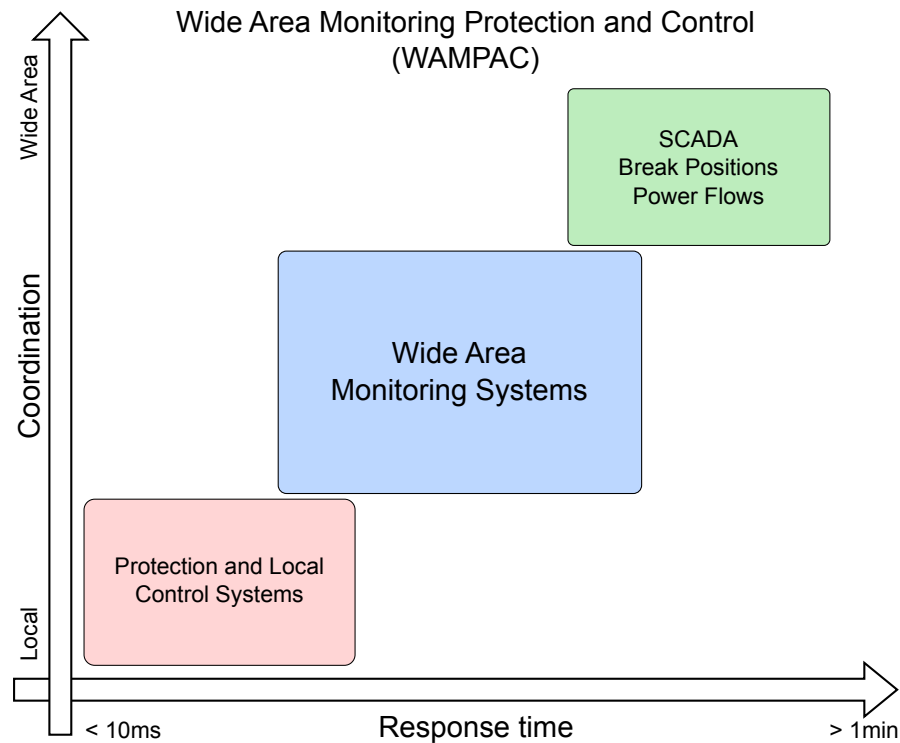


FIGURE 3.1: Wide Area Monitoring Protection and Control (WAMPAC) applications

In the interim WAMS can be seen to bridge the gap between the network wide SCADA monitoring solutions and more localised systems such as those of protection applications or dedicated control systems. WAMS has the potential to provide a new platform, to combine a number of existing applications together, offering improvements to operational and planning systems.

At NG, SM delivers a critical service to aid the understanding and management of Transmission System performance within statutory obligations, including those stipulated in the Transmission Licence. Historically it has been developed on an ad-hoc basis, and comprises a mixture of fixed and portable offline systems that supervise and record system conditions and disturbances at strategic transmission locations and critical generation and demand connection interfaces.

The on going changes towards the future network landscape brings about a number of uncertainties around system dynamics through reducing system inertia and increasing variability of supply and this consequently presents a significant number of challenges to NG. These have to be understood and managed accordingly, but

this is all heavily dependant on access to reliable system data so that the necessary analysis can be undertaken.

## **3.2 Supervisory Control and Data Acquisition (SCADA) systems**

The SCADA systems observe changes in grid conditions approximately every 5-10 seconds, by polling remote terminal units (RTUs), this is deemed too slow to track dynamic events on the grid. In addition the measurements are not time-stamped at their source; monitoring equipment feeding into the central SCADA system are time-stamped upon arrival. The systems currently employed at substations and grid connection points can be considered obsolete, working on old technology that is no longer considered suitable for the evolving network.

The systems are essentially all performing similar tasks, but do not all feed into the central system, meaning data analysis and comparisons can be quite convoluted [79]. This large number of systems points to an unnecessary level of complexity, in addition to commissioning and maintenance issues.

In essence the operation of the existing monitoring systems work through analogue voltage and current data that is provided from the secondary side of instrument transformers (ITs). This is then sampled/digitized for processing, all be it at varying resolutions. From this point a number of applications are carried out to provide information on the status of the electricity network from different perspectives.

The current arrangement of the substation systems, as can be seen in Figure 3.2, results in a convoluted and excessive amount of data processing, with some of the legacy monitoring data having to be manually retrieved through dial up systems such as the public switch telephone network (PSTN), this also makes data comparisons between sites unnecessarily complicated.

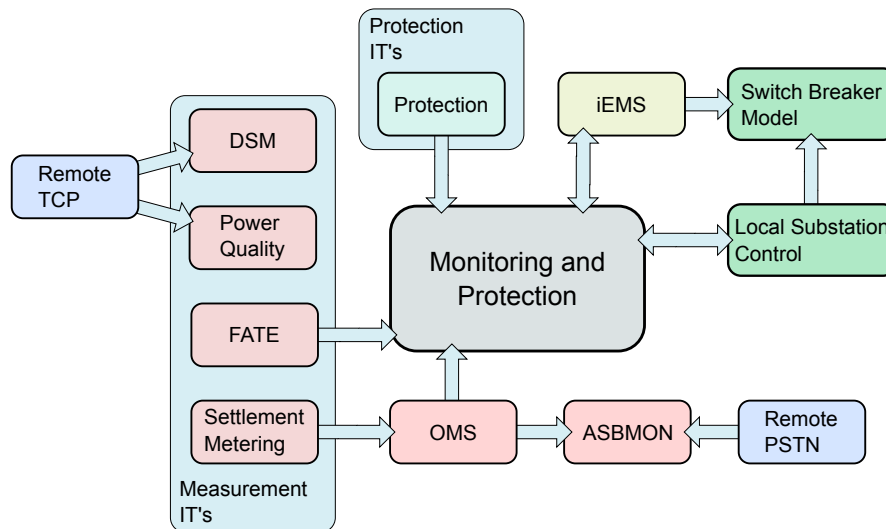


FIGURE 3.2: Monitoring and Protection systems at National Grid [79]

It is proposed that, as a number of the existing monitoring systems are at end of life, their services could be provided by PMUs or similar devices based on time-synchronised data, making use of a central data repository to facilitate simple access and analysis of the data. This serves to increase the penetration of synchronised measurements onto the network and improve the accuracy of the existing applications [79]. However, based on the statistics from NG UK construction, the currently achievable replacement rate for protection and control devices is about 5% per annum [80]. It would therefore take around 20 years to complete a whole cycle of replacement. The typical asset life for numerical equipment is 15 years, and in many cases, the digital relays can hardly stay in service for more than 10 years before becoming obsolete, due to fast technology change and availability of technical support. All of these issues are seriously challenging the sustainability of secondary system assets, which threaten the required availability and reliability of electricity transmission and distribution networks [80]. For these reasons it is important to understand the SM requirements throughout NG, so that a robust SM strategy can be developed to ensure the future monitoring requirements of the network are catered for.

The following sections detail the existing monitoring applications at NG and propose potential improvements through the use of PMUs.

### 3.2.1 Frequency and Time Error (FATE)

The Operational frequency is monitored through the FATE system; around 10 sites on the England and Wales network monitor the local frequency at 5Hz resolution. This information is sent back to the control room, where one of the readings is chosen to represent the system frequency for the whole network. This is normally taken from the electrical centre of the network, which should be an area of stability, less susceptible to the deviations that occur on the outskirts of the network.

Based on this frequency information, it is the requirement of the National Balancing Engineer to endeavour to maintain Electric Time, in accordance with the standards outlined in the NETS Security and Quality of Supply Standard (SQSS) and the Gridcode. This is to remain within  $\pm 10$  seconds of Standard Time, either by means of generation despatch or through changes to Target Frequency, which should nominally be  $50\text{Hz} \pm 0.05\text{Hz}$ , except in exceptional circumstances as determined by NGET, in its reasonable opinion when this may be  $50\text{Hz} \pm 0.1\text{Hz}$  [81, 82].

This FATE data is refreshed on a second by second basis in the control centre, which is not fast enough to track dynamic changes in the system. In addition, as the information is not time synchronized, direct comparisons cannot be made between different areas of the network. Online comparisons could add significant ability to the system to identify emerging power system conditions, playing a key role in situational awareness and could prove particularly useful to combine with information from the Irish networks or the European System, as the relative “health” of these networks could affect interconnector flows in the future. This information would also be vital during post-event analysis, allowing the progression and impact of an event to be accurately viewed as it ripples through the system. Potentially offering information on any system weaknesses through, for instance, lack of inertia or voltage support, and allow comparisons with the offline network models to improve their accuracy.

It is important to note that, at present, data is not provided from the Scottish transmission network and so there is no frequency data available for analysis. With growing concern over reduced inertia on the GB system, time-synchronised frequency information is becoming vital to the understanding of regional inertia issues and is now deemed vital for offline analysis [29]. This will be covered in greater detail in Chapter 6.

### 3.2.2 Settlement Metering

Settlement Metering Systems accurately record the flow of electricity either as an import or export from a site for each half hour period. The information is used by ELEXON to calculate any energy imbalance charges, which are applied to all Balancing and Settlement Code (BSC) parties who use more or less energy than they have contracted to buy or generate [83].

Balancing mechanism units (BMUs) are used as units of trade within the Balancing Mechanism (BM). Each BMU accounts for a collection of plant and/or apparatus, and is considered the smallest grouping that can be independently controlled. As a result, most BMUs contain either a generating unit or a collection of consumption meters.

Settlement Metering for the transmission system must comply with the requirements that are outlined in the relevant Code of Practice (CoP), typically this is CoP 1 [84], dealing with the metering of circuits with a rated capacity greater than 100MVA.

As this is a regulated area of monitoring with its own ITs, it is expected to always remain a separate service. For this reason it would not be suitably adopted by PMUs or combined with any other application. The information is however also required for operational purposes.

### 3.2.2.1 Operational Metering

This metering is intended to provide both NG and the generators with real-time information on power flowing both to and from connection points all around the network. This is used for system control and more recently to inform process for offline modelling [29]. At present this data is provided via a pulsed output from the Settlement meters; this in itself is prone to errors, of around  $\pm 1\%$  [79]. If this information was also time synchronized at source true comparisons could be made when modelling the system, as an exact “snap-shot” could be taken of the generator outputs. However, it is appreciated that this would require a PMU type device for every single BMU, which in the short term is not realistic.

### 3.2.3 Ancillary Services Business Monitoring (ASBMON)

National Grid has a licence obligation to control system frequency within the limits specified in the “Electricity Supply Regulations”, to  $\pm 1\%$  of nominal system frequency with an allowance for abnormal or exceptional circumstances. NG must therefore ensure that sufficient generation and/or demand is held in automatic readiness to manage all credible circumstances that might result in significant frequency variations.

NG maintains the system frequency through frequency response balancing services. Full details of the frequency response requirements of the GB system are provided in Chapter 6.

Mandatory frequency response is an automatic change in active power output in response to a significant frequency change. All generators operating under the requirements of the Grid Code must be capable of providing this. The generators connecting to the GB Transmission System are required, as a condition of their Generation License to comply with the Grid Code (CC 6.3.7) [82]. In turn the Grid Code places technical obligations on Generators in respect of their ability to provide frequency response.

The Grid Code specifies requirements for system monitoring in CC 6.6 and monitoring of users of the transmission system in OC 5.4. Specifically OC 5.4.1(c), imposes a Grid Code obligation on NG as the SO, to monitor the performance of the provision by users of ancillary services, which they are required or have agreed to provide [82].

The monitoring of frequency response performance confirms contracted response from providers is actually supplied when it is required. Without such specific monitoring, other systems (such as operational metering) do not provide sufficient resolution of data to establish whether the output of generators selected varies appropriately with frequency. Frequency response has to be dispatched economically. In order to do this and only despatch sufficient response at any point in time, it is necessary to have confidence that the providers selected will provide the expected levels of response. Monitoring response performance and following up on instances of under performance enables NG to reduce the amount of response held to mitigate the risk.

The existing ASBMON system is used to collect data for generators selected for frequency response to determine their performance against their contracted arrangements. Monitoring devices are currently installed at 60 sites, monitoring approximately 130 BMUs. It is important to note that the current ASBMON units have been in service for over 15 years and are currently connected via a serial connection to the Operational Metering Summator (OMS), which in itself receives information via a pulsed output from the Settlement Meter.

The ASBMON unit logs second-by-second frequency and MW data for each generator. This information is then stored on the ASBMON hard drive on a rolling 2 weeks basis such that data older than 2 weeks is overwritten.

Data is retrieved from the units as required using a stand alone PC and bespoke software, sites are then manually contacted via PSTN. Current practice is to assess frequency performance of all generators selected to provide response whenever a frequency excursion outside of operational limits ( $50\text{Hz} \pm 0.2\text{Hz}$ ) for longer than 2 minutes occurs.

Due to the age and antiquated nature of the existing system, the replacement should fall in line with new PMU installations. The reliance on manual processes could be averted through event detection type algorithms, designed to automatically detect incidents or deviations and collect data surrounding frequency performance. The increased resolution and time-synchronised data being far better equipped to analyse the generators performance. This will be vital in the future GB system with greater penetration of wind, when the amount of generation kept online in reserve will become increasingly contentious and costly. In addition if Wind farms and interconnectors are expected to provide response or synthetic inertia type services, the ASBMON could become increasingly complicated.

### **3.2.4 Power Quality**

Power Quality (PQ) monitoring is intended to encapsulate all deviations from nominal system conditions, this includes harmonics, voltage unbalance, voltage sags and swells, transients, frequency deviations and flicker. In addition PQ monitoring is required to provide evidence of Grid Code compliance whilst facilitating customer connections through identification and management of power quality parameters.

The increasing use of power electronics and converter interface connections such as those of HVDC interconnectors and Wind farms, is resulting in increasing concerns over power quality, through additional levels of electronic interaction with the AC system. If there is not suitable visibility of this issue and it is not managed correctly it could result in rising constraint costs, or lead to damage of system assets such as plant owned by NG and its connected customers. There is an urgent requirement to better manage the impending PQ issues by confirming the background harmonic distortion at PQ sensitive areas and limit the harmonic emissions from customers and resonance shifts from cable infrastructures.

At present there are 35 fixed PQ monitoring units with 10 portable devices available to enable adhoc testing. However, the draft NG System Monitoring policy



[85] states that in the future PQ monitoring should be provided as a minimum at the following areas:

- Transmission circuit Feeders and Generator bays at Generation sites having a capacity of 5-times Large Power Station as defined by the Grid code to be sites greater than 500MW ( $5 \times 100\text{MW}$ ).
- New SVC & Robust SVC (RSVC) infrastructure schemes to monitor dynamic performance because of the interaction with the main system.

In addition sites that have been identified as a “Significant Interconnection”, shall also be monitored:

- $\geq 8$  feeder circuits
- Interconnectors, PQ monitoring shall be provided at the point of interconnection.
- Offshore network connections, monitoring shall be provided at the onshore point of connection.
- Series compensation, monitoring shall be provided by NG at all ends of any series compensated circuit and at the next remote bus with the shortest electrical distance from each end of the compensated circuit.

With this in mind an additional 100 PQ units are planned to be installed over the next 3-5 years [85]

### **3.2.5 Fault Recording and Dynamic System Monitoring**

Dynamic System Monitoring (DSM) is an important tool used by NG to monitor transmission network performance and plant dynamics to provide post event analysis for system incidents and customer complaint investigations. The data produced is primarily used for Grid Code compliance monitoring and also enables:-

- The cause of specific incidents to be established.
- Lessons to be learnt from system incidents and issues.
- The improvement of system performance.
- Increased understanding of system behaviour.
- System stability assessment leading to the need for transmission reinforcement schemes.

The dynamic performance of anticipated network changes could have a significant effect on the overall performance of the connected network and the local users.

There are currently around 160 DSM devices installed on the system of England and Wales, all of which have to be manually contacted through TCP connection over the NG BLAN. Going forward, DSM devices are required to be provided at the same sites as PQ monitoring.

It is felt that this could all be combined into one SM function and could also incorporate the requirements of the FATE system [79, 85]. With the impending installation of new devices to meet these SM requirements, it would seem beneficial to NG and the overall SM strategy to, either install a PMU at the required sites to adopt these roles or to provided PMU type functionality to the new equipment.

### **3.2.6 Protection Systems**

Monitoring and Protection systems are very separate, as they have different requirements in terms of accuracy, and as outlined in Figure 3.1 they require much faster response times due to the criticality of the application to the transmission network. There two systems also have very different requirements with regards to data access and cyber security, with the protection or control systems allowing access to switches and breakers that could have a severe impact to the operation of the network, security is obviously a major concern.

The protection systems employ separate ITs, as they require current to be monitored over the full range of a fault, up to 63kA. This greater monitoring range limits the resolution available to cover normal operating conditions and hence the accuracy. The systems are also required to be integrated within a much faster communications network and at NG they sit within the OpTel network that ensures an end-to-end latency of less than 5ms.

In the conventional protection relay, a method of synchronization is required to ensure that samples are taken simultaneously by relays in substations at opposite ends of power transmission lines/cables. This operates under the premise that the propagation delays in the communication paths are equal for both send and receive. However, the technology for high speed data communication can exhibit different propagation delays between the send and receive paths, with the result that the conventional method of achieving synchronized sampling cannot be applied [86].

As a result new “line current differential” relays that can achieve synchronization based on GPS were developed [86]. Furthermore, a unique back-up mode function that can maintain the performance of the protection in the unlikely event of failure of the GPS reception system was also employed. The newly developed relays were installed in the North Hyde and Iver substations of NG and were successfully commissioned in June 2002 [86].

Although these devices provide synchronised phasor measurements, the data is unlikely to be offered as a streaming service back to a centralised system, as this would pose a security risk to the protection services. In addition, the devices would be categorised as P class PMU devices and would potentially not provide the necessary accuracy for monitoring applications.

### **3.3 The IEMS and the State Estimator**

The Integrated Energy Management System (IEMS) is the central monitoring system installed in the control room. It displays the state of the transmission

network in near real time; this includes busbar, circuit breaker, and isolator status. In addition the system status can be modified through a telecommand from remote systems.

The method of state estimation (SE) employed in the control center is based on asynchronously gathered data, collected by polling remote terminal units (RTUs) that provide information to the SCADA system. The RTUs measure data locally at 1Hz, which is not time stamped at source. Due to the time taken to scan the entire network the data has an arrival rate of 1 complete set of samples every 4-10s. The system is therefore at a slightly different state by the end of the scan allowing for potentially inconsistent results to be returned in the SCADA system, for instance, current can be indicated as flowing in a line with an open breaker.

A “snap-shot” of the SCADA data, based on the latest pole, is taken every time the SE is run; the process itself takes around 60s to converge a solution, so considering the 10s taken for the SCADA polling the corresponding estimate provided can be considered as about 70s out of time, as shown in Figure 3.3. While the delayed estimate may not be considered a problem during normal operating conditions, it can be more problematic during system incidents, whereby the SE will not be capable of accurately representing the state of the network. The occurrence of any form of system event will eventually change the network to a new steady-state condition, so such an incident should act as a trigger for the SE to be re-run, so it is always providing the most accurate quasi-steady state approximation of the network [40].

The SE has been configured to calculate a load flow every 10-minutes with contingency analysis performed by the Power Network Analysis (PNA) system. A quasi-steady state solution for the network is then provided, with an assumption that the network is static during the 10-minute period. If lines or nodes are exceeding a limit then the operator will be notified, and may take corrective action. Any discrepancy in meter readings is also picked up at this stage.

It is important to note that, at present, the result of SE is not directly used to provide operators with a view of the network, the file produced is not in a visually

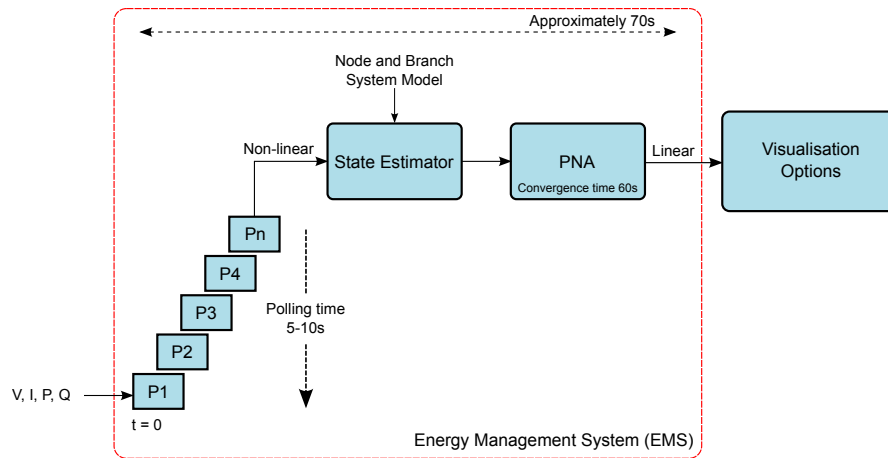


FIGURE 3.3: State Estimation process and application at NG [40]

useful form. The work demonstrated in [87] shows the possibility of using the generated file to produce geographic contour plots detailing voltage magnitude or phase angle difference around the network, thus enabling the “state” of the network to be readily determined, along with voltage profile. It is important to note that at NG the real-time systems are run from SCADA data, rather than the SE solution.

The inclusion of phasor measurements within SE has already been addressed in [23, 88] and the practical application of the measurements to static SE has been reported by some utilities [89–92]. It is however understood that the number of available PMU measurements installed in the power system compared to conventional SCADA measurements is, at present, too limited to have a significant or noticeable impact on the overall estimated solution.

The work in [24] informs that PMUs need to be installed at between 1/5 and 1/3 of the number of system buses for the system to be completely observable and it should be noted that this does not take redundancy into consideration; this certainly, on the GB system is some way off. To determine where and how many additional PMUs need to be placed in the system, different objectives need to be considered. It is important to capitalize on the use of devices, which have been installed for other applications, and with a potentially large number of devices scheduled to be installed on the GB network that could offer PMU functionality, system observability is increasing. However, on the GB network there are a number

of monitoring black-spots with low visibility over large parts of the network. It is proposed that the inclusion of PMUs to the SE should form part of a wider review of the overall SM approach.

### **3.4 Remote Asset Management and Monitoring**

The main concerns with SM are obsolescence and communication problems between the devices and the end user. The growing importance of the devices requires a robust network infrastructure with provisions for adequate volumes of storage.

Equipment concerned with DSM, PQ and ASBMON are not required to offer data streaming services, as their information is only required in the case of specific events. This can be problematic, if the devices are not regularly contacted it cannot be guaranteed they are working.

The roll out of the Remote Asset Management and Monitoring (RAMM) project is aiming to improve access across NG, ensuring secure access to sites via the internal BLAN, which should improve the communication system resilience to SM equipment at site. Figure 3.4 shows all the equipment connected through the RAMM system.

This system arrangement is suitable for monitoring equipment that provides localised storage that does not require constant high-resolution streaming services.

When determining a communications infrastructure for SM it is thought that the following still needs to be determined, based on the resolution of data to be transmitted and how often the data is required, whether it be a constant streaming service or only accessed on a post-event basis.

- Identification of communication system requirements for each different SM function,

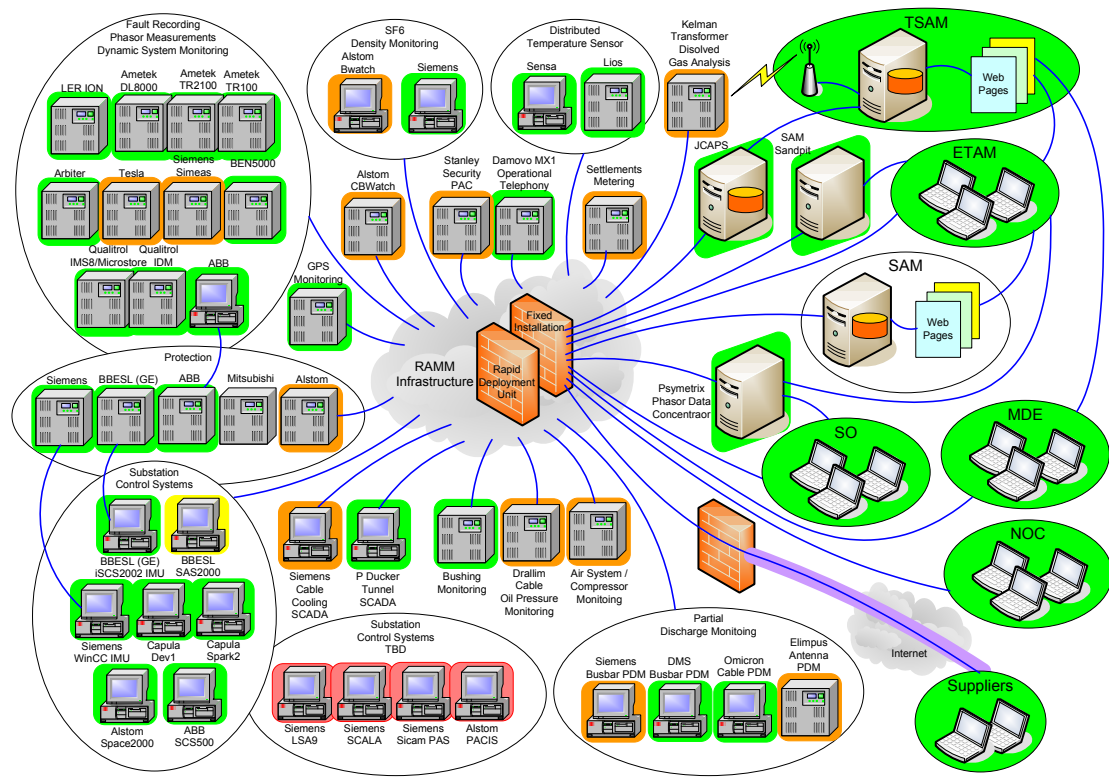


FIGURE 3.4: All the equipment connected through the RAMM system [93]

- Identify the need for and capacity of data storage, either locally, remotely or both.

PMUs are currently communicating back to the NG PDC via the RAMM system, this is not considered to be appropriate and will be examined along with the rest of the communications system in detail in Chapter 4.

### 3.5 Power System Dynamics Monitoring

The first 3 defined incidents of dynamic instability on the GB transmission system occurred towards the end of 1978 [94], these events were unexpected and consequent experience from these events enabled empirical, but correct control actions to be implemented when the oscillations reappeared.

The GB system, in the late 1970's and early 1980's, experienced large oscillations in the order of 800MWs, as can be seen in Figure 3.5, whereby generator groups in

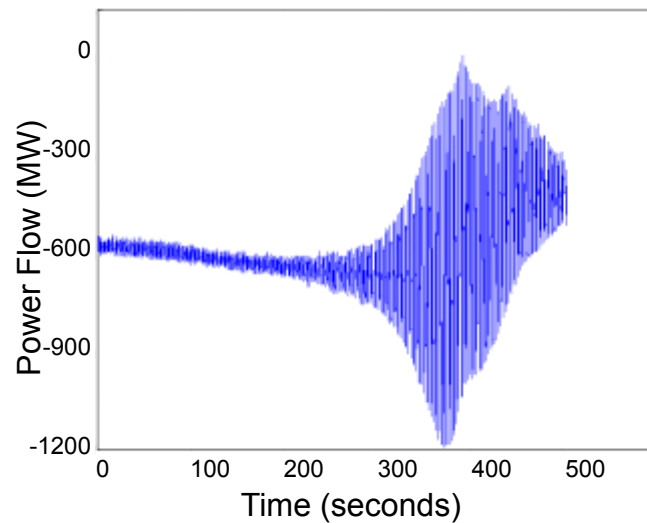


FIGURE 3.5: Example of unstable 0.5Hz oscillations in the Scotland-England transfer, 1982 [78]

the Scottish network oscillated in unison at approximately 0.5Hz against generator groups in the network of England and Wales. It is however, important to emphasise that the low-frequency oscillations involved the whole of the GB system.

The post-event analysis identified the most significant system factors in producing the oscillations and these were avoided by setting flow limits on the Anglo-Scottish interconnection [13], the capacity was severely constrained. As the power flow increases the damping of the oscillation reduces, and at some power flow levels negative damping was experienced resulting in large oscillations.

Merely reducing the power flow across the interconnection was not considered to be an economical and effective solution to the problem. Following the recurrence of large sustained oscillations in February and March of 1982, Power System Stabilisers (PSS) were consequently installed on 3 Scottish generators, Peterhead, Longannet and Hunterston [95]. However, due to the dynamic characteristics and uncertainty in dynamic network simulation, there was still a significant constraint in the export of power from Scotland to England [78].

A system was consequently developed, by Psymetrix to carry out continuous analysis of the dynamics of the GB system, extracting the frequency, amplitude and damping of the modes of oscillation. The first Wide Area Monitoring System



(WAMS) was deployed in the GB electricity national control centre (ENCC) in 1998 [78]. This system provided information to the ENCC in real time, with alarms generated if the damping of the inter-area modes exceeded a pre-defined threshold.

To effectively monitor the inter-area modes information is required from the respective centres of inertia for each area (Scotland and England). In the absence of data from the Scottish system, monitoring devices were installed, one in the North of England, close to the Anglo-Scottish boundary to detect for any oscillations between England and Scotland, and another device was installed close to the centre of inertia for England and Wales, at a known “electrically strong” area of the system. By comparing the amplitude of any oscillations between the two locations it was possible to determine whether the source of the oscillation was in the North or the South of the network.

Operational rules were setup, governing the amount of power to be transferred over the interconnector, provided that a suitable margin of damping was available [78]. If damping of the inter-area mode became poor, transfer was temporarily restricted until the oscillation dissipated. The dynamics monitoring system was instrumental in achieving a very substantial increase in power transfer without compromising system security [78].

The system was upgraded in February 2011 to make use of PMUs. Two devices, in upgraded Digital Fault Recorders (DFRs), were configured to transmit 50Hz phasor data back to a central PDC installed in the ENCC. The PDC is maintained by Psymetrix and is running the PhasorPoint [96] application for stability analysis. In the same vein as the previous system a PMU was installed close to the Anglo-Scottish boundary and another device was installed close to the centre of inertia for the England and Wales network, as shown in Figure 3.6.

The current system has the ability to identify whether the oscillation damping on the system has fallen below predefined stability margins and can determine whether the source of the oscillation is in the North or the South of the network. The reduction in damping, as identified by the system, generates an alarm that is

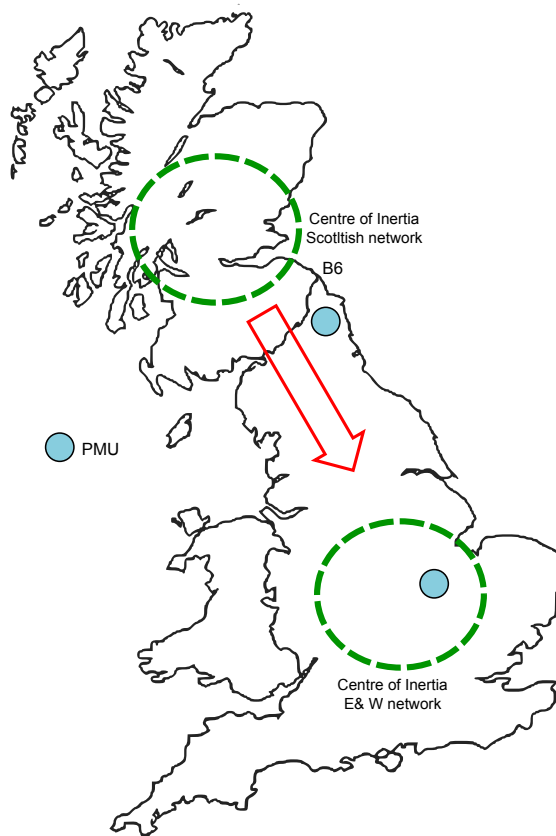


FIGURE 3.6: PMU placement - Dynamic Stability Monitoring of the Anglo-Scottish interconnection

sent to the iEMS to alert system operators that the system may be approaching instability. It should be noted that there is no means, at present, to indicate the root cause of the oscillation, be it a fault with a specific part of a generator or an excessive amount of power flow. The system employs Psymetrix's patented method of modal analysis, this remains part of Psymetrix's intellectual property and so specific details of the approach for oscillation identification are unknown. This remains a very active area of power systems research and there are a number of ongoing works analysing the inter-area modes of the GB system, which have been reported in [97–99].

In addition to the 2 PMUs configured for the PhasorPoint system, a total of 40 devices have been installed to the transmission network of England and Wales through a series of upgrades to DFRs and the installation of 4 dedicated PMUs, the majority of which are configured to report back to the central PDC at the ENCC, through the internal NG Business LAN.

It is important to emphasise that NG are not currently receiving any PMU data from either of the Scottish TOs, this would be the optimum approach to monitoring the inter-area mode, as monitoring devices are ideally required to be located at sites that represent the centres of inertia for each “area”. The inclusion of intra-network HVDC links and TCSC will also make this vitally important to the operation of the future networks. With PMU data becoming increasingly important to NG for the application of inertia estimation, provision of data from the Scottish part of the network is becoming crucial to accurate analysis methods. This will also facilitate greater understanding of the inter-area modes of the system and potentially offer improvements to the operation of the Anglo-Scottish interconnection. This is one of the intended outputs of the VISOR project [59].

### **3.5.1 Power System Oscillation Detection Procedure**

Although approximately 40 PMUs have been installed on the England and Wales Transmission System, only 2 of the devices are currently required for operational analysis of the power system oscillations, as shown in Figure 3.6. A PMU has been installed at Blyth in the North East of England and Staythorpe near the centre of the network. The Blyth PMU is best positioned to detect any oscillations between England and Scotland, as it is the closest PMU electrically to the Anglo-Scottish boundary. The Staythorpe PMU is located close to the centre of inertia of the England and Wales system. By comparing the amplitude of any oscillations between the two locations it should be possible to determine whether the source of the oscillations is in the north or south of the network. The PhasorPoint system carries out constant oscillation analysis on the Active Power signals calculated from the PMUs and provides updates to the frequency, amplitude and damping of the inter-area modes.

In addition Scottish Power have their own Power Dynamic Monitor (PDM) that is also provided by Psymetrix, and they may be able to provide additional information on request to help locate the source of oscillations relating to specific events. This would typically be an offline activity, as a means of post-event analysis to

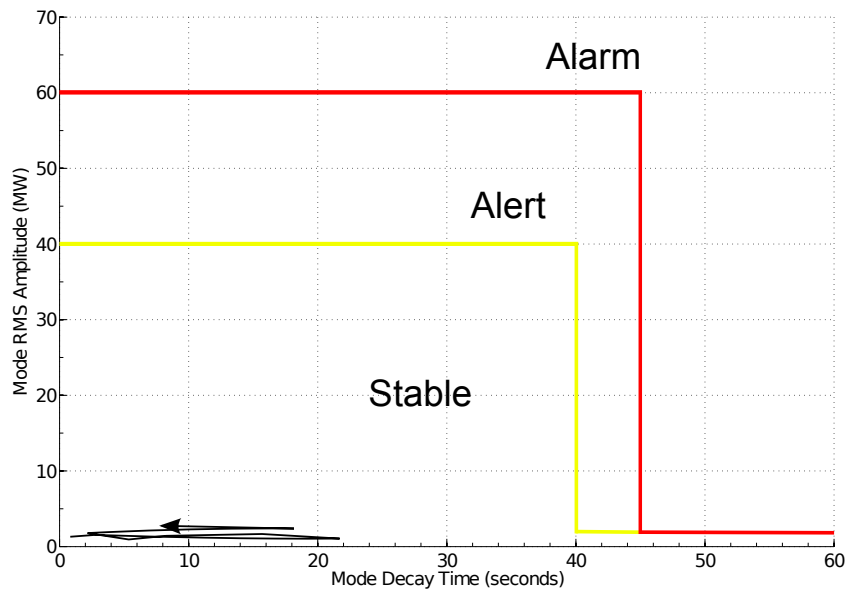


FIGURE 3.7: Psymetrix PhasorPoint oscillatory analysis Locus plot [100]

attempt to understand the cause of the incident. However, it may offer some real-time perspective on the issue, this is dependant on time-scales, as the information from the Scottish system is not readily available to NG.

In operational time-scales specific alerts and alarms have been configured based on unacceptable oscillations following advice from Psymetrix. As can be seen from the Locus plot in Figure 3.7 an Amber alert will be triggered if the magnitude of an oscillation exceeds 40MW or if the mode decay time exceeds 40s. Similarly a Red alarm will be triggered if the magnitude of the oscillation exceeds 60MW or if the mode decay time exceeds 45s. Any oscillations  $< 2$  MW are deemed insignificant, regardless of their decay time.

Any oscillations that trigger an amber or red warning should be recorded in the daily Control Room Management Report to enable post event investigation to be carried out. Since the PhasorPoint system went live at the ENCC in May 2011, there have been no recorded incidents of system instability, this is due to the conservative nature under which the Anglo-Scottish boundary is operated.

In order to attempt to establish the cause of the oscillation that generated the alert/alarm to determine the remedial action, the procedure is as follows:

- Determine which PMU/node is affected and what the frequency of the oscillation is.
- Are the oscillations sustained or are they transitory?

If there are excessive oscillations in the range of 0.4Hz to 0.7Hz then this is assumed to be as a result of excessive flow across the Anglo-Scottish corridor. It has been agreed with Scottish Power (SP) that if an alarm is initiated then this information should be passed to their control room. This way if SP have detected any oscillations with their own monitoring equipment, then this information may also help to locate the cause. The oscillations should be discussed with SP and then consideration should be given to reducing transfers from Scotland.

In the case of an Amber alert the Scottish transfer is to be reduced in 100MW blocks, as quickly as system conditions will permit, until the Dynamic Stability Monitor returns back to the stable region. Similarly in the event of a Red alarm transfer is to be reduced in 150MW blocks, as quickly as system conditions will permit, until the monitor indicates the system is stable. Having re-established a secure power transfer, the cause of the reduction in stability should be investigated in association with SP [100].

Following an oscillatory event, the restoration of the original power transfer from Scotland can be resumed if:

- The cause of the breakdown in damping has been determined and the necessary remedial actions taken.
- The amplitude of oscillation has remained within the stable region for at least 10-minutes.

The transfer can then be progressively increased in 50MW blocks at one minute intervals up to the transfer set by planning studies, provided that this does not cause any further alerts or alarms to be generated.

It must be emphasised that planning studies will continue to be used to set the upper limit for transfers from Scotland to England, even if the Dynamic Stability Monitor shows that higher transfers could be accommodated, as transient stability is the binding constraint, rather than damping.

In the future a more economical approach could be taken when operating the link. This would require information from the Scottish TOs and greater experience of PMUs on the GB system. This should then in turn lead to the development of advanced damping applications, such as the WAPOD approach by Stanett in the Nordic system.

In addition, future work has been proposed to employ a phase angle based logic to the operation of the Anglo-Scottish connection [59], as opposed to the existing practice where the link is restricted by transient stability, at a limit of 2500MW.

### **3.6 Concluding Remarks**

In this chapter a review was provided of the existing SM practices at NG. The current approaches, some of which having been in place for up to 20-years, were not deemed suitable to meet the requirements of the evolving network. With growing levels of system variability and complexity, the traditional network assessment approach is deemed to be conducted too far in advance of operations and as such is becoming increasingly unreliable.

Greater accuracy is proposed in terms of real-time system monitoring through the installation of PMUs. The PMUs will also permit massive improvements to offline studies, through the relative ease of collating and time-aligning the data.

However, unlike the power networks in the US, Europe and China, no direct funding has yet been made available for the deployment of PMUs. All implementation is deemed to be part of “business as usual” practices. PMUs have predominantly been provided to the network through the upgrading of DFRs, as part of a bottom-up approach whereby the provision of synchronised data and how it can benefit

areas of planning, operations and eventually control actions, is expected to develop business cases.

It has been suggested that PMUs could provide improvements to a number of existing monitoring practices, through increased data resolution and the added benefit of time-synchronised measurements. The installation of PMUs at the locations specified in [85] would offer a means to combine the SM requirements of DSM, PQ and FATE, this would also provide visibility for ASBMON requirements.

This could result in a potentially large quantity of PMUs, the following would therefore need to be confirmed:

- The data resolution requirements for individual SM applications.
- Identification of communication system requirements for each different SM function.
- Identify the need for and capacity of data storage, either locally, remotely or both, for all SM equipment.

With the increasing connection of HVDC and Wind farms to the network, concern is growing around power quality through increased interactions with the AC system and displacement of system inertia. To that extent much greater knowledge is required over the systems dynamics.

The provision of data from the Scottish TOs is becoming vitally important to securing such future networks, as a large amount of the generation and technology is being installed in this part of the network, increasing the amount of uncertainty around system performance.

It is also suggested that, as European market integration continues to develop, shared PMU data with the neighbouring TSOs of Ireland and Europe may also be required, as the relative security of one system will have increasing impact on the others.

A detailed analysis of the existing PMU deployment and WAMS infrastructure is provided in [Chapter 4](#).



# Chapter 4

## Wide Area Monitoring on the GB System

### 4.1 Introduction

As discussed in the previous 2 chapters, the WAMS deployment on the GB system has not been funded through any large initiatives born out of a series of system incidents, or from any specific system concerns, as has been the case for other TSOs. Moreover, PMUs were installed on the GB system primarily through a series of upgrades to DFRs, in addition to four newly installed PMUs at permitted substations from convenient outages. The initial focus of the PMU deployment was designed to improve dynamic system state monitoring by upgrading the oscillation monitoring system for the control centre.

The existing WAMS can be considered as providing a strictly monitoring role of the transmission network, with no critical emphasis on the need to provide active control to any operational systems. The current PMU deployment strategy can be viewed as a bottom-up approach, whereby the provision of synchronised phasor data and how it can benefit specific areas of planning, operations and eventually control actions, is expected to develop business cases and provide the motivation for more application specific installations. Once reliability and confidence in the

use of PMUs is established on the GB network, applications may then be considered where the data contributes towards control and protection actions to improve the operation of the system, through improved oscillation damping schemes and eventually WAMPAC systems.

In the following chapter the existing WAMS deployment on the GB system is analysed, information is also provided on a University based WAMS initiative comprising PMUs installed at the domestic supply. The future requirements for PMU deployment and WAMS implementation is then discussed, looking at the anticipated number of devices out to 2050 and the realistic short term goals for the GB system. This analysis is based on the system experience of other TSOs globally and the growing requirements and motivation for system monitoring at NG.

## 4.2 National Grid WAMS Implementation

As discussed in Chapter 3, at present only 2 PMUs are used operationally by NG for the monitoring of the inter-area modes of the GB system as a direct replacement of the older dynamics monitoring system. A Psymetrix PhasorPoint (PPP) system was installed as the PDC at the ENCC that is maintained by Psymetrix remotely via a Virtual Private Network (VPN) connection. The PPP is run as a web based application with the intention that it can be accessed from any BLAN connected PC or workstation.

The installed system permits 20 licenses in terms of monitoring nodes, so more than one PMU can be configured to transmit data from a given substation. The PDC was sized to be capable of storing 50Hz data from up to 20 PMUs for a rolling one year period, after this time the data is intended to be archived off at a reduced resolution of 10Hz for up to 10 years in NG's Data Historian (DH).

With the amount of PMUs set to increase on the GB system, as additional DFRs are upgraded and new dedicated PMUs are installed, this represents a growing

challenge in terms of data analysis and storage. In addition it is now of vital importance to capture data surrounding system events as they provide the only reliable source of information on the response of the power system, these events need to be captured at full resolution to assist in inertia estimation methods [30] and continuing validation of the offline network model. Due to the growing volumes of data, importance is therefore placed on timely analysis through fast algorithms and identification of such key system events. An understanding is also required over the necessary resolution of data required for specific SM applications, as outlined in Chapter 2 it would seem logical for PMUs or similar devices capable of providing synchrophasor data to adopt a number of existing SM applications however, data at 50Hz resolution will not be required from every PMU.

### 4.2.1 Data Accuracy and Availability

The initial configuration of the WAMS network infrastructure, was as displayed in Figure 4.1. The PMUs were configured to communicate over TCP through NGs internal BLAN, routed through Multi Protocol Label Switching (MPLS). The devices were connected to the network behind a firewall governed by an Access Control List (ACL), which meant that only PMUs with IP addresses on that ACL were able to communicate through the firewall to the PDC.

This proved to be unnecessarily restrictive following the connection of the first few PMUs, as additional devices were installed with IP addresses that were not on the ACL and consequently could not transmit phasor data to the PDC. This was then further compounded by the RAMM project, which proceeded to change all of the IP addresses at the substations. The ACL was eventually amended to allow IP addresses within a given range to pass through the firewall; governed by the RAMM project this allowed all PMUs access to the PDC. This became increasingly important once all the original 20 licences had been used. PMUs were then added or removed from the PPP based on a perceived benefit to SM, based on a PMUs network location, accuracy and availability of data. This did

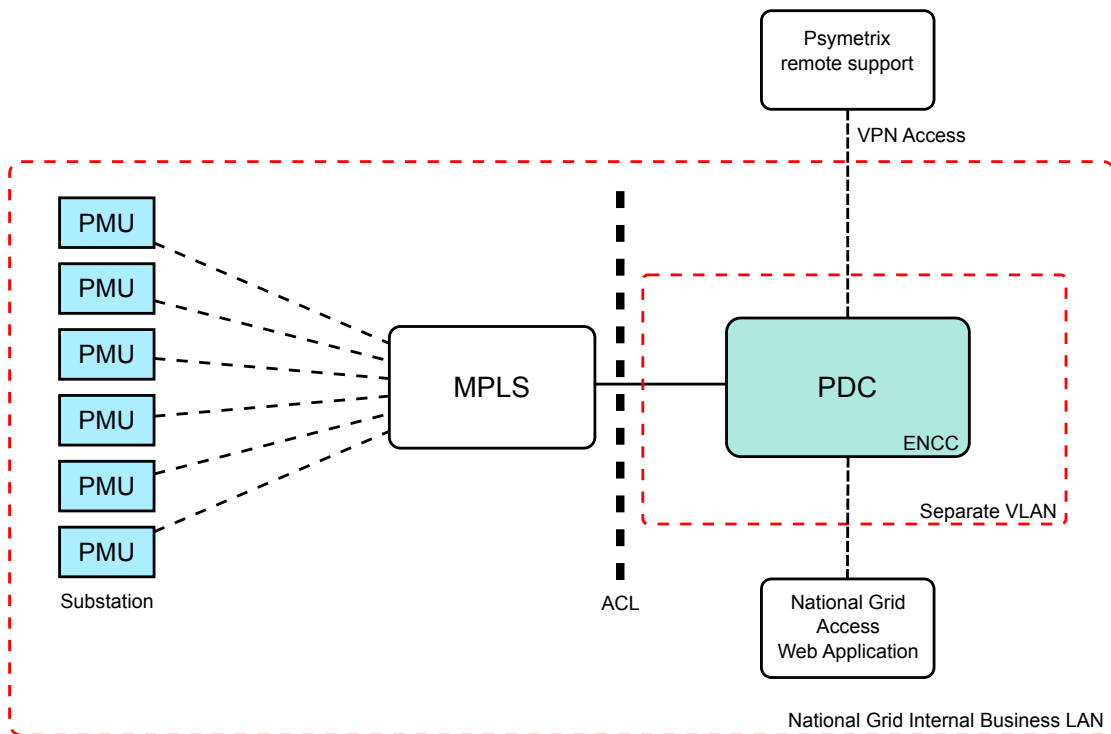


FIGURE 4.1: Initial WAMS network infrastructure within NG's internal Business LAN

also mean that data from some PMUs was permanently lost as a consequence of the limited PDC space.

As can also be seen in Figure 4.1, NG only have access to the Web Application in PPP, no provision was made to give high-level access to the server for means of any network or communications diagnosis. This proved problematic at times, as a number of the PMUs were not reporting data accurately or reliably. The PMUs, as upgraded DFRs could only be accessed for diagnosis purposes through a NG laptop capable of bypassing the BLAN firewall, this proved to be restrictive when adding new PMUs to the network, in terms of fault diagnosis or analysis of the communications infrastructure, as the laptop did not represent the same part of the network or the same environment as the PDC, which was connected on a separate VLAN.

Adding PMUs onto the GB transmission system was not without its challenges; the devices were predominantly added through upgrades to existing equipment and the issues experienced with this process were as follows:

- Out of date firmware versions running on the DFRs, preventing some of the devices from correctly using the GPS time signal and being able to accurately report data in the IEEE C37.118 format. This caused some irregular phase angles to be reported and overall poor data accuracy.
- Incorrect CT / VT ratios setup in the DFRs, resulting in some cases of the devices reporting Voltages and Currents in the mV or mA range respectively.
- Limited means of trouble shooting PMU connectivity and data accuracy.
- Insufficient bandwidth available at substations, resulting in intermittent data availability from a large number of the PMUs.

These issues have resulted in limited PMU data availability, as can be seen in Figure 4.2, the statistics for the month of October 2013 are shown. The majority of the PMUs have well below 90% data availability, with some of the devices being as low as 35%. In some cases the data is missing almost on a packet-by-packet level meaning that large volumes of the data that is received is unusable. This is predominantly as a result of insufficient bandwidth available at the substations. Sites that present relatively consistent data transmission are predominantly unmanned and so the only traffic on the BLAN for the majority of the time will be the PMU data.

A thorough analysis of the existing BLAN infrastructure is required to access the necessary amounts of dedicated bandwidth needed for consistent PMU data availability. The lack of localised PMU storage means that if the bandwidth is not available then the data is lost. This also falls under the wider scope of needing to understand the data transmission and storage requirements of each specific phasor based application.

The result of all these issues has meant that for the majority of the time, consistent and accurate PMU data has only been available from PMUs covering 3 substations, in Blyth, Staythorpe and Langage. These devices are installed in unmanned substations and so there is little if any background traffic on the BLAN.

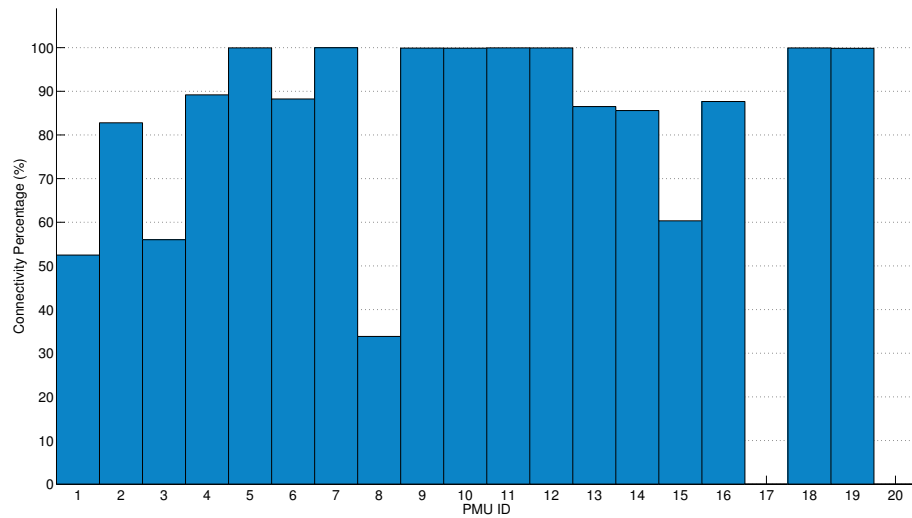


FIGURE 4.2: PMU data availability statistics October 2013

## 4.2.2 Communications Infrastructure Latency

To understand the restrictions and limitations of the existing WAMS communications infrastructure that has resulted, at times, in poor data availability, a small amount of TCPdump [101] data was provided by Psymetrix. This information enabled the calculation of the communications latency between the individual substations and the PDC at the ENCC.

The TCPdump program captures TCP packets at the PDC server and then provides a description of the contents of the packets on a network interface [101].

The file provided covered 10-seconds of data transfer and within it 3000 packets per PMU (10-seconds at 50Hz). For this period there were 6 substations communicating back to the PDC comprising a total of 8 PMUs. The connectivity at the time was as shown in Figure 4.3. All of the Substations had 1 PMU, with the exceptions of Substations 5 and 6, which both had 2. The PMU in Substation 1 was the Arbiter 1133a that sent data packets of 50 bytes, the rest of the devices were the Ametek TR2000 DFRs sending packets of 42 bytes.

In order to calculate the communications link latency two parameters are required to be known in advance, in the time stamp of the original measurement at the

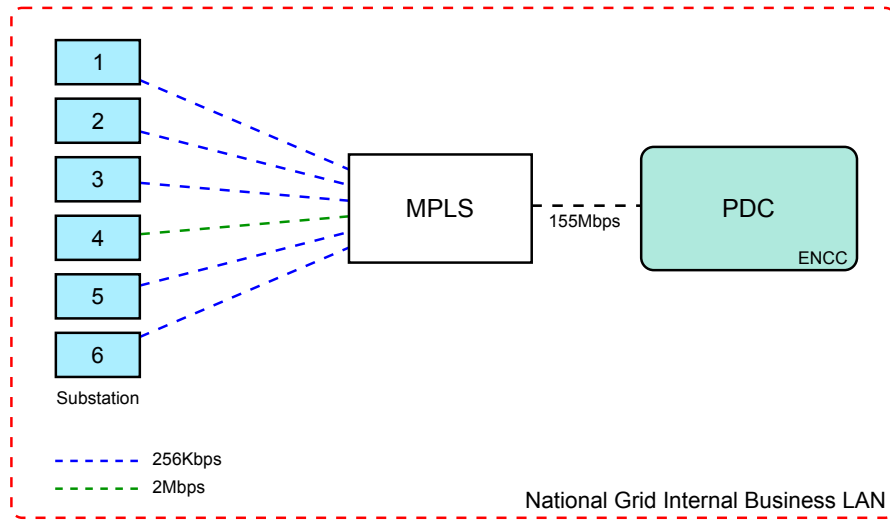


FIGURE 4.3: PMU configuration, NG Business LAN

PMU ( $PMU_{TS}$ ) and the arrival time at the PDC ( $PDC_{AT}$ ).

From [39], the contents of the PMU data packet is well understood. Inspection of the SOC (Second of Century) part of the data packet provides the time-stamp for the instant that the measurement was recorded on the PMU. In fact, the time-stamp comprises an 8 byte message consisting of 4 bytes SOC, 3 bytes fraction of a second and 1 byte time quality indicator. The SOC is the representation of the UTC (Universal Time Coordinated) in seconds, calculated from midnight on the 1<sup>st</sup> January 1970 [39]. In addition, as the PDC server is locked to an accurate time source, the accuracy of the  $PDC_{AT}$  for these purposes should be comparable to the GPS synchronised time of the PMU.

The latency for each PMU data packet can then be calculated as follows [39, 48]:

$$Latency = PDC_{AT} - PMU_{TS} \quad (4.1)$$

However, PMUs from different manufacturers calculate phasors using slightly different methods and with this each PMU will introduce different values of internal delay into the process. It is important to understand the time delay incurred inside the PMU before the data packet is available “on the wire”, as this is not part of the communications latency.

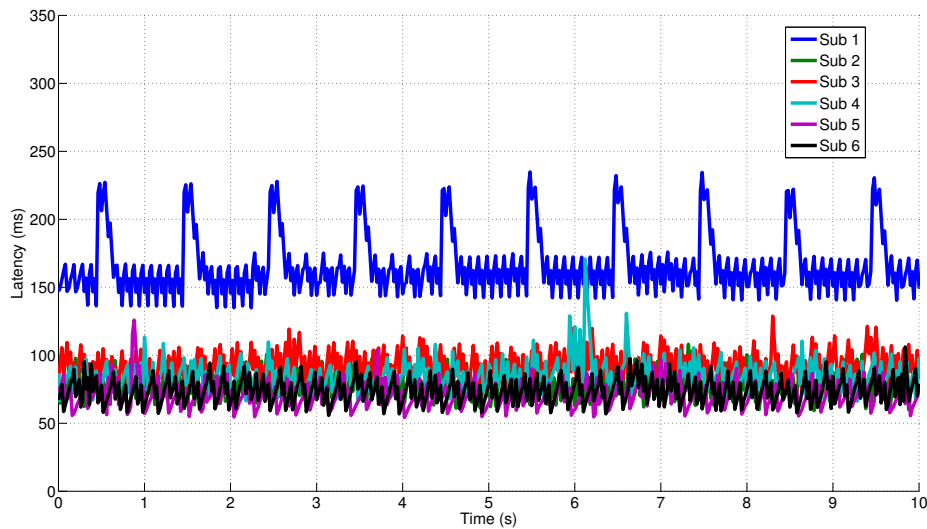


FIGURE 4.4: Network latency for 6 BLAN connected PMUs

The results displayed in Figure 4.4 show the latency as calculated using Equation 4.1 for 1 PMU from all of the 6 substations. In addition Table 4.1 shows the overall statistics for the 10-second period.

The latency varies from 60-230ms and it can be seen that Substation 1 displayed a much higher value of latency than the other 6 connections and there also appears to be some form of oscillatory behaviour visible in the results. This is in part because the internal measurement delay ( $PMU_{MD}$ ) of the PMU has not yet been taken into account. These values are not necessarily considered to be too high for monitoring applications, they are just inconsistent around the network and not as expected given the assumed knowledge of the communications infrastructure

The latency equation can be amended to [48]:

$$Latency = PDC_{AT} - PMU_{TS} - PMU_{MD} \quad (4.2)$$

It is also important to note that Substation 4 is not showing any improved performance from having the larger bandwidth link, in fact, from Table 4.1, it shows the highest latency for an individual packet.



TABLE 4.1: Individual PMU substation latency statistics

Substation	Min	Max	Mean	SD
1	39.88	139.87	71.22	22.08
2	28.89	78.05	48.94	10.13
3	40.59	98.79	62.14	10.90
4	36.17	140.84	54.27	11.50
5	24.22	95.86	40.86	9.26
6	25.76	76.07	43.76	9.09

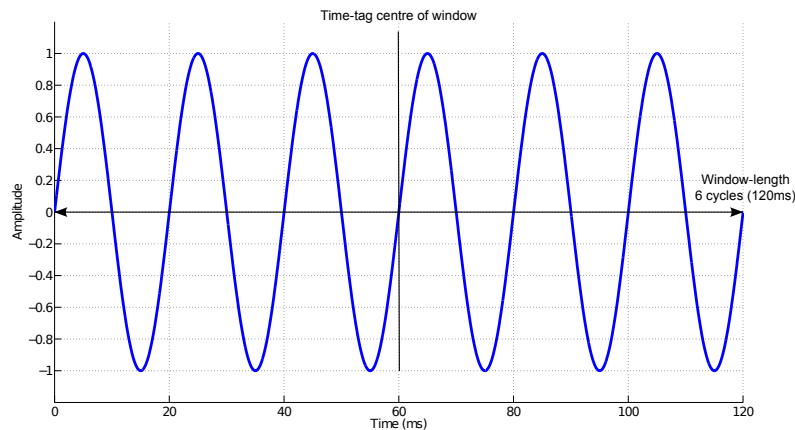


FIGURE 4.5: Arbiter PMU phasor measurement window

#### 4.2.2.1 PMU Internal Measurement Delay

For the Arbiter 1133A PMU the internal measurement delay was calculated based on information from the IEEE C37.118 standard [39] and the manufactureres operation manual [102].

Firstly, the PMU does not time-tag the measurements, moreover it measures synchronously [102]. A phasor measurement is calculated based on a user-definable number of cycles of the 50Hz waveform, in this case the measurement was taken over 6-cycles. The time-tag is placed at the center of this measurement window, as shown in Figure 4.5.

Based on this, a delay is introduced equal to half the measurement window length, as a packet will not be available until the end of the window. This is equivalent to a 60ms delay, assuming the system being measured is at a nominal frequency of 50Hz. If the system is below 50Hz the delay will increase and if the system

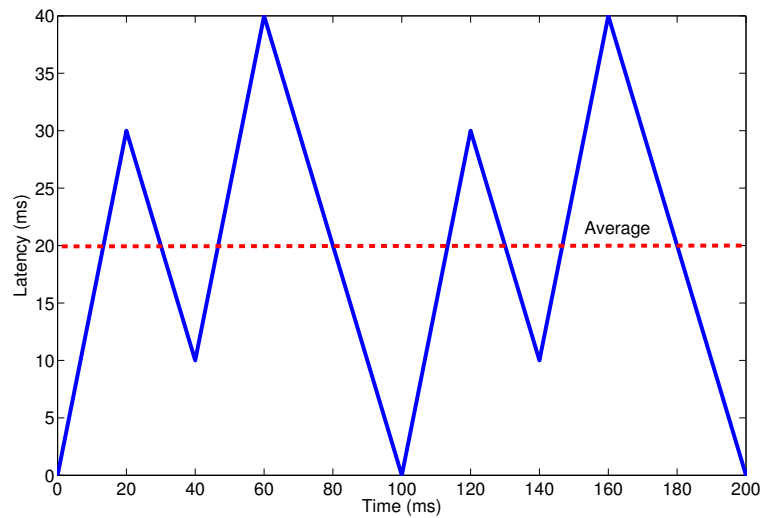


FIGURE 4.6: Arbitrator PMU data acquisition delay

is operating above 50Hz the delay will decrease. Assuming a nominal system frequency this is  $3 \times (1/50) = 60\text{ms}$ .

There is also a data acquisition delay due to the way the arbitrator batch processes the measurements, the results for all measurements are calculated each 50ms, although a phasor estimate update is provided at 50Hz resolution it will be delayed by up to 40ms in waiting for the next data acquisition slot. This is determined for each packet by how far in time (ms) it is from the next 50ms window, as depicted in Figure 4.6. For this analysis the average delay time was taken as 20ms, but it could be as low as 0 and as high as 40ms.

There is also a calculation time, which is stated in the operations manual as 15ms [102] and the data transfer time to the output of the PMU. Considering a packet size for the Arbitrator of 50 octets long and an Ethernet interface that runs at 100Mbps that gives a data transfer time of  $4\mu\text{s}$  ( $50 \times 8 / 100 \times 10^6$ ), which for these purposes can be considered negligible.

This altogether gives a total internal PMU latency time for the Arbitrator of approximately 95ms ( $60 + 20 + 15$ ). It is worth noting that the Arbitrator device, is not optimised for latency [102], moreover the PMU is concerned with the accuracy of measurement process.

Such detailed information was not available for the Ametek device, but the operation manual [103] informs that just one cycle of data is used to calculate the synchrophasor data compared with the 6 cycles used by the Arbiter. It is important to consider the impact the number of cycles used in the measurement has on the accuracy. During steady-state conditions this is less of an issue however, during dynamic conditions if the input parameters are not constant or changing across the time window, achieving a suitable estimate of the true value becomes more complicated for a larger time window and depends upon positioning of the time-stamp within the window [38].

For the Ametek device the time-stamp is at the beginning of the data window allowing for a delay of 20ms. With no knowledge of any data acquisition delay and the fact that the Ametek device is a fault recorder an additional delay of just 10ms calculation time has been assumed. This gives a total internal delay for the Ametek PMU of 30ms.

Taking into account the respective internal PMU measurement delays, the amended calculations for latency are as displayed in Figure 4.7. This is looking at the first 2 seconds of the data transfer, it is difficult to see any difference in the substations at this resolution, but it appears that Substations 5 and 6 present lower values of latency than the other sites. There is also still a significant additional delay of around 60ms introduced by the Arbiter PMU, this occurs every second on the second, so it is assumed to be associated with the GPS time-tag and then goes on to affect the first 5 - 10 samples following the time-tag, as the impact only last around 200ms. This requires further investigation, pending greater amounts of TCPdump data, as it could be specific to the substation and not anything to do with the PMU itself.

In order to get a better view of the individual differences between the substations a weighted moving average based on 30 previous samples, a ratio of 0.06, was applied and is as displayed in Figure 4.8.

Here the differences between the substations can clearly be seen, but are not as expected. Substations 5 and 6 have 2 PMUs installed at each site and only a

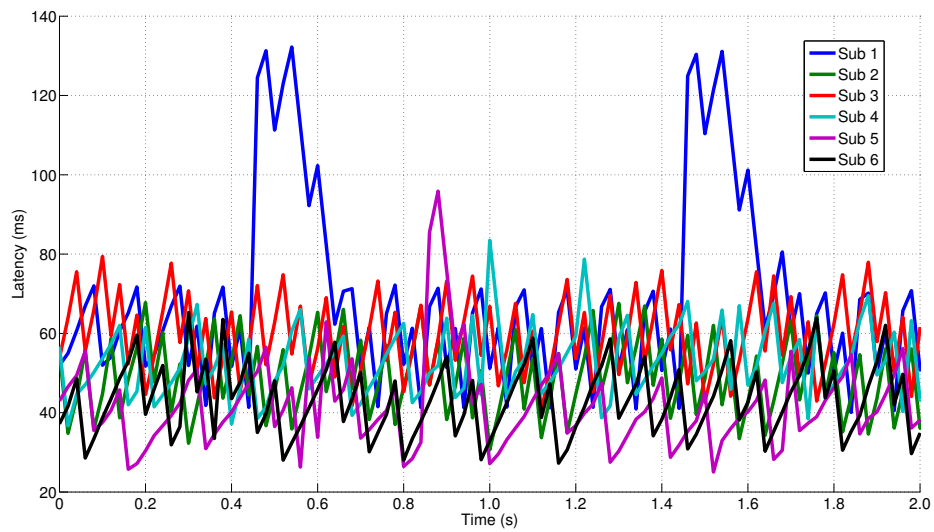


FIGURE 4.7: Network latency for 6 BLAN connected PMUs excluding internal PMU measurement delay

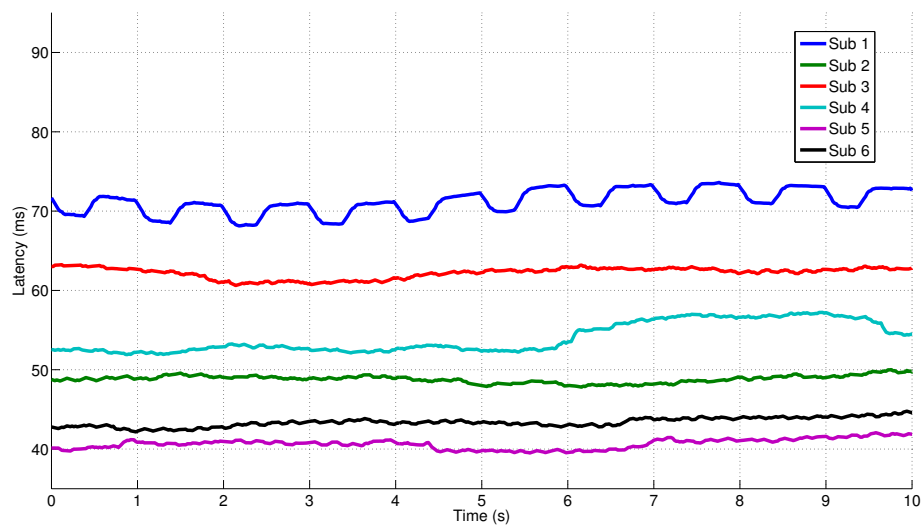


FIGURE 4.8: Smoothed network latency accounting for internal PMU latency

256Kbps communications link, but these substations report the lowest latency values. It has been confirmed by NG that these substations are unmanned and so there is unlikely to be any other traffic on the BLAN from these sites. Whilst Substation 4 is a 2Mbps link and would therefore be expected to yield the best results, this is actually restricted to 512kbps for all traffic and is known to be a manned site so BLAN traffic could potentially be very high at times and therefore a significant factor.

Substation 1 contains the Arbiter PMU, which has some significant internal latency, some of which, is still unaccounted for. This device is however considered to be very accurate in terms of the monitoring data that it reports.

It is important to note that this analysis was carried out on a single sample of 10-seconds worth of data, but a large amount of information can be understood. Further work is required to investigate the links from all substations and how they vary throughout different times of the day and therefore with different amounts of background traffic. A greater understanding is also required over the internal latencies of the PMUs.

The large variability and amount of unknowns surrounding the other traffic on the BLAN from the substations, suggest that the network is not entirely suitable for PMU streaming traffic, unless specific provision could be provided within the BLAN for PMUs. The latency requirements for the PMU communications network would ultimately be defined by the intended data application, the communications latency of 40-70ms presented in this section would be suitable, but it would have to be more consistent.

### **4.3 State Estimator Comparisons**

As described in Section 3.3 the SE has been configured to calculate a load flow every 10-minutes, using data gathered over a period of up to 10-seconds. This combined with the time to converge a solution means the SE output is delayed

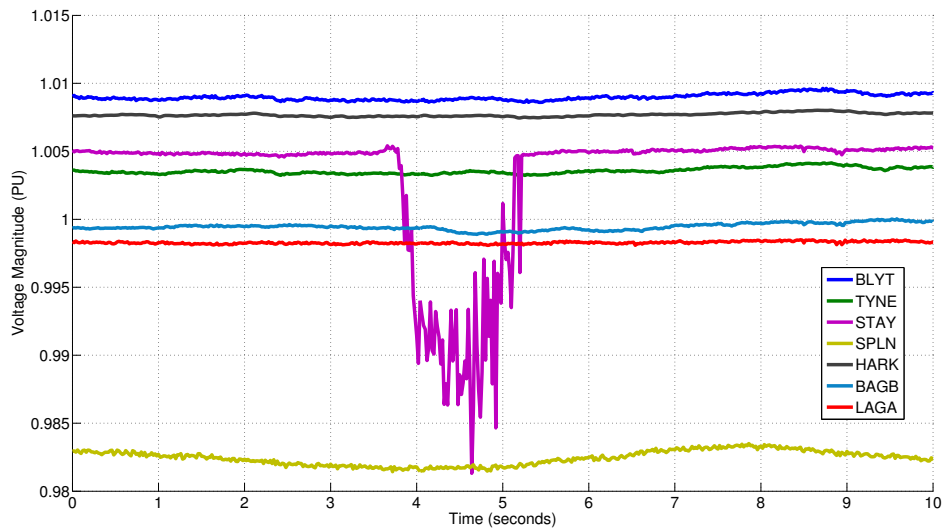


FIGURE 4.9: PU voltage magnitude from 6 PMUs over 10-second window

by about 70-seconds. The file created by the SE estimator is time-stamped from the server, so with this information the 10-second window of data acquisition that the SE is based on can be approximately established. As the SE is static, comparisons with PMU data should then be carried out between this period and a representative value should be acquired from the PMUs [40].

For a given period of 10-seconds the PMUs will have produced 500 phasor estimates ( $50\text{Hz} \times 10\text{s}$ ) and so the issue arises, as to which of these values should be used for comparison with the SE. As can be seen in Figure 4.9, this is fairly straightforward during steady-state conditions, where an average value over the period would suffice. However, as can be seen from the PMU at Staythorpe, where a transient change in voltage due to circuit switching of around 500MW in an adjacent line has resulted in a large variation in Voltage magnitude, this becomes more complicated. If the state of the network for this particular node was to be determined from this data (specifically between 3.75s - 5.25s) a low voltage problem would incorrectly be suggested in the Staythorpe area. An improved estimate of the system would then potentially not be available for another 10-minutes, depending on how often the SE is run.

When combining PMU data into the SE it is considered to be important to highlight incidents such as the above, as they distort the intended steady-state view of the network and should not be used to provide such a view of the system. These incidents should be detected and flagged to operators notifying them as to a change in the network, which should in turn require the SE to be rerun so that the most up to date view of the network can be provided [40]. In addition, an amount of filtering may be required to take into account the effects system oscillations, as this could result in periodic changes in loadflow values.

The data from these incidents is however particularly useful for applications such as the analysis of low frequency oscillations and post-mortem event analysis, as it allows, for the first time, the impact of such events on various parts of the network to be captured, investigated and then compared with the offline model response. Successful isolation of these events can also significantly assist data historian requirements, as these specific system incidents may warrant archiving at a maximum resolution for potential future investigation.

### 4.3.1 Voltage Magnitude Comparisons

The voltage magnitude was compared for 7 PMUs with the corresponding buses from the SE over a 4-hour period, in which a confirmed system incident took place in the form of a generator in the Scottish network producing more than 700MW tripping off. The average PMU value was compared along with the worst-case value, which was deemed to be the value furthest from SE solution, to indicate the complications of combining the PMU data. The results for the PMU at BLYTH, the nearest PMU to the event, can be seen in Figure 4.10.

It can be seen that the PMU values correlate well with the voltage profile from the SE, the difference being around 0.005PU for both the average and worst-case values, except for during the system incident (50-minutes in on the graph) where the difference is greater than 0.035PU with the worst-case PMU value selected. If this sample was taken from the PMU dataset it would lead to a distorted steady-state

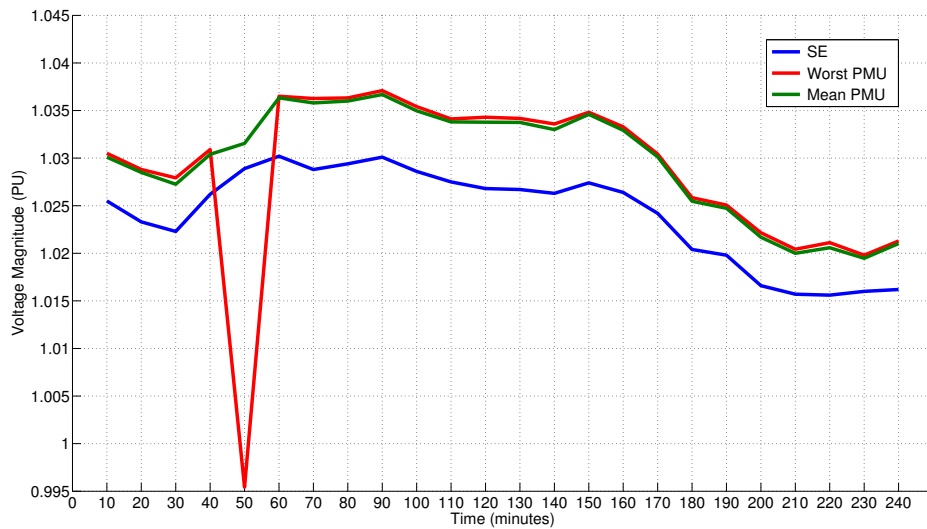


FIGURE 4.10: PU voltage magnitude comparison between BLYTH PMU and equivalent SE Bus over a 4-hour period

view of the network being represented for this bus, showing as a low voltage problem, potentially appearing as an error, when in fact the measurement is completely correct.

The difference between the average PMU value and SE value for the voltage magnitude from all 7 PMUs is shown in Figure 4.11. All of the values would appear to be comparable, with the exception of the PMU at Spalding North, this information combined with the lower voltage reading in Figure 4.9 would suggest inaccuracies on the part of the PMU. Comparisons with SCADA metering have confirmed this to be the case and the DFR was running on an old version of firmware, which has since been amended.

### 4.3.2 Phase Angle Comparisons

When comparing the phase angle the same time frame will need to be considered in terms of data acquisition. In addition a reference phasor has to be selected. The PMUs calculate a local value of positive sequence voltage phase angle that varies according to the frequency of the Bus being monitored. The SE however,



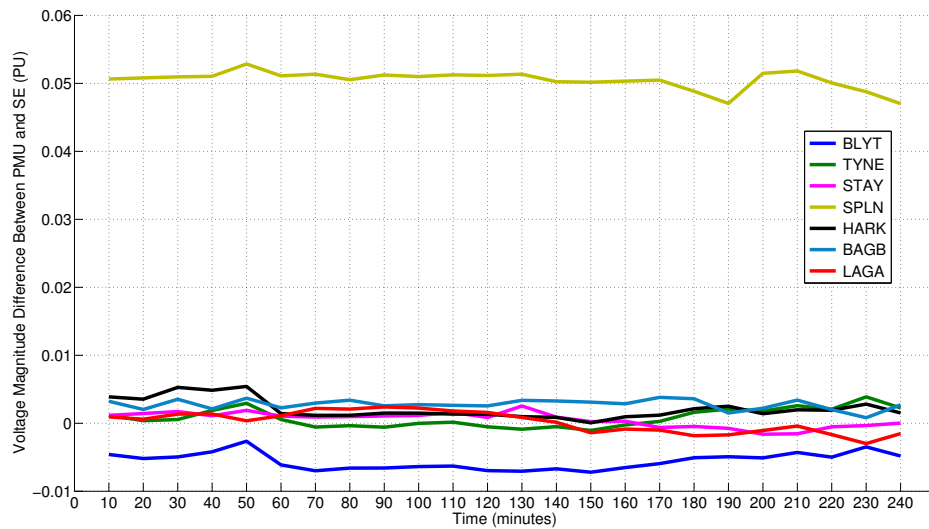


FIGURE 4.11: PU voltage magnitude difference between 7 PMUs and equivalent SE Bus over a 4-hour period

calculates phase angle with respect to a Slack-Bus, which is assumed to be a fixed point and so does not vary.

For the following analysis Harker was selected as the reference bus, as this site contains the only online PMU in the Arbiter device, the others are the Ametek DFRs. All of the phase angle values for the PMUs and the SE, are with respect to the monitoring nodes at Harker, as taken for the PMUs and SE respectively.

In the same vein as with the Voltage magnitude, the comparisons were made between both the average and worst-case PMU values. It can be seen again from Figure 4.12, during a system incident the corresponding transient measured by the PMU, in this case the PMU at Langage the furthest from the event and reference PMU, causes the values to vary wildly, as the incident has excited the inter-area mode of the system, resulting in an oscillation at around 0.5Hz. Then depending on which value in time is selected, the “state” determined, at that bus at least, will differ greatly from the rest of the buses, as transients will be captured across the network in differing magnitudes depending on the distance to the system event.

Comparisons were made with the SE over the same 4-hour period as with voltage magnitude. Figure 4.13 shows the phase angle difference between Langage, the

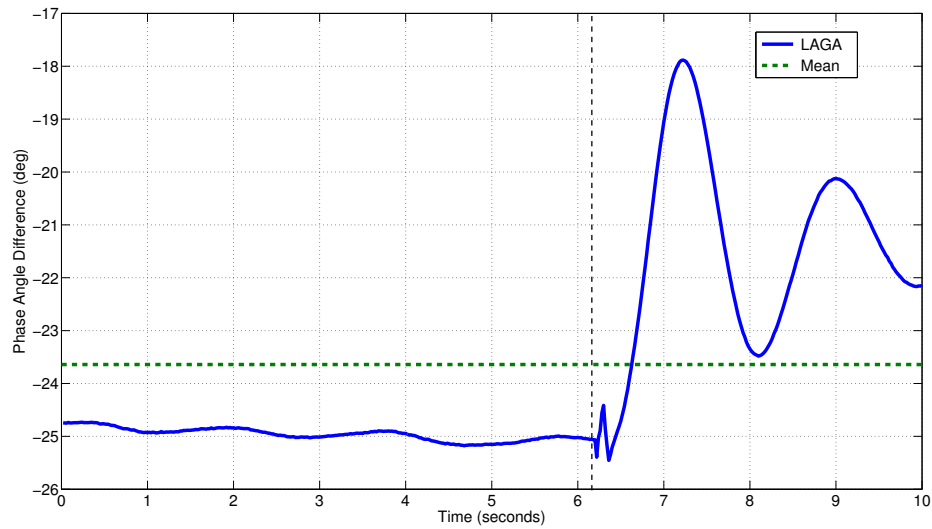


FIGURE 4.12: Phase angle difference between LAGA and HARK, and equivalent SE buses over a 10-second period

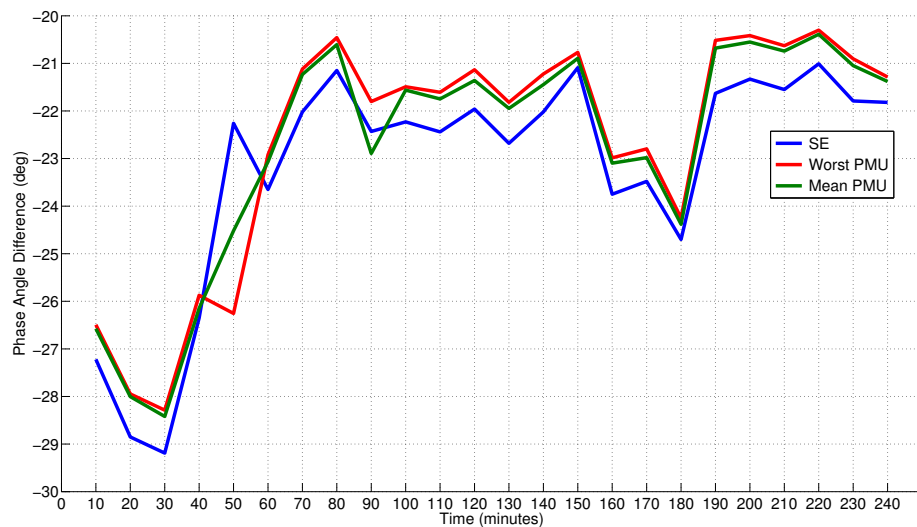


FIGURE 4.13: Phase angle difference between LAGA and HARK, and equivalent SE buses over a 4-hour period

PMU furthest electrically from the event, and Harker. It can be seen that the average PMU value correlates fairly well with the SE value, with the difference typically being about  $1^\circ$ . During the system incident (50-minutes in on the graph) the difference is seen to be around  $4^\circ$ , when the worst-case PMU value is selected.

The difference between the average PMU value and SE value for the phase angle difference from all 6 PMUs is shown in Figure 4.14. The details for HARK are

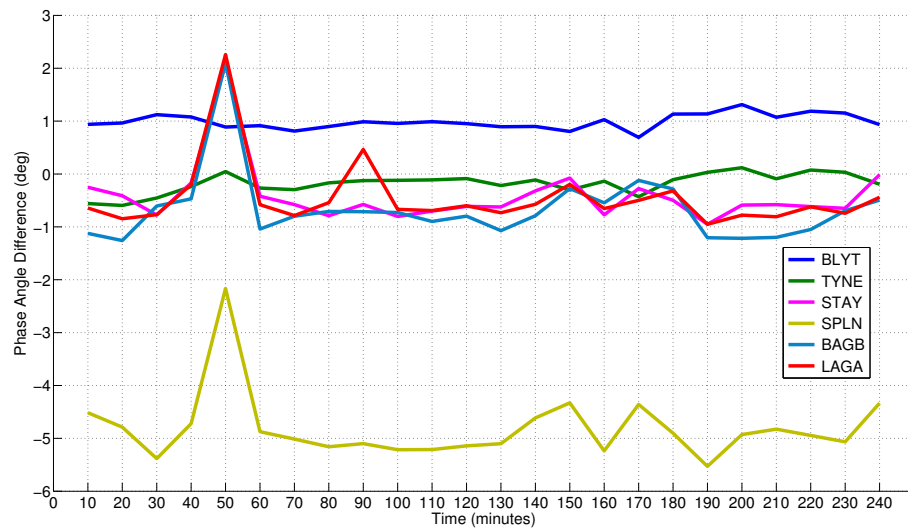


FIGURE 4.14: Phase angle difference for all PMUs, and equivalent SE buses over a 4-hour period

omitted, as this node was taken as the reference value.

The difference between the values would appear to be comparable at about  $\pm 1^\circ$ , with the exception of the PMU at Spalding North that is always around  $5^\circ$  different, this further confirms the inaccuracies with this PMU. The transients captured by the PMUs has a much greater impact to the phase angle difference than to the voltage magnitude, as the average PMU value still shows a large difference in the readings, especially the devices furthest from the reference node.

All of this information is useful to confirm the validity of the PMU measurements and can also point out potential bias in the SE values. The inaccuracies in the SE values are likely to come from the either the lack of metering in a specific part of the network or bad data.

## 4.4 Domestic Supply Based WAMS

The installation of PMUs at the Transmission level can be very costly if substation outages are required. There are also a number of challenges surrounding data access, availability and accuracy. The inclusion of PMUs at the domestic supply

has the potential to alleviate all of these issues through the relative ease of installation, with the only barrier to data availability in terms of communications being the provision of an internet connection.

The provision of phasor data through these means also alleviates the issues of data requirements that are enforced on TOs or generators through either the Grid Code or the System Operator Transmission Owner Code (STC).

With the devices being installed at the domestic supply there is also visibility of local events, as well as at the distribution level. This needs to be considered when looking at the use of such devices to monitor the transmission grid. The devices will also only typically only be able to provide information on system frequency and voltage phase angle, which will either need to be compensated for due to the number of transformers between the voltage levels, which introduce phase-shifts, or taken as a value with DC offset removed, as will be shown in the next section. This could also be confirmed through comparison with SE values, but the exact equivalent bus would need to be determined.

For applications such as event detection, a form of logic will have to be employed to differentiate an event taking place at the distribution level or lower, from one taking place on the transmission system. Depending on the type of event this would be through confirmation of the events visibility at the transmission level from other PMUs.

It should be noted that at this time there is no long term strategy around the use of LV monitoring to further the system visibility at the transmission level.

#### **4.4.1 ELPROS - University based WAMS deployment**

As part of an EPSRC project “FLEXNET” [104], PMUs have been deployed on the domestic supply at 4 UK Universities, Brunel, Birmingham, Manchester and Strathclyde, as outlined in Figure 4.15. The devices are measuring synchrophasor data, in positive sequence voltage (magnitude and phase), frequency and rate of



FIGURE 4.15: Location of Low Voltage PMUs on the GB system

change of frequency (RoCoF), locally at 50Hz. This information is then sent via the Internet to a server in Ljubljana, Slovenia hosted by ELPROS running their WAProtector application [105]. This system gives a good geographical coverage of the GB transmission system with PMUs well distributed across the Scottish to England system, providing visibility over the impact of any system events through the Anglo-Scottish connection [106, 107]. The system also provides access to data from the Scottish network, free from any issues of Gridcode or STC data requirements or questions about data ownership.

An additional advantage of this system being installed on the domestic supply is that the availability of data is not limited by circuit outages or substation works. Once installed the availability of the system is reliant on the communication medium back to the PDC, in this case the local Ethernet connection and the public Internet.

The PMUs in this system are all connected to wall outlet voltages on the domestic supply; these voltages are understood to not provide as high an accuracy of voltage reading as those typically measured by PMUs connected to the transmission level and the measured voltages are also subject to building loads. For these reasons

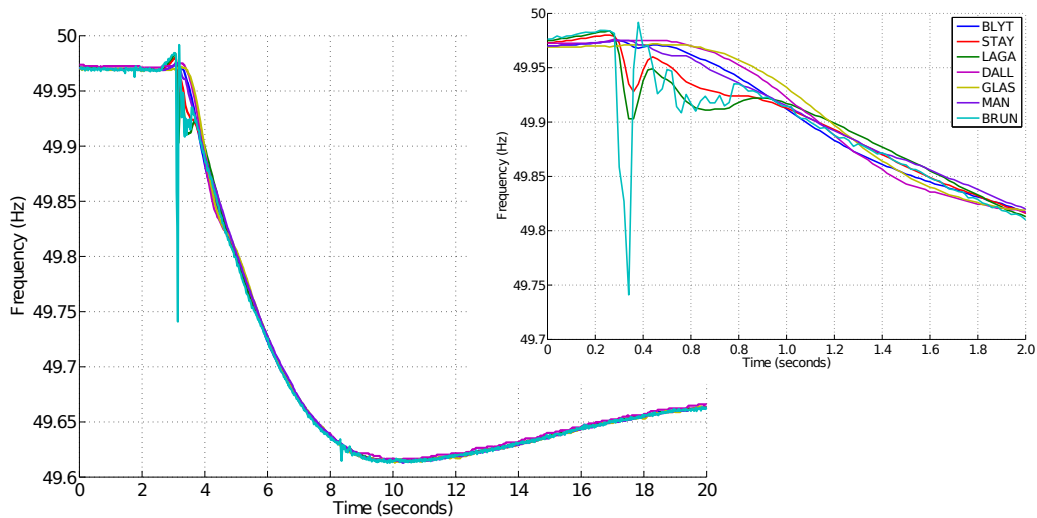


FIGURE 4.16: Generation loss of 1000MW on GB transmission system as measured by 7 PMUs from the transmission system and domestic supply level

comparisons cannot be made in terms of voltage magnitude with devices at the transmission level, a per unit value from the domestic supply would have little meaning and is therefore unsuitable for establishing the voltage profile of an area of the network.

Measurements of system frequency from this system have proved to be vitally important, as can be seen from Figure 4.16 the addition of the 4 extra PMUs provides valuable insight during post-event analysis. The data provides greater visibility of the impact of system events around the network, this will be discussed further in Chapter 6. The system also provides an additional level of redundancy [108], as has proven useful on a couple of occasion when the main NETSO PDC was unavailable and data was required to analyse major system events.

Using information on Voltage phase angle from domestic supply PMUs in conjunction with those at the transmission level is not straightforward due to the number of phase-shifts introduced by voltage transformers between the different Voltage levels, as can be seen in Figure 4.17.

The PMUs from the NG WAMS, Blyth, Staythorpe and Langage in addition to the PMUs from the ELPROS system, with the exception of the Birmingham device, are shown with respect to the reference phasor Harker, shown at  $0^\circ$ . A

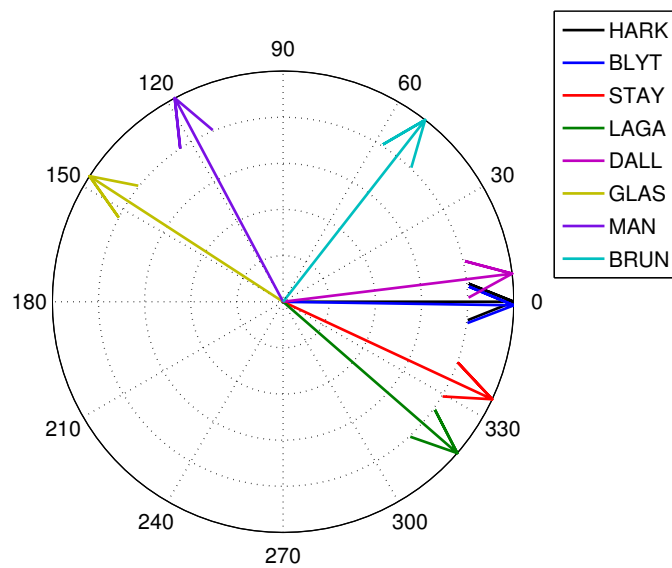


FIGURE 4.17: Phasor plot showing angle difference for NG, SPT and ELPROS PMUs with Harker as reference

small amount of data was also provided from a PMU installed in the SPT WAMS on the Dalmally-Windyhill circuit (DALL), located in a geographically similar location to the Strathclyde PMU in Glasgow.

It can be seen from Figure 4.17 that the angles for the ELPROS PMUs are some way out from the NG PMUs. From this information the Brunel PMU appears to be about  $90^\circ$  -  $100^\circ$  out as it would be expected to show similar values to LAGA. Assuming the PMU at DALL is a good representation of the SPT network near Strathclyde University the GLAS PMU is about  $140^\circ$  out of phase. The Manchester PMU would be expected to be somewhere between the Blyth and Staythorpe PMU so could be anything between  $120^\circ$  and  $140^\circ$  out of phase.

On this basis the ELPROS PMUs can not really be placed on the same phasor diagram as the transmission level PMUs with any useful meaning.

If the DC offset is removed from the phase angle differences then the information can be very useful during post-event analysis, as the separation of the different parts of the network can be seen to vary during an event. Figure 4.18 shows the separation of the phase angles from all of the 7 PMUs, for the 1000MW loss event

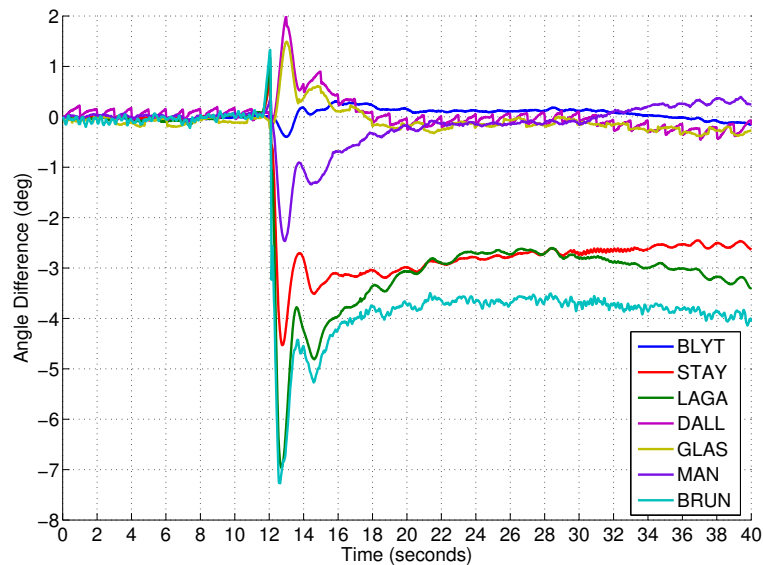


FIGURE 4.18: Angle difference minus DC offset for NG, SPT and ELPROS PMUs with Harker as the reference

of Figure 4.16. At this level the ELPROS PMUs provide additional insight as to the response from different parts of the network to generation loss. It can now be seen that the PMUs at Langage and Brunel show similar results with the phase angles both increasing by around  $7^\circ$ , in the same way as the PMUs at Dalmally and Strathclyde now show much more comparable values. In addition the phase angle difference at Manchester is now, as expected from its position in the network between the PMUs at Blyth and Langage.

The location of all of the PMUs and their relative connections on the GB system can be seen in Appendix A.1.

#### 4.4.2 FNET

In addition to the PMU installed for the ELPROS project, Brunel University have also joined the FNET project and have installed an FDR device that sends data via the public Internet to a server at the University of Tennessee. The FNET system offers a method of event detection and source location through a patented



triangulation method [57] however, additional monitoring equipment would be required on the GB system to achieve this.

The provision of FDR data from other GB institutions such as those involved in the ELPROS project would provide some interesting comparisons. These domestic supply based WAMS also provide an additional level of redundancy for the NETSO in terms of SM, these devices can further the visibility of the system during post-event analysis and improve online situational awareness.

## 4.5 Future WAMS Requirements

The requirements of the future WAMS of the GB network need to be considered as the second stage towards the ultimate goal of WAMPAC. The existing WAMS, considered as the first stage, has evolved beyond its initial requirements to improve the oscillation monitoring system for the control room. The data provided by PMUs is now becoming vital to the GB system, as a means to understand the growing challenges posed to the NETSO as the transmission system develops, not least of all the issues that are arising as a result of the reduction in system inertia and the consequent impact to stability and system security. To that extent the PMUs are now required to be integrated within a robust and scalable ICT infrastructure to ensure the continued availability of data for the now vital analysis of all transmission network events [30].

A key requirement moving forward is the provision of data from the Scottish part of the network, as this will provide greater visibility of the inter-area modes of the system and should lead to a more economic operation of the prominent constraint boundary (B6) [59]. This will also provide vital information during post-event analysis, as will be covered in greater detail in Chapters 5 and 6.

Based on the experience of other TSOs, as discussed in Chapter 2, a typical period of 3-5 years is required to establish the key benefits of PMUs on the network. It is felt that the GB system still requires a period of time to gather a sufficient amount

of accurate and reliable PMU data to be able to build suitable business cases to develop future applications, or to inform application specific device installations.

The following are considered to be important changes necessary to the existing WAMS implementation to improve both the availability and accuracy of PMU data:

- High level access to PDC server, to permit troubleshooting of PMUs and to be able to carry out a detailed assessment of the communications infrastructure.
- Commissioning procedure for PMUs to insure correct installation and accuracy of data, as confirmed over the IEEE C37.118 protocol.
- Identification of vital monitoring nodes where redundancy is required in terms of additional monitoring devices and the provision of local storage.
- Either a dedicated portion of bandwidth through the existing communications infrastructure or a SM specific communications network is required.

The number of PMUs on the GB system, as visible by the NETSO, is expected to grow from the existing 40 in 2014 to anywhere between 100 and 300 by 2020. This is dependent on the rate at which the existing DFR equipment is upgraded, located as shown in Appendix B, and the rate of installation of the new PQ devices with synchrophasor measurement capabilities, as mentioned in Section 3.2.4. The availability of data from the Scottish TOs will also be significant in determining the total number of PMUs visible by the NETSO [59].

At present Scottish Power have around 10 PMUs, which is expected to rise to 15 by 2017 and Scottish Hydro, although currently have 0 PMUs could have 5 by 2017 [59]. In addition there are in excess of 100 installed DSM devices that could offer PMU capabilities to the Scottish transmission system.

The main challenge then comes in providing the necessary ICT infrastructure to support the growing volume of devices and in storing the potentially massive volumes of data.

### 4.5.1 Data Storage Requirements to 2050

In order to consider the potential data storage requirements for PMUs out to 2050, in line with the objectives of the e-Highways 2050 project [18], 4 scenarios will be considered based on PMUs monitoring all of the transmission circuits by 2050.

The initial data requirements for the NG PDC was to provide storage for 20 PMUs at 50Hz resolution for 1 year. Assuming a data packet size based on the Arbiter PMU [102] of 50bytes, the storage requirements equate to approximately 1.43TB a year ( $50\text{bytes} \times 50\text{Hz} \times 60\text{s} \times 60\text{mins} \times 24\text{hours} \times 365\text{days} \times 20\text{PMUs}$ ). The data was then to be archived off at 10Hz resolution for up to 10 years in a separate historian system, equivalent to 0.286TB a year for 20 PMUs.

On this basis the minimum total storage requirements for 20 PMUs over 10 years is a rolling storage of 1.43TB with an archived storage facility requirement for the additional 10 years of 2.86TB ( $10 \times 0.286\text{TB}$ ). It is important to note that this does not account for the additional storage requirements of data captured surrounding system events, which would be stored at 50Hz.

The present number of PMUs installed on the transmission system of England and Wales is 40, if the ICT infrastructure was in place for all devices and the data was stored at maximum resolution, then the storage requirement would be double the existing capacity. The existing devices have been installed or upgraded over the past 3 years, at an average rate of 13.33 a year ( $40/3$ ), making the assumption that this rate continues on a linear progression, the total installed number of PMUs on the transmission system of England and Wales would be 520 by the year 2050, as shown in Figure 4.19.

This is considered to be a relatively fair assumption for the first scenario, as there are currently 513 circuits on the NGET transmission network [11] and this would allow for all these circuits to be monitored by 2050.

The corresponding storage requirements, assuming 50Hz data is required for 1 year and then data is archived off for up to 10 years at 10Hz, are provided in

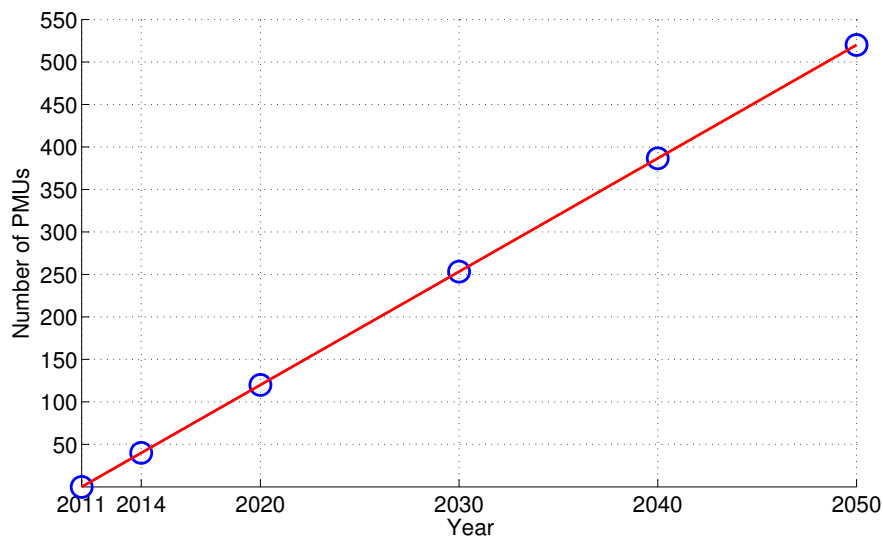


FIGURE 4.19: Anticipated number of installed PMUs with linear progression out to 2050.

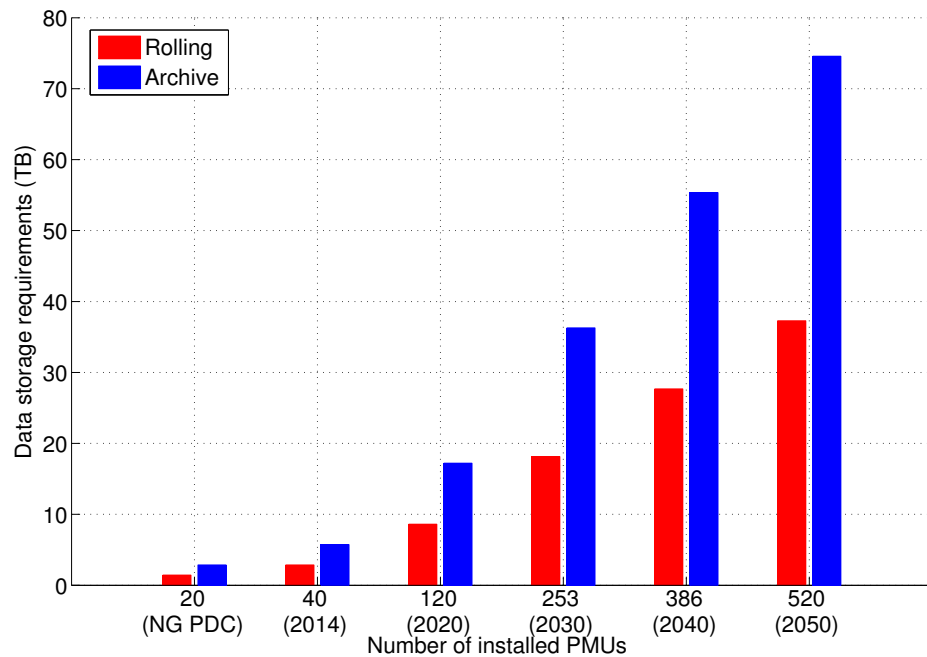


FIGURE 4.20: Data storage requirements for increasing volumes of PMUs linear progression

Figure 4.20. It can be seen that by 2050 a total of over 110TB of storage would be required from around 35TB rolling and 75TB for archived data.

The second scenario considers the developments to the transmission system by 2050. A number of new circuits will have been built and commissioned, as a result

of the increased penetration of renewables and the anticipated rise in electricity demand. From NGs latest Electricity Ten Year Statement (ETYS) [11] the planned network developments on the NGET system by 2024, is in the order of 50 new circuits, this is in line with an increased generation capacity based on the Gone Green scenario, as shown in Figure 1.1, of about 40GW from 2014. The generation capacity, based on this scenario, is then expected to increase by another 40GW by 2035.

To project these figures out to 2050, it is assumed that this rate of approximately 50 new circuits per 40GW of generation capacity every 10 years will continue, and on this basis an extra 5 circuits would have been commissioned every year from 2014 to 2050. The projected increase in the number of PMUs to monitor all of these new circuits is 180 by 2050 ( $5 \times 36$ ), making a total of 700.

In a separate scenario the availability of data from the Scottish TO's should also be taken into consideration. One of the objectives of the VISOR project [59] is to combine data from all 3 TO's of the GB system to improve the overall operation of the network. With this in mind the additional anticipated 20 PMUs of this project from the Scottish network would increase the number of PMUs visible to the NETSO by 2017 to 100, from the original 80 assumed in the linear progression scenario in Figure 4.19. In line with the linear progression scenario for NGET, to project the potential number of PMUs available by 2050, consider the total number of circuits on the GB transmission system at present of 1070 [11] that could be monitored.

For the final scenario, in the same vein as before if the number of new circuits out to 2050 for the whole GB network are considered, based on the current projections from [11] then SPT are due to commission 44 and SHE are due to commission 122 new circuits by 2024, carrying the previous assumptions forward, this is a rate of approximately 22 new circuits every year ( $(50 + 122 + 44) / 10$ ).

The projected increase in the number of PMUs now to monitor all the circuits for the whole GB transmission system, is an extra 792 ( $22 \times 36$ ) taking the total to 1862 by 2050. The projections for all 4 scenarios are shown in Figure 4.21

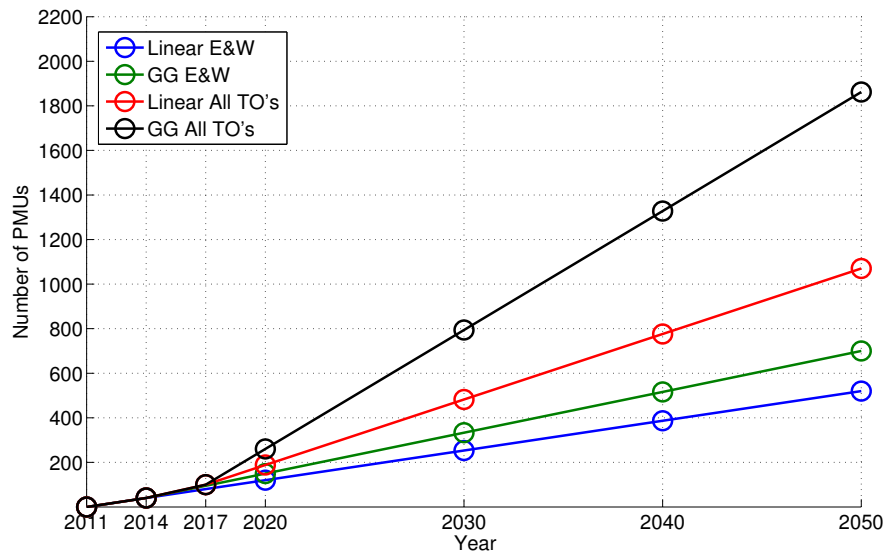


FIGURE 4.21: Potential number of installed PMUs by 2050 based on 4 scenarios.

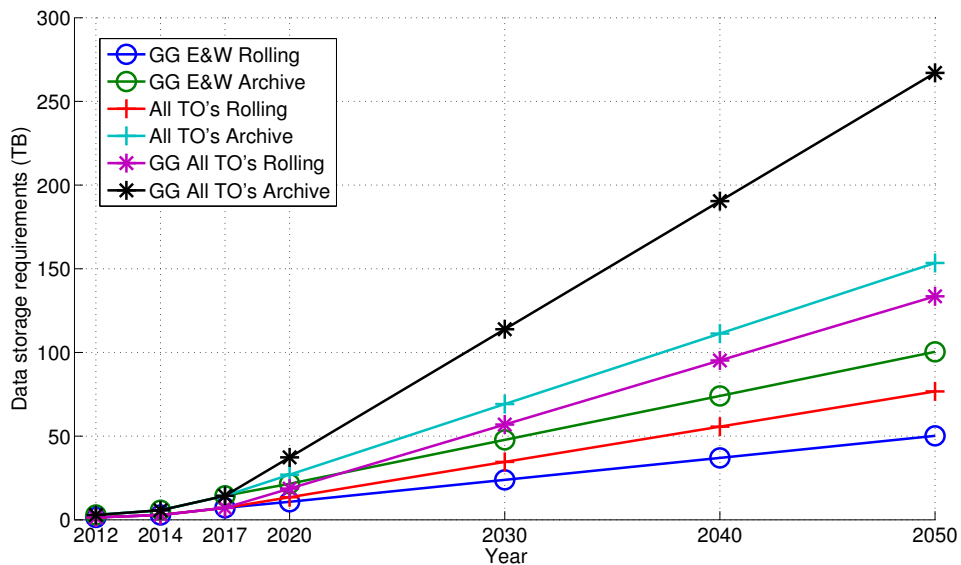


FIGURE 4.22: Data storage requirements for increasing volumes of PMUs with all circuits monitored by 2050

The implications for the storage requirements of the PMUs based on the additional scenarios is as shown in Figure 4.22. This is not necessarily considered to represent a problem to the TO's or even the TSO, but it is considered to be large increase in data in comparison with typical SCADA requirements.

In addition to the increased requirements on data storage, the growing volumes of PMUs will continue to overload the BLAN resulting in higher values of data

latency and an increase in the loss of data. Going forward as the data from PMUs becomes increasingly vital to the operation and planning of the GB network, either a dedicated portion of an existing network will need to be provided to ensure the reliability of the data transmission or a specific SM communications network will be required.

The communications requirements for any future WAMPAC applications on the GB system will need to be designed to comply with the existing requirements of the protection systems, taking note of the fact that faults need to be cleared within 80ms. This may require a large amount of investment into the communications infrastructure for PMUs of which significant benefit to the operation of the network would need to be demonstrated. In the interim applications looking at WAPOD, based on the experience of the Nordic system that recommends figures of around 30ms [76] for oscillation damping applications are more achievable.

## 4.6 Concluding Remarks

In this chapter the existing WAMS of the GB transmission system was analysed. The method of comparing the voltage magnitude and phase values of the PMUs with the GB SE was demonstrated. This served to both validate the data from the PMUs and also further highlighted some measurement errors with one of the devices. The comparison was confirmed as being straightforward during steady-state operation and it was outlined that the presence of a system event should be used as a trigger to re-run the SE so that the most up to date view of the network can be provided [40].

An analysis was also provided of the communications infrastructure of the WAMS network in the NG BLAN and it was concluded that this would only be suitable going forward if a dedicated proportion of the LAN could be reserved for SM. Monitoring nodes that are identified as vital to the operation of the transmission system should potentially be equipped with localised storage so that in the absence of sufficient communications the data is not lost. The requirements for the future

volumes of data storage was also considered out to 2050, based on the assumption that all circuits would need to be monitored. The potential for massive volumes of data also highlighted the necessity for fast acting event detection algorithms capable of analysing massive datasets.

The ability of a University based WAMS network to monitor the transmission network was discussed and demonstrated to provide greater visibility and insight to applications concerned with post-event analysis. The data was shown to provide greater insight into the response of the network to system events, through the provision of frequency and voltage phase angle difference data.



# Chapter 5

## Event Detection and Big Data Analytics

### 5.1 Introduction

As a result of the growing complexities in power systems from the increased integration of renewable generation sources and the networks ongoing expansions, it is now vital that data surrounding power system events, such as generation losses, are accurately captured [29, 30]. These events provide the only reliable source of information on the true power system dynamics, providing a means for greater understanding of system inertia, something that is of growing concern on the power system of Great Britain (GB). Timely analysis of these events is critical to understanding the necessary generation response and reserve requirements for a secure network and also permits the analysis of any trends in the behaviour of the power system under different operating conditions, providing a means to validate or improve offline system modelling tools.

Importance is therefore heavily placed on the provision of time-synchronised, accurate frequency measurements that are now vital for this analysis. To that effect, the inclusion of PMUs in the transmission system of England and Wales, with their high-resolution measurements and improved accuracy of data, is providing

greater detail on the dynamic behaviour of the power system in both real-time and during post-event analysis.

The increasing number of monitoring devices being installed in the power system is however, leading to rapidly growing volumes of data, there is therefore an increasing need for efficient and scalable algorithms, to analyse these datasets in a timely manner. This will serve to assist network operators in online time-scales and provide a more efficient approach to the analysis of the massive datasets in the offline post-event space [109]. This analysis can also assist in understanding DH requirements in terms of data storage, as already outlined, information pertaining to transmission system events should be archived at maximum resolution for the benefit of any future analysis. In addition any erroneous datasets also need to be flagged and removed.

In this chapter a novel event detection methodology based on Detrended Fluctuation Analysis (DFA) is described and presented [40]. The method provides a basic means of event source location and also determines the exact start time ( $t = t_0$ ), which is deemed to be vital to inertia estimation methodologies [29, 30]. The method also determines the suitability of a transmission system event to provide an estimate on the total inertia of the power system, with the key requirement on this being the confirmation of the instantaneous nature of the loss. The approach is then further expanded to be parallelised for the use on massive volumes of PMU data and with this an introduction to Big Data analytics is provided and the implementation of the Parallel DFA (PDFA) approach is presented in the MapReduce programming model.

## 5.2 Detrended Fluctuation Analysis

As described in Chapter 4 a method is required to detect for portions of data captured by PMUs deemed unsuitable to determine the steady-state of the network. A method is proposed that uses DFA [110] to identify any transients captured by the PMU data, indicating either gross measurement errors or that a system

incident has resulted in a transient change in voltage magnitude or phase angle. A gross measurement error would typically just be isolated to individual PMUs and be frequently occurring, whereas the presence of a system event would be captured by all PMUs just in varying magnitudes determined primarily by the electrical distance to the event. A figure of uncertainty can then be established based on the fluctuations present in the measured data. The lower the value of fluctuation, the greater the confidence in the measurement from a given PMU.

Previous works on detrending power system data [111, 112], have focused on removing trends or denoising power system data for the purposes of processing transient oscillations, this is separate from the work implied here. The purpose of detrending the data for this application is to highlight the specific changes in the PMUs measured values as a result of captured transients on the network; the process has the effect of filtering the normal variations in the signal that are predominantly a feature of the high resolution measurement, placing the focus on large changes over a very short time span. It is also possible that dynamic incidents on the network such as the presence of oscillations could cause large fluctuations in the data and these would also be captured.

### 5.2.1 The DFA Algorithm

The DFA algorithm is used to extract “extrinsic fluctuations” present in a signal in order to allow the analysis of the signals “normal” variability. The first step to implementing the DFA algorithm is the integration of the original signal  $x$ , employed to remove any DC offset, Equation 5.1.

$$y(k) = \sum_{i=1}^k [x(i) - \bar{x}] \quad (5.1)$$

Where  $k$  is the sample number of the original signal and  $\bar{x}$  is the average value of the signal over the period  $i = 1 \rightarrow k$ . The integrated signal,  $y(k)$  is then divided up

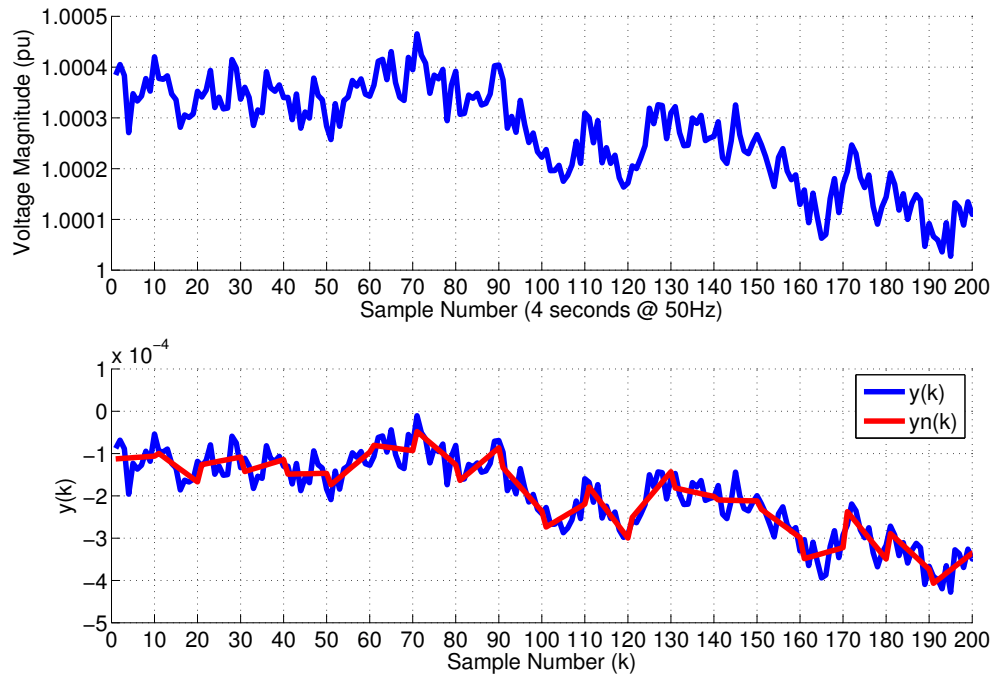


FIGURE 5.1: Data captured by a PMU over 4 seconds (200 samples at 50Hz). The integrated signal  $y(k)$  with vertical dotted lines representing a box size of  $n = 10$ , the solid red line segments representing the estimated “trend” in each box from a linear least squares approximation.

into multiple windows or boxes of a selectable length  $n$ . A least squares first-order linear approximation is then calculated for each of these boxes and this represents the “trend” of that segment of the signal.

In Figure 5.1 the top graph shows the original signal  $x$ , in the voltage magnitude data as measured by a PMU over a 4 second period. The bottom graph shows the integrated signal and a box of size  $n = 10$ , has been selected to illustrate the detrending process. The trend of the individual signal elements,  $y_n(k)$  can be considered as an approximation to the integrated signal  $y(k)$ .

The next step is to detrend the integrated time series  $y(k)$  by removing the local trend  $y_n(k)$ , for each box by subtracting it:

$$e(k) = y(k) - y_n(k) \quad (5.2)$$

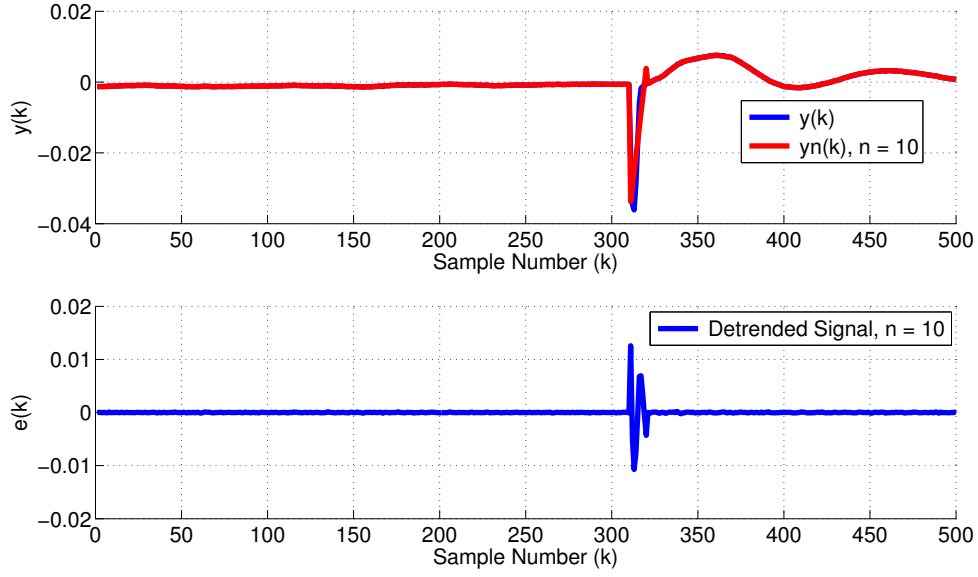


FIGURE 5.2: The integrated time series and the “trend” shown in red based on a box size of  $n = 10$ . The detrended signal has the affect of almost filtering out the “normal” portion of the signal, focusing on the captured transient

The detrended signal  $e(k)$  is now considered as the approximation error. An RMS fluctuation of Equation 5.2 is then calculated by:

$$F(n) = \sqrt{\frac{1}{n} \sum_{k=1}^n [e(k)]^2} \quad (5.3)$$

Where  $N = 200$  and is the total number of samples in the original signal, for 4 seconds of PMU data at 50Hz. Through careful selection of the box size  $n$ , the value of fluctuation calculated in Equation 5.3 can then be used to determine the presence of an incident or gross measurement error captured by the PMUs. The greater the value of  $F$ , the higher the variance in the signal and therefore the greater the captured transient or data error. It should be noted that the value of  $n$  will differ depending on the sampling frequency of the captured data. ncreasing the sampling frequency will result in a larger box size as additional data samples have to be included for the same time period. Conversely a reduced sampling frequency could result in the event not being detected, as the transient state may not be captured in the measurements.

For this analysis a box size of  $n = 10$  was selected to highlight any transient changes occurring over 10 samples, either through a captured system event or gross measurement error. It can be seen in Figure 5.2, this box size has the affect of almost filtering out the minor fluctuations in the rest of the “normal” signal, focusing on the actual transient itself. The corresponding value of fluctuation is then based predominantly on the transient, so the larger the value of  $F$ , the greater the measured transient on the network. Through comparisons with other PMUs this will enable the approximate location of the incident to be determined, as the PMU nearest the event would report the largest value of fluctuation.

The DFA analysis was carried out over the same time period as the example of Figure 4.16, to confirm the visibility of the 1000MW generator trip. The results are displayed in Figure 5.3, using phase angle difference data with the PMU at Harker as the reference. The event is clearly detected, with the varying magnitude of the fluctuation  $F$  indicating the proximity to the loss, with the PMUs at Brunel and Langage detecting it in the greatest magnitude the event is clearly in the South of the network, the larger value at Brunel would suggest its the closest monitoring node to the event. In this instance the loss was in the interconnector to France to the South East of the GB system.

The process also facilitates the use of PMUs from different voltage levels, through the inclusion of the devices from the University network, as the DC offset is removed as part of the DFA algorithm, the phase angles of the domestic supply devices is accounted for.

Even localised events will be detected to some degree all around the network, although in the Phase Angle difference, as can be seen in Figure 5.4 where circuit switching of approximately 200MW on one of the Staythorpe circuits is detected by DFA. The left plot shows the Voltage Magnitude results, where the event is only shown at the Staythorpe PMU, the right plot shows the visibility of the event in the Phase Angle difference at Langage as well.

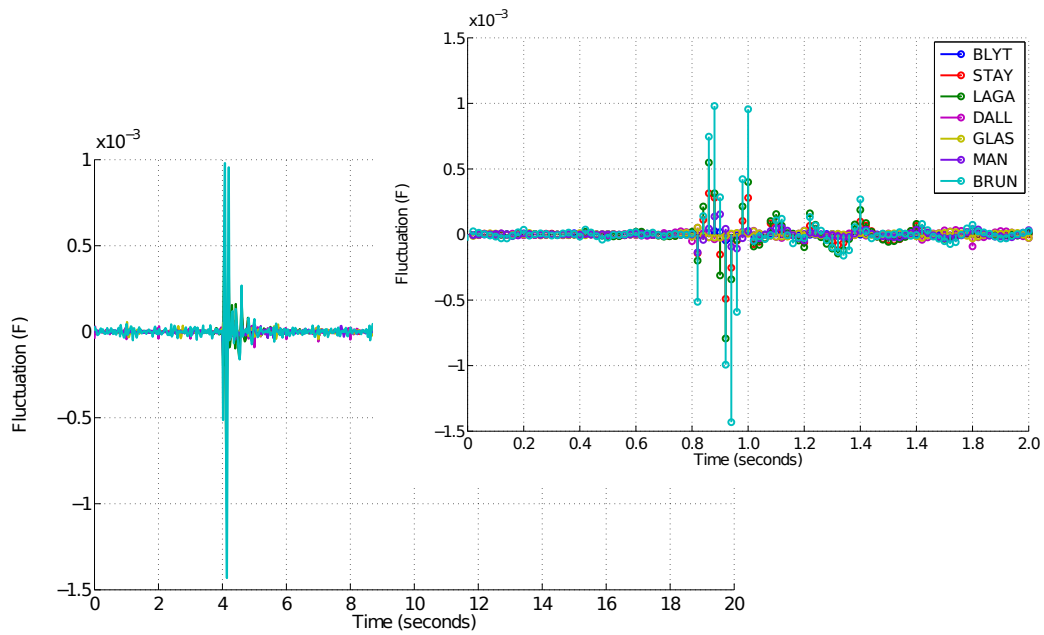


FIGURE 5.3: DFA on phase angle difference from NG, SPT and ELPROS PMUs

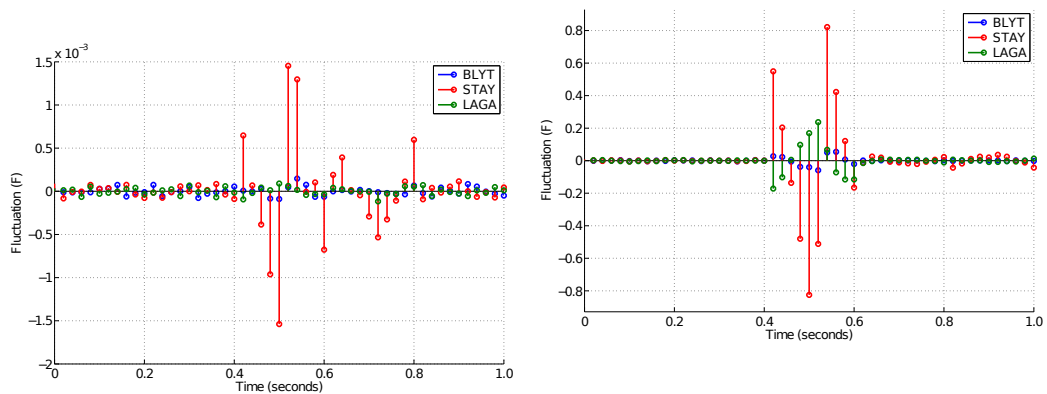


FIGURE 5.4: DFA on voltage magnitude (left plot) and phase angle difference (right) for a localised event at Staythorpe

### 5.2.2 DFA Exact Start of Event and Baseline Analysis

There is an increasing requirement to analyse generation loss events, as they provide the only opportunity to analyse the true dynamics of the power system and the corresponding response of various parts of the system [30]. The primary application being to estimate the inertia of the power system, as will be detailed in Chapter 6.

A loss of generation will cause the system frequency to fall at a rate proportional

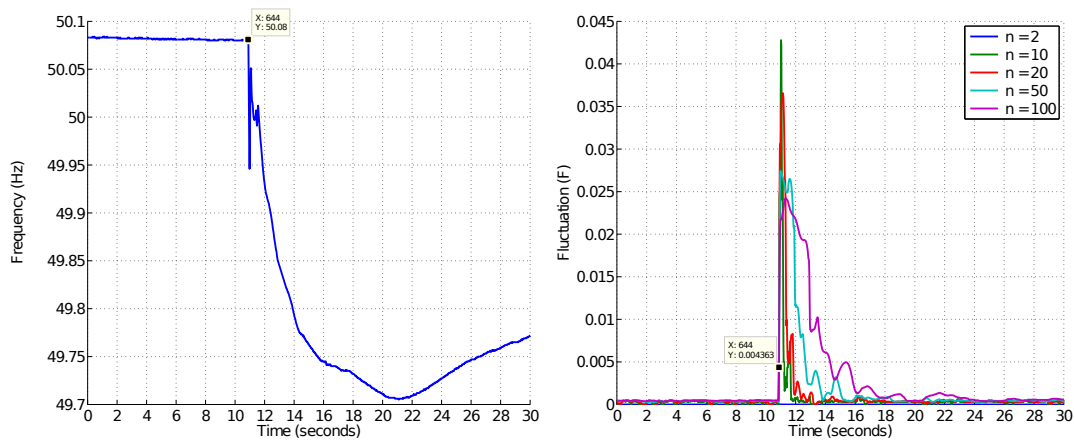


FIGURE 5.5: Frequency trace following a 1000MW generation loss from a local monitoring node (left plot). The corresponding DFA with varying box size (right plot)

to the size of the loss relative to the amount of inertia present in the power system. It is important to note that for the application of inertia estimation this has to be an instantaneous loss of generation through breaker action, so as the system experiences a moment of “free-fall” limited only by the inertia of the system [30]. In addition, in the case of a loss of plant made up of several generators, the loss could be staggered, which could pose issues when determining an accurate value on the size of the loss from SCADA measurements. As will be demonstrated in Chapter 6, the exact start time of the event ( $t = t_0$ ) is also vital to determining accurate values on the state of the power system at the time of the loss.

Using the DFA method two parameters have to be determined to achieve an accurate detection, in the box size  $n$  to divide the dataset into before detrending and the threshold value that signifies the start of an event. The method also needs to take into consideration the measured transients that will be present in the frequency following the generation loss, as these may affect the determination of the exact start time.

The graphs of Figure 5.5 show, on the left plot, the frequency trace following a generation loss of 1000MW, as measured by a PMU local to the event. At the time of the loss the inertia of the system was relatively low and so the consequent



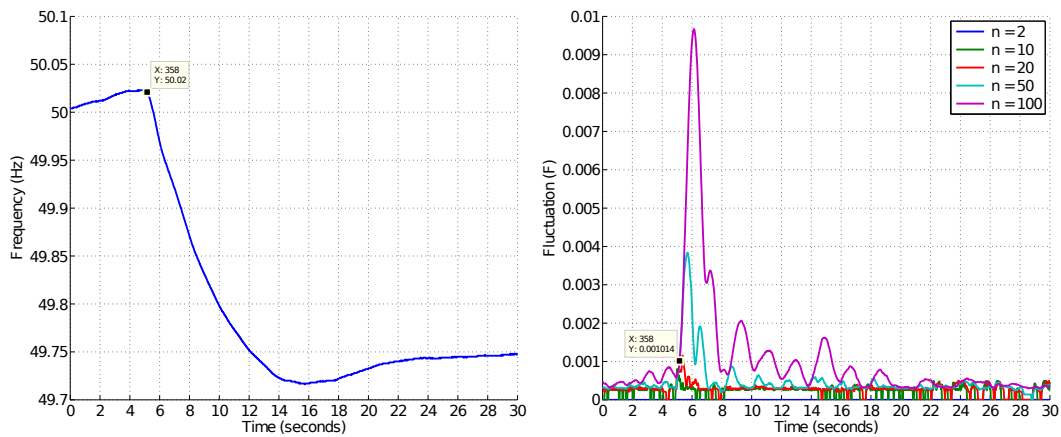


FIGURE 5.6: Frequency trace following a 1000MW generation loss with a distant monitoring node and relatively high inertia (left plot). The corresponding DFA with varying box size (right plot)

measurement contains a large transient following a fast Rate of Change of Frequency (RoCoF). The plot to the right shows DFA on the event with varying box size from  $n = 2 \dots 100$ .

The event is clearly detected for all box sizes from  $n = 10$  and above, as for  $n = 2$ , the event cannot be differentiated from the background noise. Increasing the value of  $n$  serves to reduce the level of background fluctuation, as the variance is seen to be lower in the signal however, it increases the amount of ripple after the presence of the event, as the window extends further along the dataset.

The graphs of Figure 5.6 show, on the left plot, the frequency trace following a separate generation loss of 1000MW, as measured by the furthest PMU from the event. At the time of the loss the inertia of the system was relatively high in comparison with the previous event and so the consequent measurement contains no transient and a relatively smooth decrease in the system frequency. The plot to the right shows DFA on the event with varying box size from  $n = 2 \dots 100$ .

The event is clearly detected for all box sizes from  $n = 50$  and above, with anything below this value it becomes difficult to discern the event from the background fluctuation level and so determination of an adequate threshold level becomes impossible.

Based on these 2 events, showing differing scenarios in terms of measured transients, the threshold for the  $t = t_0$  moment of the event is determined as the first value after,  $F = 1 \times 10^{-3}$ , assuming a box size of  $n = 50$ . This ensures that the event can be easily differentiated from background fluctuations. In order to confirm this, analysis was carried out on a number of transmission loss events from the GB system, using 3 PMUs with varying distances to the events, representing different levels of measured transients and background noise.

The results of the DFA are shown in Table 5.1 from 3 PMUs on the GB transmission network, it can be seen for all 10 events that the algorithm detects the event above the previously assumed threshold level of  $F > 1 \times 10^{-3}$ , the events are detected at the time the first value exceeds the threshold. Calculation of the average background level for fluctuation is also seen to be well below the threshold and so no false positives were detected.

TABLE 5.1: DFA on 10 generation loss events as identified by 3 PMUs from the GB transmission system

Event	$\Delta P$	BLYT	STAY	LAGA	Mean Background
1	380	0.001116	0.001115	0.001237	0.000321
2	360	0.001079	0.001102	0.001082	0.000301
3	999	0.001263	0.001378	0.002061	0.000677
4	996	0.001056	0.001112	0.002403	0.000358
5	263	0.001055	0.001063	0.001497	0.000343
6	998	0.003630	0.002385	0.004363	0.000689
7	996	0.002046	0.001844	0.002420	0.000539
8	999	0.001014	0.001057	0.002209	0.000423
9	980	0.001184	0.001631	0.001967	0.000398
10	530	0.001144	0.001182	0.001043	0.000341

### 5.2.3 Instantaneous Generation Loss Determination

The specific requirements for a generation loss event suitable for inertia estimation, as described above, are that the loss has to be instantaneous from a breaker action and must not be staggered, so that the value of the loss can be determined through SCADA measurements. An example of such an event is shown in

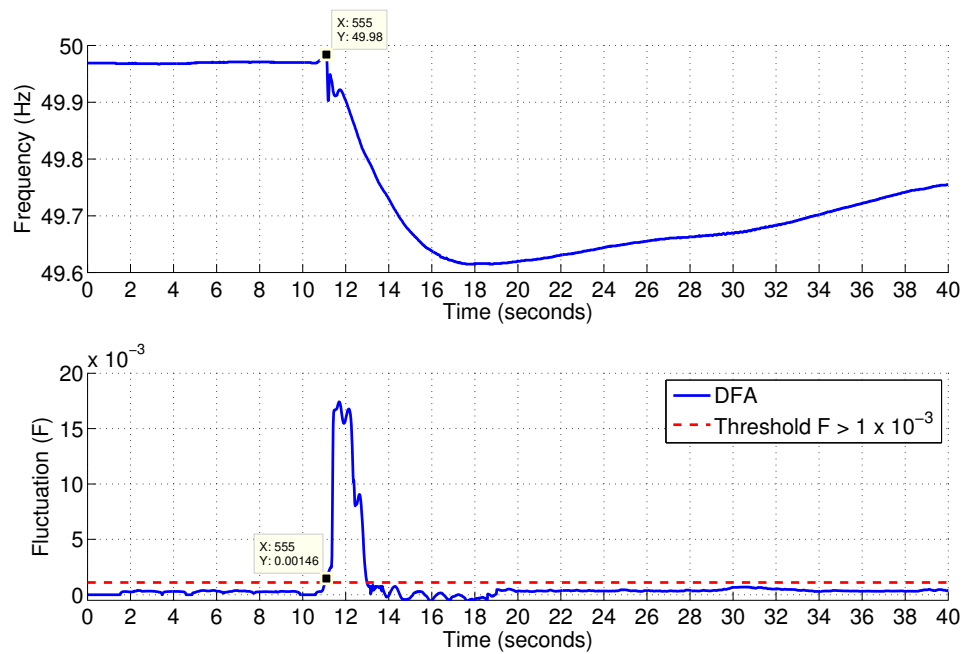


FIGURE 5.7: DFA on frequency data following an instantaneous generation loss

Figure 5.7, where the upper subplot shows the instantaneous loss of an interconnector importing 1000MW, and the corresponding transient followed by a smooth decrease in frequency.

Detecting a suitable event is achieved by observing the time-varying properties of the extracted fluctuation  $F$ , obtained using DFA. The algorithm is run over a sliding sample-by-sample window with a length of 50 samples (one second of data), as determined from the previous section. When the fluctuation is first detected to increase above a threshold fluctuation level of  $F = 1 \times 10^{-3}$ , the beginning of a potentially suitable event is indicated. A suitable event is determined by the narrow fluctuation pulse, with the threshold not being exceeded again within 1 second. Any additional fluctuations pulses, within this period would indicate additional in-feed loss events, and due to the sampling rate of supervisory control and data acquisition (SCADA) systems being less than 1Hz, an accurate value for the in-feed loss,  $\Delta P$  would not be possible.

The upper subplot of Figure 5.8 displays an event where the generation appears as two small distinct loss events, leading to a non-monotonic frequency deviation. The corresponding results from the DFA algorithm are shown in the lower subplot,

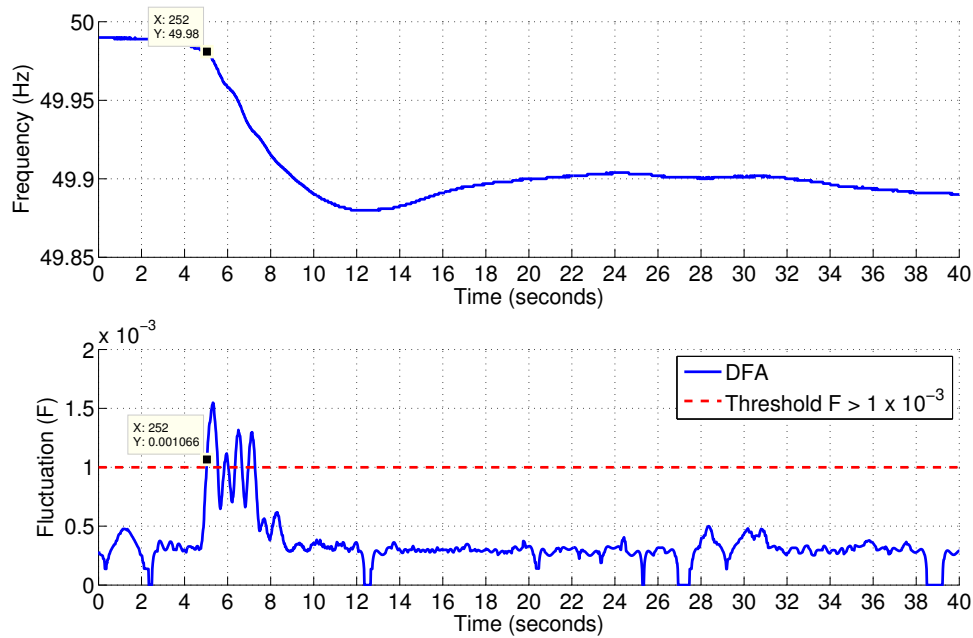


FIGURE 5.8: DFA on frequency data following a staggered generation loss

where the suitability of the measured event to provide an estimate of inertia is determined. In this instance multiple peaks are displayed in quick succession, indicative of the non-simultaneous generation loss. Thus, the unsuitability of this event for inertial estimation is confirmed. An accurate value of  $\Delta P$  would not be achievable from SCADA and so the corresponding accuracy of inertia estimation would be unreliable.

### 5.3 Overview of HPC and Big Data Analytics

With the advent of the smart grid the power system is becoming increasingly complex and computationally intensive. The power systems community faces the challenge of finding suitable methods to solve growing computational issues, for instance, processing massive volumes of PMU data. Such methods can be found in the field of high performance computing (HPC) through parallel processing methods.

### 5.3.1 Parallel Processing Methods

The message passing interface (MPI) is a parallel programming model used to parallelize computation across multiple processors or computers. The MPI model has been used to distribute computation tasks over grid computing nodes [113] and in [114] it was deployed in the HPC environment to parallelize a contingency analysis algorithm. However, the MPI model still requires improvement in areas such as parallel I/O, scalability and topology awareness.

An alternative approach can be found in cluster computing. In [115] a High-Performance Hybrid Computing approach was applied to reduce the execution time of massive contingency analysis algorithms. In this work the algorithm was parallelized using a XMT multithread C/C++ compiler on Gray XMT (multithread HPC computing platform) and conventional cluster computers. In addition, the work in [67] proposed a large scale smart grid stability monitoring application using a conventional cluster of computers to speed up the analysis of PMU measurements. These two separate approaches can increase the speed of program execution by adding more processing nodes however, they rely on centralized management, which can be vulnerable to node failure.

Gao et al. [116] used the parallel computing toolbox within MATLABs Distributed Computer Server (MDCS) to parallelize their contingency analysis algorithm on multiple processors, whilst in [117] a parallel processing method for two monitoring techniques in Prony analysis and an extended complex Kalman filter on multicore systems is explored. Similarly in [118] a genetic algorithm was parallelized. However, these approaches are not resilient and fault-tolerant. The aforementioned approaches can significantly reduce the execution time of large complex computation however, applying these approaches in power system applications is not simply a case of adding more processing units, they require careful design of programs and middleware to make the applications compatible with underlying hardware and software. Furthermore, these approaches (cluster and MPI based) can be scaled by adding more processing nodes. However, they lack the ability to respond to node failures. For example, if any processing node fails as a result of a hardware

or software problem, they do not have any remedy to migrate the running tasks to another available node.

Alternatively the work in [117, 119] proposes the cloud computing platform for smart grid data storage and real-time analysis. The processing is parallelized in cloud computing environments to achieve faster computation. To reduce the risk of data accessibility during node failures, data is replicated on multiple machines however, in the instance of node failures no solution is provided to gracefully assign the running computation to another node.

A robust solution to these issues can be found in the Hadoop MapReduce framework, proposed in a number of areas [120–123], offering a reliable, fault-tolerant, scalable and resilient framework for storing and processing massive datasets. In [120] a machine learning technique is applied whilst in [121] simple statistic calculations (maximum, minimum and average) are used to process PMU datasets. However, both of these works leave out the implementation details and provide no evaluation of their methodology or results. The work [122, 123] uses the Hadoop HDFS (Hadoop distributed file system) for storing data and Pig scripting language for simple statistical calculations. The main focus of both works is to compare the performance of the Hadoop distributed processing with the Multi Core system.

### 5.3.2 MapReduce Programming Model

MapReduce is a parallel and distributed programming model originally developed by Google for processing massive amounts of data in a cluster computing environment [124, 125]. Due to its remarkable features such as fault-tolerance, simplicity and scalability, MapReduce has become a major software technology in support of data intensive applications [126]. MapReduce is a highly scalable model; thousands of commodity computers can be used as an effective platform for parallel and distributed computing.

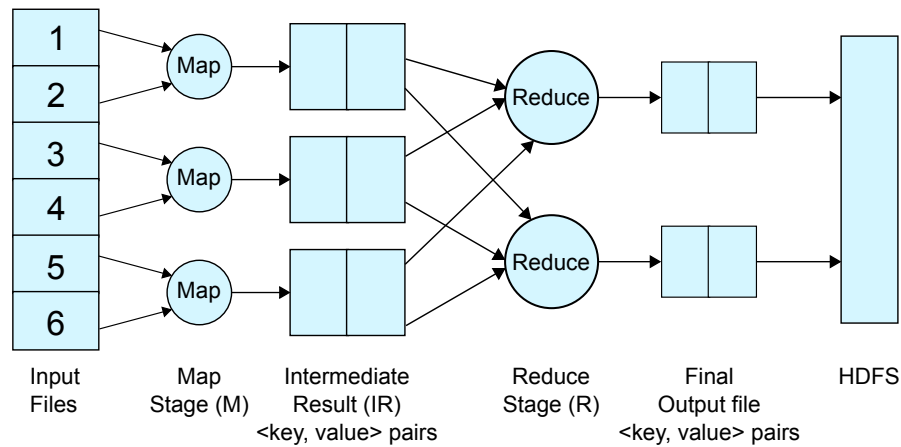


FIGURE 5.9: The MapReduce model.

As shown in Figure 5.9, the MapReduce model divides computational tasks into Map and Reduce stages. In the Map stage, the computation is divided into several Map tasks to be executed in parallel on cluster computing nodes or virtual machines (VMs). Each Map task (a user-defined Map function) processes a block of the input dataset and produces an intermediate result (IR) in the form of key/-value pairs, which are then saved in local storage. In the Reduce phase, each Reduce task (a user-defined Reduce function) collects the IR and combines the values together corresponding to a single key to produce the final result. It should be noted that the Map and Reduce functions are executed independently.

### 5.3.3 MapReduce Implementation with Hadoop

The MapReduce programming model has been implemented in a number of systems such as Mars [127], Phoenix [128], Dryad [129] and Hadoop [130]. Hadoop is the most popular implementation of MapReduce and has been widely employed by the community due to its open source nature. Hadoop was originally developed by Yahoo to process huge amounts of data (over 300TB) across a cluster of low-cost commodity computers [131]. It is worth noting that Hadoop not only works in cluster computing environments, but also in cloud computing systems such as the Amazon EC2 Cloud [132].

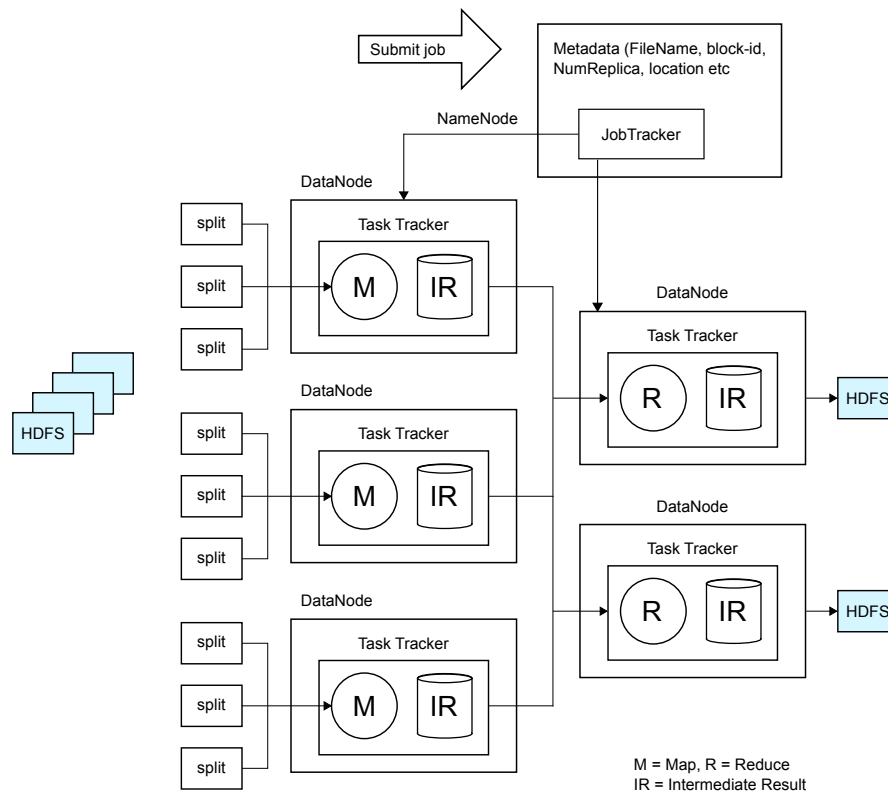


FIGURE 5.10: The Hadoop framework.

The architecture of the Hadoop framework, as shown in Figure 5.10, comprises its own file system, the Hadoop Distributed File System (HDFS) [133]. HDFS is designed to store massive amounts of data (terabytes or petabytes) over a large number of computer clusters and provides fast, scalable access to that data. The system follows a client-server architecture, where there is a NameNode acting as the server and multiple DataNodes that act as clients. The HDFS has high availability (HA) features by providing the option to configure two NameNodes in the same cluster in the form of an active NameNode or a passive NameNode (Standby NameNode). This feature is used to reduce the risk of single points of failure, providing a more robust solution. The passive NameNode deals with fast failover in case the active NameNode crashes as a result of software or hardware malfunction [134].

HDFS automatically splits input files into equal size blocks (64 MB or 128 MB by default) that are distributed across the DataNodes. Each data block has multiple replicas (3 by default), which are stored on different data nodes. If the cluster



network topology has more than one rack then the block replicas will be stored on different rack machines. The purpose of data replication and distribution on different machines is to maximise reliability and availability of data.

The NameNode manages the namespace of the file system and regulates the clients access to files. It does not store data itself, but rather it maintains metadata files that contain information such as the file name, block id and number of replicas, mapping between blocks and DataNodes on which the blocks are stored and the location of each block replica. The DataNodes manage the storage directly attached to each DataNode and execute the Map and Reduce tasks.

The JobTracker runs on the NameNode and is responsible for dividing user jobs into multiple tasks, scheduling the tasks on the DataNodes, monitoring the tasks and re-assigning the tasks in the instance of a failure. The TaskTracker runs on DataNodes, receiving the Map and Reduce tasks from the JobTracker and periodically communicates with the JobTracker to report the task completion progress and requests for new tasks.

Furthermore, the Hadoop MapReduce cluster has over 180 configuration parameters. The system automatically assigns a default value for these parameters if the user does not specify one during a job submission. It has been widely recognized that setting an optimum value for these parameters can have a high impact on the performance of a Hadoop job [135, 136]. Out of all the configuration parameters, precise tuning of the following can have a significant impact on a jobs performance:

- `io.sort.mb` - Specifies the size of a buffer in memory (MB) used by a map task when sorting a file. The default value is 100MB; however, higher values can improve the performance by reducing the spill to the local disk.
- `io.sort.spill.percent` - Controls when the system will start the background thread to spill the contents of the memory buffer to local disk. The default value is 0.8 (80%).
- `io.sort.factor` - Determines the number of spill files to be merged. The default value is 10 and can be up to 30 depending on the RAM of the system.

- `mapred.reduce.tasks` - This parameter controls the number of Reduce tasks to be set for a job. The default value is 1. However, the user can set more Reduce tasks for a job depending on the structure of the application and requirements of the user.
- `dfs.block.size` - Controls the size of data block. The default value is 64MB/128MB however, it can be set to a larger size for improved performance.
- `dfs.replication` - This parameter controls the number of replicas for each data block. The default value is 3. Increasing the number of replicas improves the reliability however at cost of storage space.
- `mapred.tasktracker.map.tasks.maximum` - This parameter controls the number of Map tasks executed in parallel on a DataNode.
- `mapred.tasktracker.reduce.tasks.maximum` - This parameter controls the number of Reduce tasks executed in parallel on a DataNode.
- `mapred.map.child.java.opts` - Specifies the amount of memory for the TaskTracker to use when launching jvm (Java Virtual Machine). The default value is `Xmx200m`.

## 5.4 The Design of PDFA

With the anticipated volumes of PMU data on the GB system set to increase significantly over the next 5 years, algorithms need to be considered for timely analysis of potentially massive datasets in near to real-time. For these reason the DFA algorithm has been parallelised in the Hadoop MapReduce framework to demonstrate the scalability of the algorithm and its ability to efficiently analyse massive volumes of data [109].

The Parallel DFA (PDFA) has been tested and demonstrated in two stages, the first through a laboratory based online setup, using a PMU installed at the domestic supply and the openPDC platform [137] with a localised Data Historian

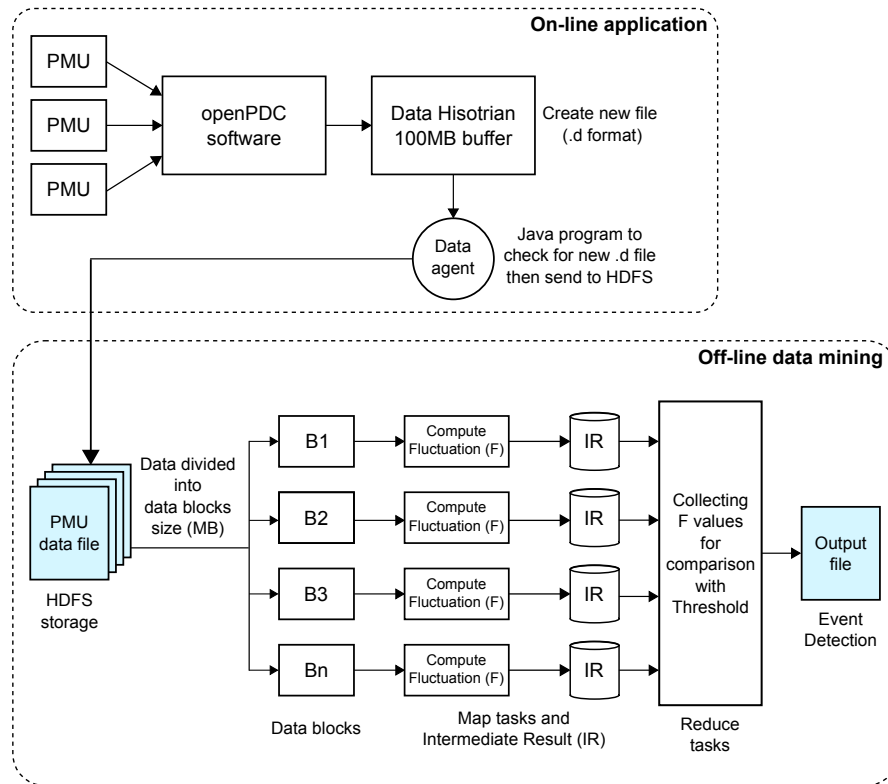


FIGURE 5.11: Architecture of PDFFA implementation.

(DH) to collect and store 50Hz resolution frequency data. The second, is the application to the WAMS installed on the transmission system of GB, as an offline Data Mining approach.

### 5.4.1 PDFFA Implementation

The original DFA algorithm was implemented in MATLAB specifically for the offline application of event detection and assessment for inertia estimation, the approach focuses on small datasets and the determination of the  $t = t_0$  moment or exact start time of a specific event.

The PDFFA, is intended for the analysis of massive volumes of PMU data and therefore has been implemented in the Hadoop MapReduce framework using the Python programming language due to its flexibility and open source. The algorithm has been implemented as depicted in Figure 5.11.

A laboratory based setup at Brunel University comprises a domestic supply connected PMU measuring positive sequence voltage values, frequency and RoCoF at 50Hz. This data is sent through a Local Area Network (LAN) to an openPDC historian. The openPDC software is configured in such a way that when the historian data size reaches 100MB, a new data storage file is created in .d format with a corresponding time-stamp.

A data agent has been created in the Java programming language using a number of Hadoop core libraries and the Java directory watch service package. The application code is encapsulated in the while loop statement to execute continuously, monitoring the historian folder to detect for the presence of new .d files. Once the new file is created in the historian folder, the data agent application automatically moves it to the Hadoop cluster HDFS storage.

It should be noted that the HDFS storage system is not capable of working with the .d file format. At present this file is manually converted to .csv format using the historian playback module within the openPDC software. This process will be automated at a later stage.

Having proven the online data collection side of the system, the following analysis can either be performed as a complement to this process or alternatively it can work in a Data Mining sense where massive datasets are provided directly to the HDFS storage in the .csv file format.

The Hadoop MapReduce facility supports a number of programming languages such as Java, Python, and C++. Java is the native language of Hadoop and so programs written in Java can be directly executed. Programs written in any other language require application program interfaces (APIs) to execute them. For example, programs written in C++ are executed through the Pipes API and programs written in Python will execute through the Streaming API [138].

The PDFFA was written in Python in the form of Map and Reduce functions, as Python is an open source language and unlike Java contains a large amount of the

required mathematical functionality for the DFA algorithm. The PDFA is then executed through the Streaming API in the Hadoop MapReduce environment.

When a dataset is moved onto a Hadoop cluster, the HDFS automatically divides it up into blocks  $B$ , as shown in Figure 5.10. The block size is specified in the cluster configuration file (`hdfs-site.xml`), for instance, if a historian dataset is 16MB and the block size value has been set to 2MB, then the total number of blocks for that dataset will be 8 ( $16/2 = 8$ ). The total number of Map tasks is equal to the total number of blocks.

When the PDFA program is submitted to the Hadoop framework, the framework automatically divides the PDFA program into a number of Map and Reduce tasks. A block of the PMU dataset is assigned to each Map task and the number of Map tasks executed in parallel to process the dataset depends upon the number of Map slots specified in the cluster configuration file (`mapred-site.xml`). For the PDFA, one slot was configured on each VM, as a result 8 Map slots were configured in the cluster and so 8 Map tasks were executed in parallel to process the historian dataset. The number of Map slots configured on a VM depends on the processing capacity (physical memory and number of CPU cores) of the VM.

Each Map task processes the assigned data block on a sliding window of 50 samples (as per the DFA algorithm) and calculates the fluctuation value  $F$ . The  $F$  values are buffered in memory of size 100MB, which can also be set in the configuration file. When the content of the buffer memory reaches a threshold value of 80% (80MB) a background thread is started to spill the contents of the memory buffer to a local disk as an intermediate result (IR). The number of IR files is equal to the number of Reduce tasks.

After completion of the Map phase, the PDFA Reduce tasks are initiated and collect the calculated  $F$  values. The number of Reduce tasks is also configurable by the user in the configuration file. The number of Reduce tasks to be executed in parallel depends on the number of Reduce slots configured in the configuration file. For the PDFA, 8 Reduce tasks and 8 Reduce slots were configured, so as to fully utilize all the available Reduce slots. Each Reduce task compares every value

of  $F$  with the threshold value  $F = 1 \times 10^{-3}$ , any value greater than this threshold is flagged as an event for further analysis.

Most of the conventional cluster-based approaches have issues of reliability and fault-tolerance. The PDFA is implemented in a Hadoop based cluster computing environment, as it offers built-in remarkable features such as high availability, fault-tolerance and scalability. The framework supports multiple replicas of the data blocks and distributes them on different computers/VMs to overcome any fail situations and delays. The cluster can easily be scaled by adding more processing nodes to increase the speedup of computation. During the job execution, if any processing nodes crash due to software or hardware failures, the jobTracker will automatically detect it and assign the running tasks to another available node.

## 5.5 Evaluation and Results

The performance of the PDFA is compared with the original sequential DFA in terms of efficiency and accuracy, using 6000 samples of frequency data (2 minutes at 50Hz), provided by a PMU on the NG WAMS. The data contained a known system event, in the loss of a generator exporting approximately 1000MW. In order to create a Big Data scenario, this dataset was replicated a number of times to provide a relatively large dataset with over 32 million samples.

### 5.5.1 Experimental Setup

The experiments were carried out using a high performance Intel Server machine comprising 4 Intel Nehalem-EX processors running at 2.27GHz each with 128GB of physical memory. Each processor has 10 CPU cores with hyper thread technology enabled in each core. The specific details of the hardware and software implementation are displayed in Table 5.2. The analysis of the sequential DFA was carried out on just one of the VMs, whereas the PDFA was run on up to 8 VMs.

TABLE 5.2: Experimental configuration of the Hadoop cluster

Hardware	CPU	40 Cores
	Processor	2.27GHz
	Storage	2TB and 320GB
	Connectivity	100Mbps Ethernet LAN
Software	Operating System	Ubuntu 12.04 TLS
	Python	Version 3.3
	JDK	Version 1.6
	Hadoop	CDH 4.5
	Oracle Virtual Box	Version 4.2.8
	openPDC	Version 1.5

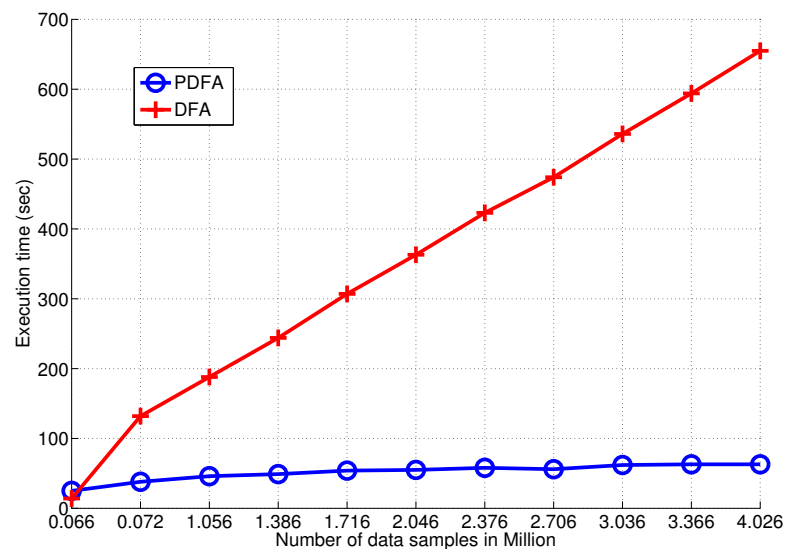


FIGURE 5.12: Analysis of PDFA efficiency.

## 5.5.2 Results

A number of experiments were carried out to evaluate the efficiency and accuracy of the PDFA method. From Figure 5.12, it can be seen that the PDFA outperforms the sequential DFA in computation significantly using 8 VMs. The execution time of the sequential DFA increases with an increasing number of data samples, while the execution time of the PDFA remains relatively constant.

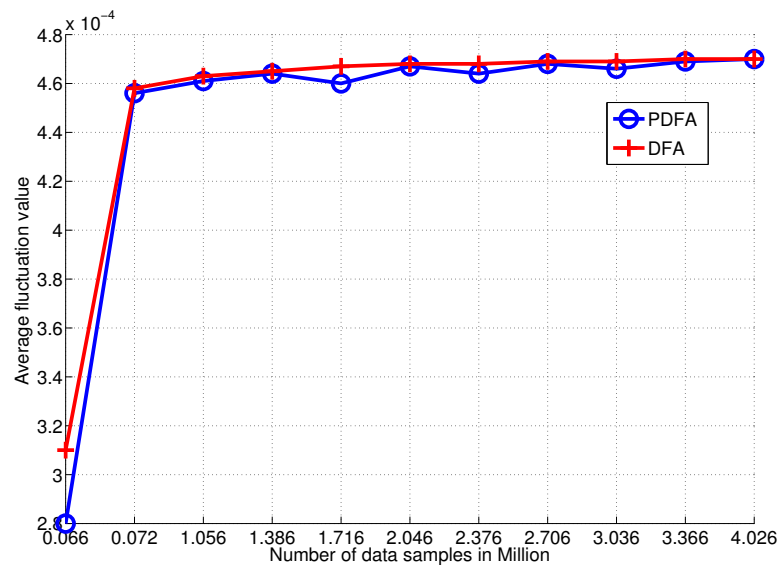


FIGURE 5.13: The relative accuracy of PDFFA compared to DFA.

The DFA algorithm works on a sliding window, so when comparing the output of the sequential DFA with PDFFA it is important to note the possibility of discrepancies in results caused by data partitioning due to the way in which the datasets are divided up for parallelization. This does not affect the PDFAs ability to detect events; it just means that the  $F$  values could differ slightly from the DFA results, as they may be analysing a slightly different set of samples. The results of the PDFFA are compared with that of the DFA and are displayed in Figure 5.13, the relative accuracy of PDFFA is very close to that of the sequential DFA, especially in the cases of larger datasets, as the difference converges to zero.

The scalability of the PDFFA in terms of a varied number of both VMs and data samples was evaluated. Figure 5.14 shows the execution times of the PDFFA when processing 3 different sizes of dataset and a varied number of VMs from 1 to 8. The PDFFA clearly performs best in scalability on the largest dataset with 32 million data samples. It can be observed that the execution time of the PDFFA on each dataset decreases with an increasing number of VMs employed. When processing 8M data samples, 4 VMs generated 2 times speedup, whereas 8 VMs generated 2.5 times of speedup. However, when the number of data samples is increased to 32M, 4 VMs generated 3.3 times of speedup whereas 8 VMs generated 5.4 times



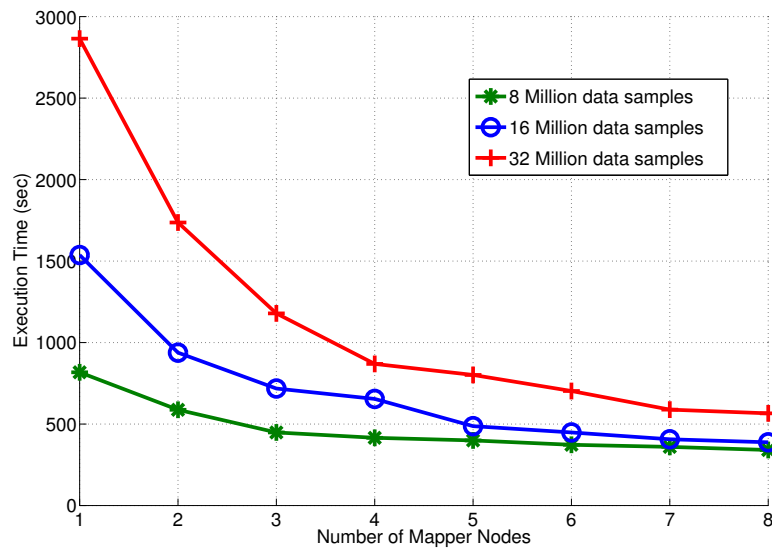


FIGURE 5.14: The scalability of PDFFA, execution time against number of Mapper nodes (VMs).

of speedup. With increasing numbers of data samples, the times of speedup will be increased closer to the number of VMs.

Based on the results presented in Figure 5.14, the speedup of the PDFFA in terms of computation when processing the 3 different sized datasets was calculated using Equation 5.4.

$$Speedup = \frac{T_s}{T_N} \quad (5.4)$$

Where  $T_s$  is the execution time of the PDFFA on a single VM and  $T_N$  represents the execution time of the PDFFA on  $N$  number of VMs. The results of this calculation are displayed in Figure 5.15. Again, the PDFFA achieves the best speedup in computation on the largest dataset with 32 million data samples. However, as shown by the dotted line in Figure 5.15, the results never achieve that which are to be expected from Amdahl's law [139].

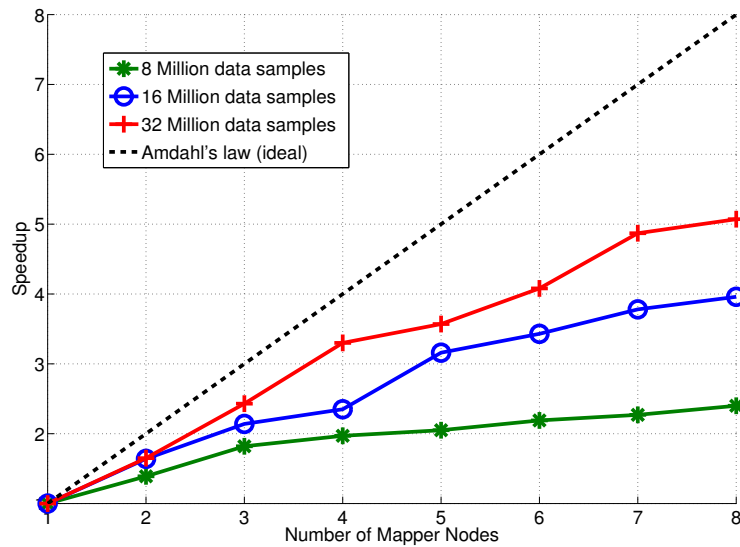


FIGURE 5.15: Speedup analysis of the PDFFA algorithm.

### 5.5.3 Speedup Analysis

When parallelizing a sequential program, the speedup in computation can be calculated using Amdahl's Law [139], defined in Equation 5.5.

$$Speedup = \frac{1}{(1 - P) + \frac{P}{N}} \quad (5.5)$$

Where  $P$ , represents the portion of the sequential programme in percentage that can be parallelized and  $N$  represents the number of computers used in the computation. Theoretically, in the case when a sequential program can be fully parallelized ( $P = 1$ ), as was the case with PDFFA, the speedup of the parallelized program should be equal to the number of computers used in the computation  $N$ . Therefore:

$$Speedup = \frac{1}{(1 - P) + \frac{P}{N}} \leq N \quad (5.6)$$

However, as shown in Figure 5.15, the closest speedup to Equation 5.6 that the PDFFA achieved in all the computation scenarios was 3.3 times faster than the

sequential DFA when 4 VMs were used in the process. The speedup of the PDFA never achieved  $N$  times in a Hadoop cluster with  $N$  computers even though the sequential DFA was fully parallelized. This means that Amdahls Law in the form of (5.6) is not sufficient in calculating the speedup of a parallelized program that is executed in a cluster computing environment. This is because Amdahl's Law in this form does not consider the communication overhead of a user job in cluster computing. For this purpose, a revision to Amdahls Law is proposed in the form of Equation 5.7, to better reflect the speedup gain when parallelizing a sequential program in cluster computing.

$$Speedup = \frac{1}{(1 - P) + \frac{P}{N} + R} < N \quad (5.7)$$

Where  $R$ , represents the ratio of the communication overhead to the computation of a user job, and  $R > 0$ .

The revised Amdahl's Law (5.7) better explains the speedup of a parallel program running in cluster computing. The larger a dataset is, the higher overhead in computation will be incurred. As a result, the lower the ratio of communication to computation would be achieved, which leads to a higher speedup in computation. This well explains the speedup of the PDFA in computation when processing the 3 datasets with varied sizes.

To achieve an optimal performance in speedup, the ratio of communication to the communication of a parallel program should be minimized. In the case of Hadoop MapReduce clusters, the size of the segmented data blocks shall be large. On one hand, a large size of data block will generate a small number of tasks that incurs a small overhead in communication. On the other hand, a large size of data block will lead to a high workload in computation. Therefore, a large size of data block will lead to a low communication to computation ratio generating a high speedup.

To evaluate how the size of a data block affects the computational performance of PDFA, the algorithm was run on a dataset of 352MB using 8 VMs with varied sizes of data blocks ranging from 2MB to 32MB. From Figure 5.16 it can be observed

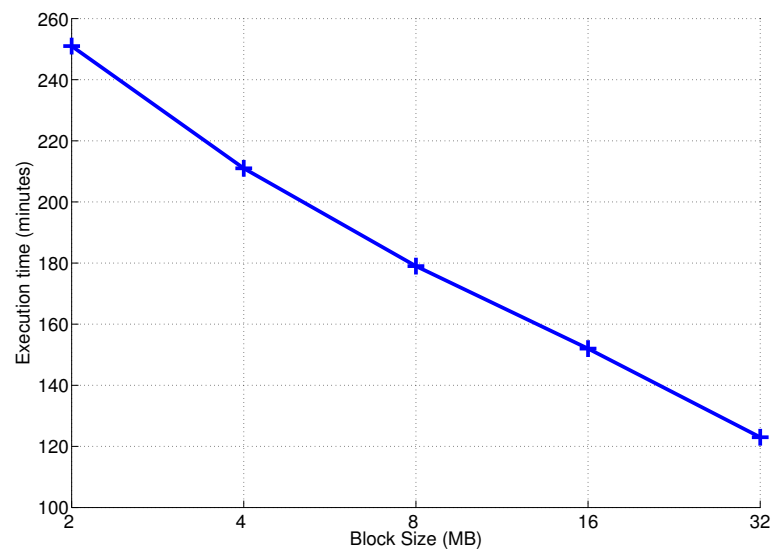


FIGURE 5.16: Computational overhead of PDFFA against data block size.

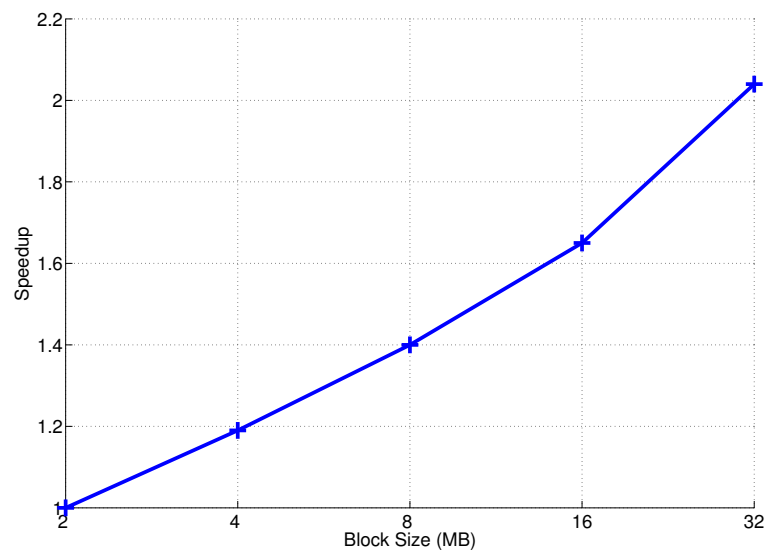


FIGURE 5.17: The speedup of PDFFA against data block size.

that the execution time of PDFFA decreases with an increasing size of data block. The speedup of PDFFA in computation goes up with an increasing size of data block, as shown in Figure 5.17. It can be seen that PDFFA is 2.04 times faster in computation using 32MB data blocks than when using 2MB data blocks, thus confirming a greater improvement in performance with larger datasets.

## 5.6 Concluding Remarks

In this chapter a novel event detection methodology based on Detrended Fluctuation Analysis (DFA) was presented. The method was demonstrated as a basic means of event source location through identifying the closest PMU to an event, and also the determination of the exact event start time ( $t = t_0$ ), deemed vital to inertia estimation methodologies.

The suitability of a transmission system event to provide an estimate on the total inertia of the power system was defined, the key requirement on this being the instantaneous nature of the loss. The identification of such events was demonstrated, again using the DFA algorithm.

The approach was then further expanded to be parallellised for the use on massive volumes of PMU data. With this an introduction to Big Data analytics was provided and the implementation of the Parallel DFA (PDFA) approach presented in the MapReduce programming model.

The experimental results have shown the speedup of PDFA in computation whilst maintaining relative accuracy in comparison with the sequential DFA. Based on the analysis in the speedup of computation, an improvement to Amdahls law was proposed, introducing the ratio of communication to computation to enhance its capability to analyse the performance gain in computation when parallelizing data intensive applications in a cluster computing environment.

Further work is proposed to investigate the methodologies to automatically optimize the configuration settings of Hadoop MapReduce parameters. This will further improve the performance of the PDFA algorithm.

# Chapter 6

## Inertia Estimation of the GB Power System

### 6.1 Introduction

The GB system is required to accommodate an increasing volume of renewable energy, predominantly in the form of offshore wind, asynchronously connecting to the periphery of the transmission system. This displacement of traditional thermal generation is leading to a significant reduction in system inertia, thus making the task of system operation more challenging.

The inevitable shift towards a more dynamic system compounds the existing issues of calculating generator response and reserve requirements, which traditionally assume that system inertia varies linearly with demand. With demand being met by a growing percentage of asynchronous generation, such as renewables and HVDC interconnectors, this assumption is becoming increasingly invalid. Frequency services are becoming more complicated and less predictable throughout the day, forcing reassessment of generation patterns and limitations on single circuit risks, making it more difficult to maintain security for all credible contingencies.

It is therefore necessary to gain an improved understanding of both the inertial frequency response of the power system and the security of the system in real-time. This will ensure the impact of incidents to specific areas of the network is understood, facilitating more economically efficient operation of the power system.

In this chapter a method is proposed for estimating the total inertia of the GB power system, by dividing the network into groups or regions of generation based around the constraint boundaries of the GB network [11]. The inertia is first estimated at a regional level before it is combined to provide a total estimate for the whole network. This estimate is then compared with the known contribution to inertia from generation, to provide an estimate for the currently unknown contribution to inertia from residual sources; namely synchronously connected demand and embedded generation. The approach is first demonstrated on the full dynamic model of the GB power system before results are presented from analysing the impact of a number of instantaneous transmission in-feed loss events, using phase-angle data provided by the 3 PMUs from the GB transmission network and also the devices installed at the domestic supply at 4 GB Universities.

## 6.2 Frequency Response Requirements

The GB power system has no synchronous connection to any other national electricity networks, and therefore must rely on the actions of generators, DC converters and additional demand services to control the system frequency as part of an Ancillary Services Agreement [140]. The Security and Quality of Supply Standard (SQSS) [81] details the GB transmission system obligations on frequency, which should nominally be kept at 50Hz, but is to be maintained within the defined statutory limits of 49.5Hz and 50.5Hz ( $\pm 1\%$ ). For an abnormal event that is considered to be an instantaneous in-feed loss  $>1\text{GW}$  but below the greatest instantaneous loss, which as of 1st April 2014 is 1800MW, the system may deviate beyond these limits, but must be regulated to a minimum of 49.5Hz within one minute.

In addition to the SQSS limits, NG imposes its own operating limits of 50Hz  $\pm$ 0.2Hz for losses up to 300MW, and a maximum frequency deviation of -0.8Hz for events considered to be abnormal. If the rate of change of frequency (RoCoF) following such an event exceeds a predetermined limit, then protection systems designed to monitor for loss of mains (LoM) and prevent the islanding of generation embedded in the distribution network, may operate and further exacerbate the fall in frequency. This is particularly problematic for NG, as there is little if any visibility as to the amount of embedded generation online or whereabouts exactly in the network it is.

To ensure that these limits are adhered to, a predetermined amount of synchronous spinning reserve is held at any time for frequency response. It is important to note that, at this point in time, there is no Automatic Generation Control (AGC) implemented on the GB system. In addition, there are on-going actions to review generation patterns and ensure additional fast acting reserve is made available if required [12].

In order to establish the impact on system frequency of the increasing volumes of variable speed wind turbines and HVDC convertor technology, NG formed a Frequency Response Technical Sub-Group on 15<sup>th</sup> November 2010 [141]. To quantify the future frequency response requirements, NG evaluated various generation backgrounds based on its “Gone Green” scenario, at demand levels ranging from 20GW to 65GW. Each of the scenarios considered High, Average and Low Wind conditions and was studied using the full dynamic system model implemented in Digsilent Power Factory in order to ensure that the SQSS conditions could be satisfied for the largest loss of 1800MW. The recommendations concluded that a Fast Frequency Response (FFR) capability should be developed as it is less challenging to implement than the alternatives of synthetic inertia services, considered to reduce the risk of further power reductions from the interaction with wind turbines in the recovery period and avoid additional complications with RoCoF sampling [141].



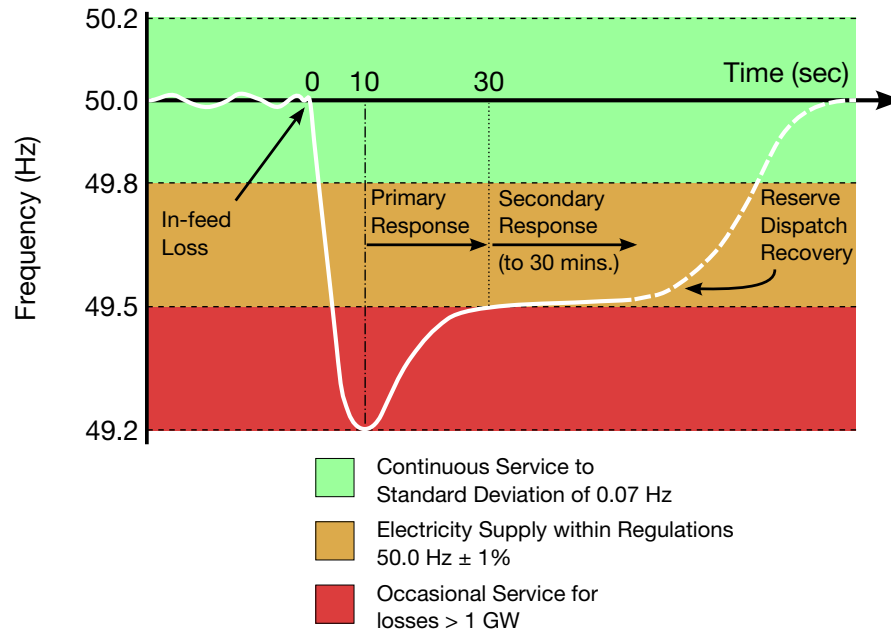


FIGURE 6.1: Frequency response requirements on the GB transmission system.

A typical frequency trace following an in-feed loss, as a consequence of an abnormal event, and the corresponding deployment of reserves to restore the system frequency can be seen in Figure 6.1. Primary frequency response reserves must have activated within 2-seconds of the instance of a loss ( $t = t_0$ ) and be fully deliverable to the system at 10-seconds; these reserves must also be maintained, where necessary, for a further 20-seconds. Secondary frequency response is deliverable following primary response timescales, and can be required for up to 30-minutes after an event. The purpose of primary response is to arrest the initial frequency deviation, whilst the secondary response is required to restore the frequency back to within operational limits.

The move towards FFR and rapid frequency response will require Primary response services to have activated within 1-second of a -0.5Hz change in frequency and have to be fully delivered to the system within 5 seconds, for users bound by the provisions of the Grid Code including asynchronous generation, this allows frequency response volumes to be reduced significantly [142].

### 6.2.1 Inertia Contribution

Large synchronous generators provide the majority of the inertia to the GB system, for which accurate power plant models and operating information are typically available. The remaining system inertia termed as the residual contribution and currently assumed to contribute around 20% to the total, is provided by small and micro generation, which is embedded in the distribution network, where less specific information is available and by industrial, commercial and domestic demand, for which there is very limited information available [12].

The existing assumption is that system inertia varies linearly with demand, as will be shown, this assumption is becoming increasingly invalid, with growing volumes of the demand being met by electronically decoupled generation such as HVDC interconnectors and wind farms.

Large frequency deviations as a result of instantaneous in-feed losses are a rare occurrence on the GB system, but at present these provide the only reliable source of information on system frequency behaviour, and with it the only opportunity to calculate estimates of total system inertia. Provision of accurate synchronized frequency information pertaining to such events becomes vital when attempting to perform these estimates. Additionally, an understanding of the measurement algorithms employed and any limitations of a devices transient performance is now also necessary [29, 30].

## 6.3 Power System Inertia Constant

The inertia of the power system is defined by the stored energy,  $E$  in the synchronously rotating masses of the power system [58], defined as follows:

$$E = \frac{1}{2} J \omega_r^2 \quad [MVAs] \quad (6.1)$$

where  $J$ , is the moment of inertia of a rotating shaft with the units  $\text{kg} \cdot \text{m}^2$  and  $\omega_r$  is the angular velocity of the rotor in  $\text{rad/s}$  (mech). In this format the amount of stored energy  $E$  is seen to vary with the velocity of the rotor, for this reason it is common practice to define the stored energy with respect to an inertia constant,  $H$  defined as the ratio of the stored kinetic energy at synchronous speed,  $\omega_{r_0}$  to the VA rating of the machine,  $S_{\text{base}}$ . This determines the amount of time in seconds that the stored energy  $E$  could supply power to the system at an equivalent value to the  $S_{\text{base}}$ .

$$H = \frac{1}{2} \frac{J\omega_{r_0}^2}{S_{\text{base}}} \quad [\text{s}] \quad (6.2)$$

The Equation 6.2 is valid for all of the individual synchronous machines of the power system, therefore the total inertia of the power system has to be calculated as a summation for  $n = 1 \dots N$ .

$$H_{\text{Tot}} = \sum_{n=1}^N \frac{1}{2} \frac{J_n \omega_{r_0,n}^2}{S_{\text{base},n}} \quad [\text{s}] \quad (6.3)$$

Representing the inertia of the power system with respect to  $H(s)$  implies an average value for the system. The work demonstrated in this thesis is concerned with the total inertia of the power system, as a representation of a physical spinning mass, for this reason the inertia is represented with respect to H·MVA.

## 6.4 Inertial Frequency Response Estimation

The inertial response of the GB system is considered to be the period up to one second immediately following an in-feed loss, prior to the activation of primary frequency response reserves. During this time, the system frequency response is unregulated, and its behaviour is dictated primarily by the inertia present in the power system. The RoCoF following such an imbalance between supply and demand depends on the inertia present in the system at the time of the offending

disturbance, as well as the size of the loss. This can be calculated from the swing equation [58].

An unbalance in the torques acting on the rotor of a given machine, as a result of a disturbance will cause an acceleration in torque

$$\Delta T = T_m - T_e \quad (6.4)$$

where  $\Delta T$  is the change in torque due to the acceleration,  $T_m$  is the mechanical torque and  $T_e$  is the electromagnetic torque, all in N·m. The swing equation is therefore

$$J \frac{d\omega_r}{dt} = \Delta T \quad (6.5)$$

where  $\omega_r$  is the angular velocity of the rotor in *rad/s* (mechanical) and  $t$  is time in seconds  $s$ . Combining Equation 6.2 into Equation 6.5 gives

$$J = \frac{2 \cdot H \cdot S_{\text{base}}}{\omega_{r0}^2} \Rightarrow \frac{2 \cdot H \cdot S_{\text{base}}}{\omega_{r0}^2} \frac{d\omega_r}{dt} = \Delta T \quad (6.6)$$

we are concerned with system frequency,  $f$  at the electrical output of the generator, so accounting for the number of field poles  $p_f$  of the generator and utilizing the relationship  $\omega_r = 2\pi f_r$ , the synchronous speed of the generator rotor in Hz (electrical) is calculated as

$$f = \frac{p_f}{2} f_r. \quad (6.7)$$

incorporating into Equation 6.6 in terms of electrical frequency  $f$  gives

$$\frac{2 \cdot H \cdot S_{\text{base}}}{f_0^2} \frac{df}{dt} = \Delta T \quad (6.8)$$

It is more convenient to work with power as this can be more easily measured as opposed to torque. The power is equivalent to the product of the torque and the frequency of the rotor  $f$  [143], therefore

$$\frac{2 \cdot H \cdot S_{\text{base}}}{f_0} \frac{df}{dt} = \Delta P \quad (6.9)$$

where  $\Delta P$  is the difference between,  $P_m$  the mechanical power and  $P_e$  the electrical output power of the machine, all in  $W$ . Rearranging leads to the more commonly expressed equation relating the RoCoF to the total system inertia,

$$\frac{df}{dt} = \frac{-\Delta P}{2H_{S_{\text{base}}}} f_0, \quad (6.10)$$

where  $\Delta P$  is the change in active power due to an in-feed loss in MW relative to the systems load base in MVA, and  $f_0$  is the system frequency at the time of the disturbance ( $t = t_0$ ).

With the amount of inertia from transmission connected generation on the decline it is becoming increasingly important to understand the amount of inertia available from residual sources. Accurate information on the availability of additional inertia could serve to reduce frequency response requirements.

The known contribution to inertia from the transmission-connected generation provides an upper limit to the maximum possible value of RoCoF; an accurate measured value should thus always be less than this to account for inertia from residual sources, namely generation embedded in the distribution network and demand services in the form of electric motors.

On this basis the RoCoF,  $df_{c,G}/dt$  applicable to the centre of inertia [144] based on generation only can be determined as

$$\frac{df_{c,G}}{dt} = \frac{-\Delta P}{2H_{\text{GEN}}} f_0, \quad (6.11)$$

where  $H_{\text{GEN}}$ , is the total inertia provided by transmission connected generation, relative to the  $S_{\text{base}}$ .

The residual inertia contribution can then be calculated, assuming an accurate measurement for the  $df_{c,T}/dt$  applicable to the centre of inertia based on the total system contribution, as the difference between the total system inertia,  $H_{\text{TOT}}$  and  $H_{\text{GEN}}$ , where  $H_{\text{TOT}}$  is

$$H_{\text{TOT}} = \frac{-\Delta P}{2 \cdot \frac{df_{c,T}}{dt}} f_0 \quad (6.12)$$

From this the inertia contribution from residual sources can be defined as:

$$H_{\text{RES}} = H_{\text{TOT}} - H_{\text{GEN}} \quad (6.13)$$

#### 6.4.1 Factors Affecting Inertia Estimation

The ability to estimate the inertia of the system based on this swing equation method is dependent on the accuracy of the measured data utilized in Equation 6.10, and can be summarised as follows:

- Precise data on the size of loss - dependant on the availability of accurate metering.
- Online plant inertias, for the estimate of the residual contribution - accurate knowledge of the connected plant to determine the total contribution to inertia from generation.
- Identification of event start time ( $t = t_0$ ) - vital to determining the initial conditions of the network in terms of system frequency, online plant and the size of the loss.
- Accuracy of frequency measurement - poor resolution will limit the ability to capture the inertial response of the system.

- Method of RoCoF ( $df/dt$ ) calculation - over the correct time-frame and taking into account any measured transients.
- Location of measurement point relative to in-feed loss - respective localised inertias and network connectivity.

The specific parameter estimated from online measured system data is the  $df/dt$  or RoCoF experienced by the system during the loss of generation. It has been shown in [30] that the location of the frequency measurement relative to the loss is also a pertinent factor in the estimation. For an identical event, a measurement taken from a location in the network which is weakly interconnected and has low localised inertia will produce a higher magnitude estimate of RoCoF, relative to the estimate yielded from a measurement taken from an electrically strong part of the network with a relatively high inertia.

## 6.4.2 Frequency Calculation

The frequency measurements available on the GB system are predominantly provided through the upgraded DFR-type PMU devices. Although the measurements are time-synchronised at source, they employ the zero-crossing method to calculate frequency [103]. This frequency calculation method, compounded with potential errors due to quantization, has at times resulted in poor frequency resolution, as can be seen in Figure 6.2. For this reason, the analysis of the GB system is carried out using frequency measurements calculated from the time derivative of the voltage phase angle [36],

$$\hat{f} = f_n + \frac{d\delta}{dt} \cdot \frac{f_s}{360}, \quad (6.14)$$

as this provided better frequency estimates. Here,  $f_n$  is the nominal system frequency,  $\delta$  is the voltage phase angle, and  $f_s$  is the sampling frequency of the measurement device.

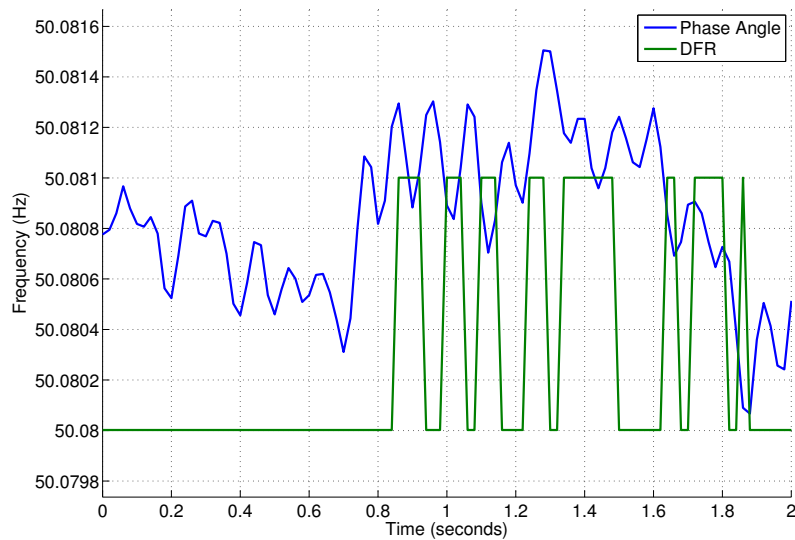


FIGURE 6.2: Frequency resolution from voltage phase angle compared with DFR

### 6.4.3 RoCoF Calculation

It has been shown in [26, 27, 30] that a method of curve fitting is required to mitigate the impacts of measured transients in frequency following a loss in generation, otherwise the calculated RoCoF may be significantly larger than anticipated for the given system loss. Without some form of signal conditioning, the electrical distance between the measurement and the location of the event is the primary factor influencing the calculated RoCoF, as can be seen in Figure 6.3.

The upper subplot in Figure 6.3 shows the system frequency as measured from 3 installed PMUs located in the North, Midlands, and South of England, in response to an in-feed loss of 1000MW in the South of England. It can be seen that the PMU nearest to the event initially records the most significant frequency deviation, and therefore yields the largest magnitude estimate of RoCoF, as shown in the lower subplot. It should also be noted that the PMUs are from the same manufacturer and are all the same model.

The RoCoF, as seen in the lower subplot, also has to be estimated over the relevant time interval, between the start of the event and the onset of primary response.



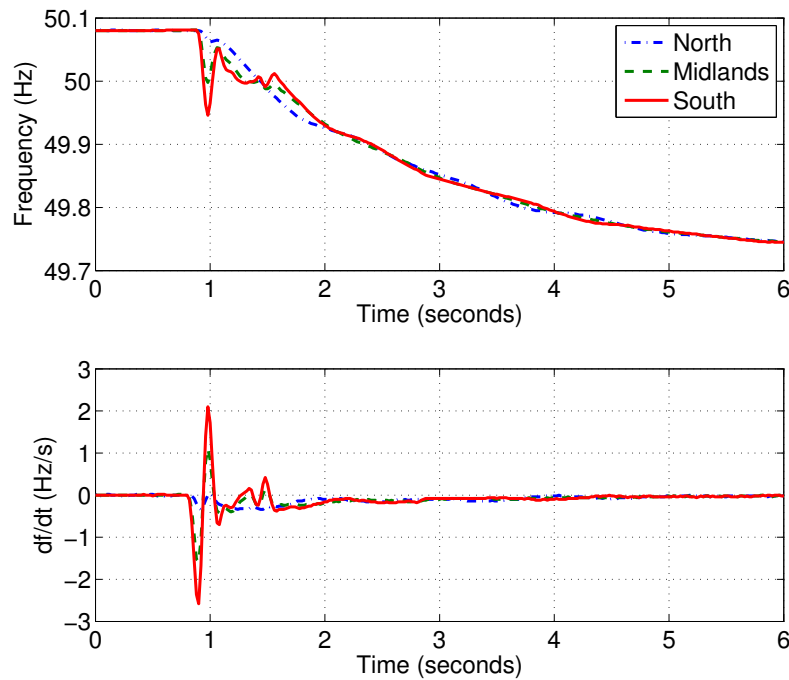


FIGURE 6.3: Frequency trace and calculated  $df/dt$  following a 1000MW in-feed loss of generation in the South of the Network.

In the GB system, primary response can be observed deploying within one second following an in-feed loss event.

For the GB system, previous works [30], based on the methodology of [26], have demonstrated the use of a fifth order polynomial fit to the frequency data to minimize the influence of the measured transients before estimating the RoCoF. This has since been found to be unsuitable, as the fitting of the polynomial is too dependant on frequency effects well outside inertial time-scales, due to the curve having to be aligned with up to 20 seconds of data. The impact of primary response services are well under operation during this time.

Following analysis of these measured transients in the frequency domain, it was identified that in all cases the signal energy resulting from the transient distortion was predominantly present above 0.5Hz, as shown in Figure 6.4, so a lowpass Butterworth filter with a 0.5Hz corner frequency was utilized to isolate the dominant system inertial frequency response, as shown in Figure 6.5. It should be noted

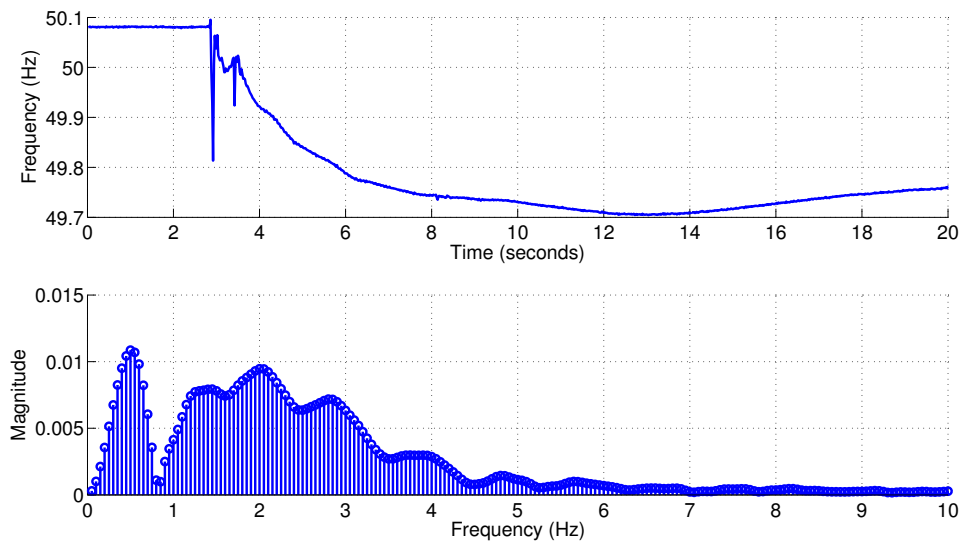


FIGURE 6.4: FFT on measured frequency transients following 1000MW generation loss

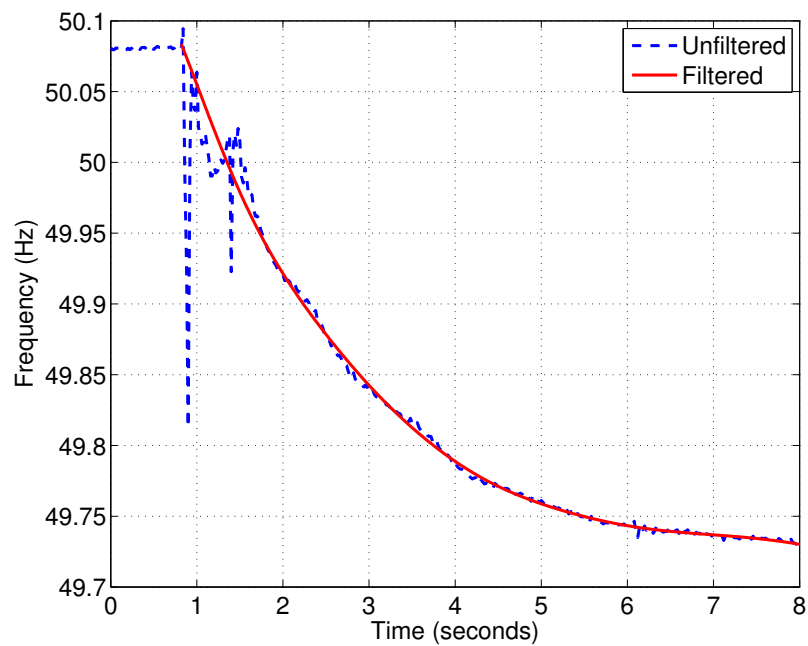


FIGURE 6.5: Low pass filter applied to measured frequency transient.

that any delay introduced by the filter is considered negligible in this analysis, as the filter is applied with the data purely from post event at  $t = t_0$ .

Following the detection of a suitable event for inertia estimation, as defined in Section 5.2.3, the RoCoF was then calculated using a 500ms sample-by-sample sliding window, over a one second period following the in-feed loss. The maximum value

TABLE 6.1: 22 generation loss events captured from the GB transmission system

Event	$\Delta P$	System	MVA	H	H·MVA	$df_{c,G}/dt$
		Demand (MW)	Rating			
1	380	37,648.40	50,658.89	5.01	253,932.63	0.0374
2	360	34,857.11	44,654.24	4.68	209,139.06	0.0430
3	354	24,243.20	34,149.15	4.56	155,858.45	0.0568
4	240	39,358.40	52,114.80	4.82	251,204.53	0.0239
5	590	22,809.65	36,568.45	4.93	180,125.10	0.0819
6	300	40,017.81	55,700.38	4.89	272,310.84	0.0275
7	212	34,924.69	51,022.18	5.10	260,056.55	0.0204
8	316	23,315.90	41,343.34	4.65	192,428.56	0.0411
9	320	23,145.50	39,123.14	4.50	176,032.93	0.0454
10	312	44,843.81	58,736.29	4.23	248,224.95	0.0314
11	324	46,085.60	59,201.60	4.29	253,840.30	0.0319
12	328	45,086.90	57,655.89	4.95	285,612.67	0.0287
13	312	39,928.30	52,593.65	4.98	261,934.93	0.0298
14	228	39,200.77	54,885.90	4.85	266,418.37	0.0214
15	999	23,190.70	37,918.44	4.96	187,890.67	0.1329
16	996	39,714.41	50,814.05	5.04	256,306.14	0.0972
17	263	23,551.20	34,341.95	5.41	185,821.70	0.0354
18	998	25,282.74	34,738.15	4.26	147,920.44	0.1686
19	996	32,919.81	39,119.95	4.47	174,881.98	0.1424
20	999	49,972.75	59,875.85	4.35	260,402.39	0.0959
21	980	38,305.31	49,649.10	4.07	201,902.08	0.1213
22	530	39,096.19	50,270.50	4.09	205,614.39	0.0644

was then taken to represent the free-fall period of frequency deviation following the event before any frequency response services started to take effect.

## 6.5 Results and Analysis

A total of 22 events were detected on the GB transmission system using the DFA method, for which data from 3 PMUs was available. The details of all 22 events are shown in Table 6.1.

The final column shows the theoretical maximum value of RoCoF,  $df_{e,G}/dt$  applicable to the centre of inertia based on generation only, calculated using Equation 6.11. It is then understood that a measured value, which accurately represents the centre of inertia for the whole system should be higher than this to allow for the residual contribution to inertia.

Using Equation 6.12 the total inertia for the GB power system was estimated based on the measured values of  $df/dt$  from the 3 PMUs. The results are shown in Table 6.2 for the total inertia estimation, it can be seen that the results vary quite considerably. This is due to the localised inertias of the monitoring points and the electrical distance of the monitoring points to the event. The location of the disturbance governs the electrical distance to any monitoring point and consequently how much of the loss is actually captured. In addition if a monitoring point has a relatively high localised inertia the relative size of the loss will also be smaller.

This will also affect the accuracy of any measurements of residual inertia and the variance of the corresponding estimates can be seen from Figure 6.6. The results are seen to vary amongst the events from between 4% to 45% and between individual monitoring nodes, in the instance of Event 20, the variation is as much as 40% between Langage and Staythorpe. This is all largely determined by the amount of generating plant online at the onset of the event, or more specifically whereabouts in the network the plant is connected.

The majority of the generation on the GB system is typically connected around the Midlands of the GB system, with this in mind the PMU at Staythorpe is located central to around 50% of the generating plant online, the location of the PMUs relative to the generation on the GB system can be seen in Appendix A. Taking the values exclusively from Staythorpe reduces the variance to between around 9% and 45% but it is still too inconsistent, as the behaviour of the generators on the outskirts of the network are not accurately represented.

TABLE 6.2: Variation in measured  $df/dt$  from 3 PMUs

Event	$df/dt$	$df/dt$	$df/dt$	$H_{\text{Est}}$	$H_{\text{Est}}$	$H_{\text{Est}}$
	BLYT	STAY	LAGA	BLYT	STAY	LAGA
1	0.0263	0.0263	0.0323	361,630.2664	361,795.1843	294,175.8995
2	0.0345	0.0310	0.0341	261,078.5841	290,325.1098	263,871.3902
3	0.0420	0.0442	0.0436	210,859.8794	200,315.7764	203,193.1844
4	0.0229	0.0165	0.0203	262,127.2843	363,758.8599	295,787.2209
5	0.0594	0.0591	0.0677	248,148.6939	249,434.8745	217,796.7794
6	0.0215	0.0205	0.0220	348,587.4514	366,078.8346	341,536.2808
7	0.0179	0.0179	0.0195	295,506.4795	296,759.7907	271,172.5215
8	0.0320	0.0336	0.0357	247,087.8813	235,460.5390	221,115.0023
9	0.0377	0.0378	0.0377	212,169.6551	211,726.9200	212,181.4624
10	0.0238	0.0246	0.0253	327,611.7979	317,010.4946	308,025.3200
11	0.0268	0.0258	0.0280	302,423.3158	314,444.3265	289,452.6500
12	0.0239	0.0233	0.0242	342,853.0812	351,815.6166	339,390.6887
13	0.0266	0.0265	0.0283	292,918.8148	293,858.6445	275,439.9078
14	0.0172	0.0195	0.0202	331,696.3957	293,044.2919	281,651.7977
15	0.1256	0.1154	0.1027	198,768.5132	216,316.2892	243,065.0822
16	0.0812	0.0723	0.0802	306,656.4225	344,308.0800	310,630.4934
17	0.0289	0.0285	0.0291	227,658.1972	231,090.8987	225,920.1979
18	0.1493	0.1474	0.1515	167,045.0629	169,237.5321	164,634.1217
19	0.1195	0.1025	0.1361	208,484.0475	243,026.0156	182,953.8572
20	0.0693	0.0581	0.0899	360,119.1917	429,562.0288	277,677.3799
21	0.0769	0.0723	0.0748	318,448.6215	338,502.4655	327,398.0341
22	0.0359	0.0358	0.0384	369,222.0229	370,148.6630	344,818.3122

A method is required that factors in the regional variations in the measurement of  $df/dt$  relative to the localised inertias, whilst also accounting for the electrical distance to the disturbance.

## 6.6 Regional Inertia Estimation

In this analysis, estimation of the total system inertia and not the average throughout the network is of primary concern, so all of the results are presented with respect to  $H \cdot \text{MVA}$  as opposed to  $H$ .

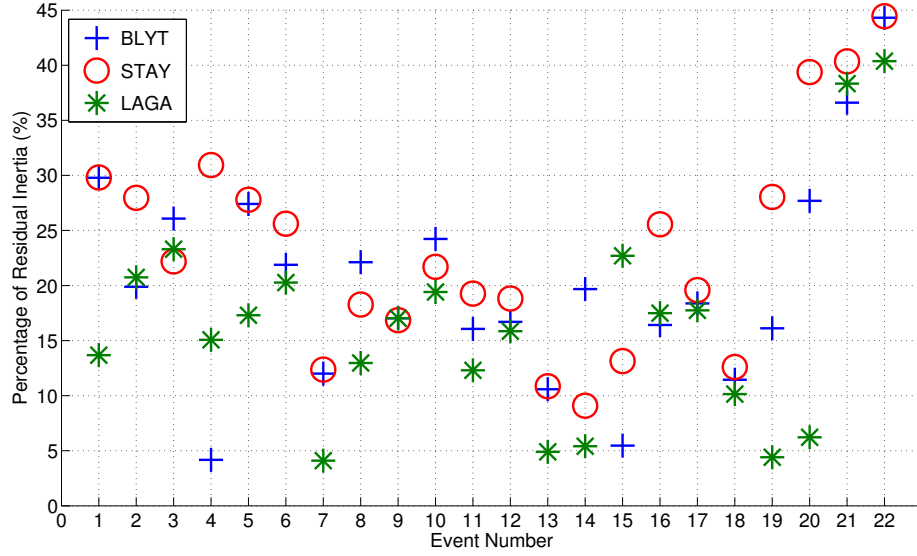


FIGURE 6.6: Variation in residual inertia estimation from 3 separate PMUs

The location of an event within the power system defines the specific electrical distance to generators and this in turn determines the corresponding frequency response of those generators. The response of generators closer to the disturbance will be more rapid and severe than the response of more distantly located generators [145]. Regardless of the electrical distance to a disturbance, the response of a generator will still be in proportion to the size of the loss relative to the generator's inertia.

From the swing equation for the  $i$ th ( $i = 1 \dots N$ ) generator the relative proportion of the loss  $\Delta P_i$  as seen by a generator,  $i$  can be determined. It should be noted that this is a time dependent variable, not all generators will 'see' the event at the same time, due to the propagation delay through the power network.

$$\Delta P_i = \frac{2H_i}{f_0} \cdot \frac{df_i}{dt} \quad (6.15)$$

If the  $df_i/dt$  for all generators can be precisely measured, for example, from a PMU installed at every generation bus, and with accurate information regarding

the inertia of the  $i$ th generator, then the summation of  $N$  swing equations can be used to determine the exact size of the loss,  $\Delta P$ .

$$\Delta \hat{P} = \sum_{i=1}^N \Delta P_i \quad (6.16)$$

Conversely, in the real system case for GB, if the size of the loss and total inertia from generation is accurately known in advance, then the total inertia for the whole system can be estimated from the ratio of the estimate of the loss  $\Delta \hat{P}$  to the known loss  $\Delta P$ . In simple terms, how much additional inertia must there be in the system in addition to that which is known about from transmission connected generation to achieve an accurate estimation for the size of the loss.

$$H_{Total} = \frac{\Delta P}{\Delta \hat{P}} \times H_{Gen} \quad (6.17)$$

The estimate of the loss  $\Delta \hat{P}$  for the GB system should always be less than the actual known value of the loss  $\Delta P$ , to account for the residual contributions to inertia.

### 6.6.1 Modelled Examples

In the following example the full dynamic model for the GB transmission system was used, as represented and simulated in Digsilent PowerFactory. The modelled scenario consisted of 104 individual generators, comprising 48 gensets, which have been represented by 41 monitoring nodes, with electrically local generation grouped together, as shown in Figure 6.7, as these points provided an accurate representation of the frequencies of the individual generators.

A simulation was run for 7 events spread across the network of England and Wales, to provide insight into the visibility of events around the system, located as shown again in Figure 6.7.

For the first simulated event a generator exporting 520MW to the network was tripped off, the system demand in MW and the total inertia of the system in H·MVA are as shown by the totals at the bottom of Table 6.3. The  $df_i/dt$  for the individual nodes was calculated following a lowpass filter at 0.5Hz cutoff over 500ms and is also provided, along with the relative proportion of the loss  $\Delta P_i$  that was seen by each node. The system frequency,  $f_0$  at the time of the disturbance ( $t = t_0$ ) was 50Hz.

It can be seen from Table 6.3 that for this simulated event the size of the loss was accurately estimated, coming out at 520.0035MW. In order to emphasis the effect that the relative location of the event to the monitoring node can have on this type of estimation, if the maximum and minimum values of  $df_i/dt$ , as measured to be -0.2373Hz/s and -0.0327Hz/s respectively, are taken and assumed to represent the total system, from Equation 6.15 and the totals of Table 6.3 this would result in a loss estimation of 2151.61MW and 296.49MW and respectively.

In order to understand how accurate the estimate can be based on the equivalent monitoring nodes of the 3 PMUs installed on the GB transmission network, the GB system was divided up into the North, Midlands and the South, according to the system constraint boundaries, as outlined in [11]. The boundaries were determined following detailed analysis looking at circuit flows, voltages and generator stability risks following faults and the loss of circuits. This process went on to identify critical circuits that can limit the flow of power from a specific area, in turn informing the boundaries of the transmission system [11].

As can be seen in Figure 6.8, the North of the system was grouped as all generation above constraint boundary B7a, combining all the generators in Scotland with the North of England. The South of the network was combined as everything below boundary B9 and the Midlands comprised of the generation in between the two.



TABLE 6.3: Loss estimation on a modelled example from 41 monitoring nodes

Node	MW	MVA	$H_i$	$H_i \cdot \text{MVA}$	$df_i/dt$	$\Delta P_i$
	Generated	Rating				
1	2	11	3.25	35.75	-0.0443	0.0633
2	485	660	4.98	3286.80	-0.2373	31.1957
3	261	156	5.00	781.25	-0.0416	1.2996
4	1200	1554	4.38	6806.52	-0.0462	12.5874
5	75	162	7.55	1226.12	-0.0351	1.7200
6	4	8	2.47	19.76	-0.0473	0.0374
7	1424	2118	4.71	9965.19	-0.0439	17.5140
8	140	170	6.50	1105.00	-0.0439	1.9397
9	2570	4432	4.44	19673.65	-0.0358	28.2018
10	6	16	4.79	76.64	-0.0473	0.1450
11	795	1764	3.48	6138.72	-0.0853	20.9556
12	958	1176	4.46	5244.96	-0.0486	10.2008
13	3225	3880	3.79	14705.20	-0.0392	23.0830
14	22	28	3.10	86.80	-0.0413	0.1432
15	537	776	3.19	2475.44	-0.0740	7.3232
16	1231	1612	3.44	5545.28	-0.0434	9.6242
17	1332	1764	4.12	7267.68	-0.0400	11.6193
18	686	1179	7.62	8976.63	-0.0933	33.5008
19	1450	2352	3.50	8232.00	-0.0343	11.2838
20	400	900	8.90	8010.00	-0.0333	10.6680
21	657	956	4.39	4196.84	-0.0636	10.6771
22	55	160	6.28	1004.80	-0.0405	1.6291
23	1596	2298	6.02	13838.56	-0.0329	18.2348
24	590	776	3.15	2444.40	-0.0418	4.0862
25	2421	3132	3.52	11034.04	-0.0383	16.9081
26	909	1552	3.15	4888.80	-0.1155	22.5823
27	635	1552	3.84	5959.68	-0.0438	10.4406
28	1719	2940	3.50	10290.00	-0.0327	13.4515
29	480	1715	5.45	9346.75	-0.0468	17.4997
30	930	1176	4.46	5244.96	-0.0390	8.1893
31	404	818	7.12	5820.07	-0.0492	11.4602
32	54	462	5.71	2638.02	-0.1135	11.9766
33	20	36	4.10	147.60	-0.0478	0.2822
34	438	1040	7.70	8008.00	-0.1671	53.5351
35	1594	2065	4.81	9938.98	-0.0379	15.0599
36	1845	2352	4.46	10489.92	-0.0471	19.7513
37	68	85	5.00	425.00	-0.0638	1.0845
38	740	1236	3.61	4461.96	-0.0600	10.7166
39	1250	1638	4.00	6555.28	-0.1479	38.7810
40	56	93	2.24	208.32	-0.0488	0.4067
41	1	24	3.10	74.40	-0.0486	0.1447
Totals	33265	50823	4.46	226675.76		520.0035

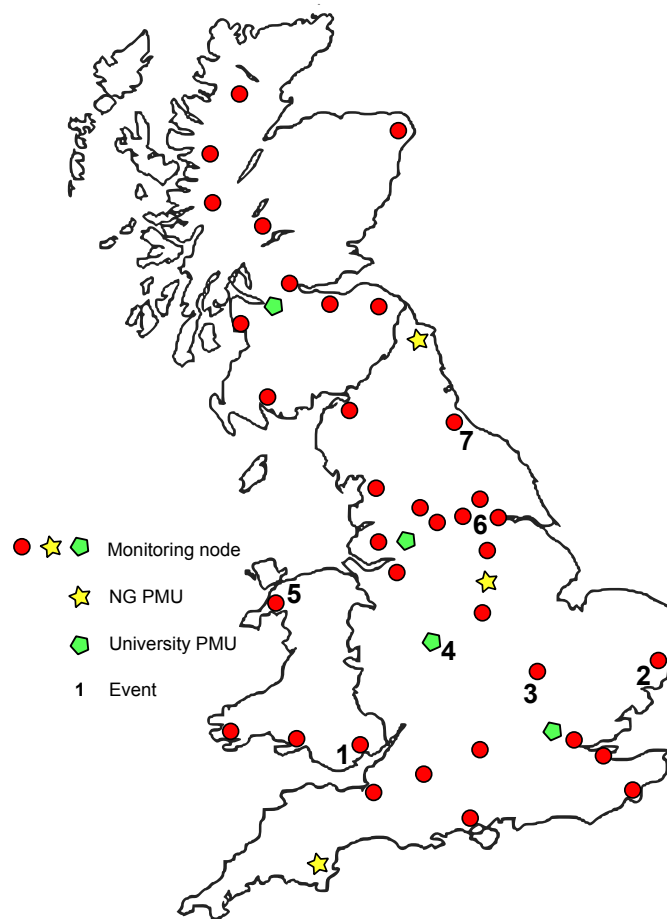


FIGURE 6.7: Location of monitoring nodes, installed PMUs and simulated events

It can be seen from Table 6.4 that the PMUs for the North, Midlands and the South correspond to nodes 3, 9 and 26 respectively. The grouped generation in terms of demand and inertia are also displayed along with the estimated proportions of the loss  $\Delta P_i$  and  $df_i/dt$ , which remain the same as for the previous table. As previously discussed the Midlands accounts for approximately 50% of the generation and hence the inertia. The other two system groups are considerably lighter. The estimate for the loss is now 3.6% higher than the known value however, if the  $df_i/dt$ , from the Staythorpe monitoring point is used solely to represent the whole the system, using Equation 6.15 and the totals from Table 6.3, the estimate for the loss would be 324.5997MW, which is only 62.4% of the known value, with this in mind the regional method can be considered extremely accurate.

To incorporate the available monitoring nodes from the University based WAMS,

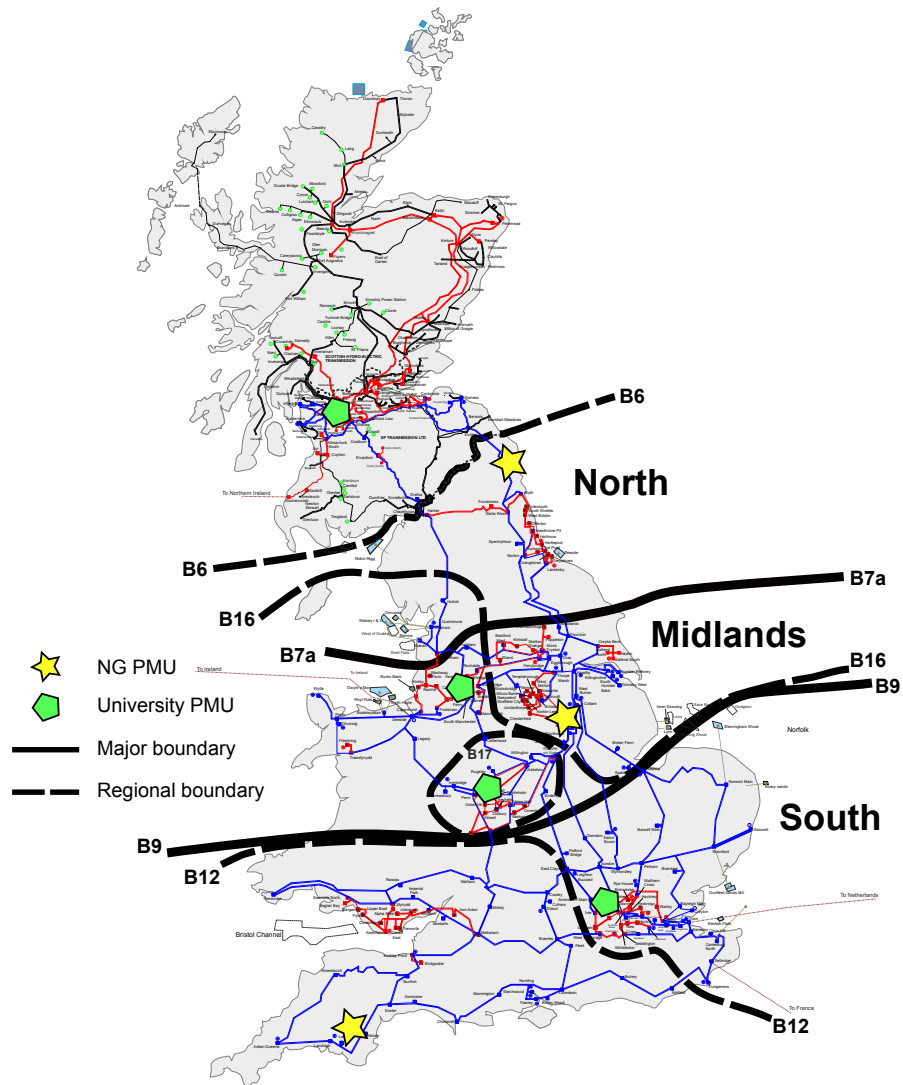


FIGURE 6.8: Generator groupings relative to PMU monitoring nodes

the network was divided again based on additional constraint boundaries, as shown in Figure 6.8 by the dashed lines. The corresponding monitoring nodes representing the Strathclyde, Manchester, Birmingham and Brunel PMUs are 5, 10, 12 and 37, as shown in Table 6.5.

The inclusion of the extra 4 PMUs from the Universities has a large impact on the results reducing the error to just -0.25% with the estimate for the loss being just over 1MW out.

The same procedure was applied to all 7 loss events from Figure 6.7 with the results of the estimation displayed in Table 6.6. With all 41 monitoring nodes available the approach can be considered reliably accurate, with the results always being within

TABLE 6.4: Inertia estimation on modelled example 1 based on 3 monitoring nodes

Node	MW	MVA	$H_i$	$H_i \cdot \text{MVA}$	$df_i/dt$	$\Delta P_i$
	Generated	Rating				
3	7348	11607	4.12	47829.99	-0.0416	79.5891
9	15478	25497	4.52	115161.36	-0.0358	164.9111
26	10439	13719	4.68	63684.41	-0.1155	294.2220
Totals	33265	50823	4.46	226675.76		538.7222

TABLE 6.5: Inertia estimation on modelled example 1 based on 7 monitoring nodes

Node	MW	MVA	$H_i$	$H_i \cdot \text{MVA}$	$df_i/dt$	$\Delta P_i$
	Generated	Rating				
3	3327	4224	3.38	14265.45	-0.0416	23.7303
5	2603	5479	3.91	21406.62	-0.0351	30.0549
9	11372	14490	4.21	61019.86	-0.0358	87.4707
10	4021	7383	4.28	31564.54	-0.0473	59.7226
12	2803	3928	4.51	17734.88	-0.0486	34.4922
26	4052	6951	5.38	37407.10	-0.1155	172.7909
37	5087	8368	5.17	43278.30	-0.0638	110.4358
Totals	33265	50823	4.46	226675.76		518.6975

about 1MW of exact, the approach accurately represents the whole network. The results for 7 monitoring nodes showed notable improvement over the results for 3 nodes, which in itself is considerably more accurate than the method employing just 1 node. Event 5 displaying the worst results because of its location in the system, isolated at the end of a long line, it can be determined from this study that a PMU is required local to that part of the system.

### 6.6.2 Results from Genuine GB System Events

Using the DFA method 22 suitable events were detected on the GB system, as previously outlined in Section 6.5 and detailed in Table 6.7 where the known size of the loss,  $\Delta P$  and total inertia from generation,  $H \cdot \text{MVA}$  are provided.

TABLE 6.6: Inertia estimation accuracy based on 7 modelled examples

Event	$\Delta P$	$\Delta \hat{P}$		$\Delta \hat{P}$		$\Delta \hat{P}$	
		N = 3	% diff	N = 7	% diff	N = 41	% diff
1	520	538.72	3.60	518.70	-0.25	520.00	0.00
2	601	644.50	7.24	633.73	5.45	600.32	-0.11
3	404	418.30	3.54	414.19	2.52	404.75	0.19
4	490	474.05	-3.26	492.27	0.46	490.41	0.08
5	486	494.76	1.80	492.45	1.33	487.51	0.31
6	645	669.43	3.79	657.29	1.91	644.87	-0.02
7	590	585.88	-0.70	588.78	-0.21	589.65	-0.06

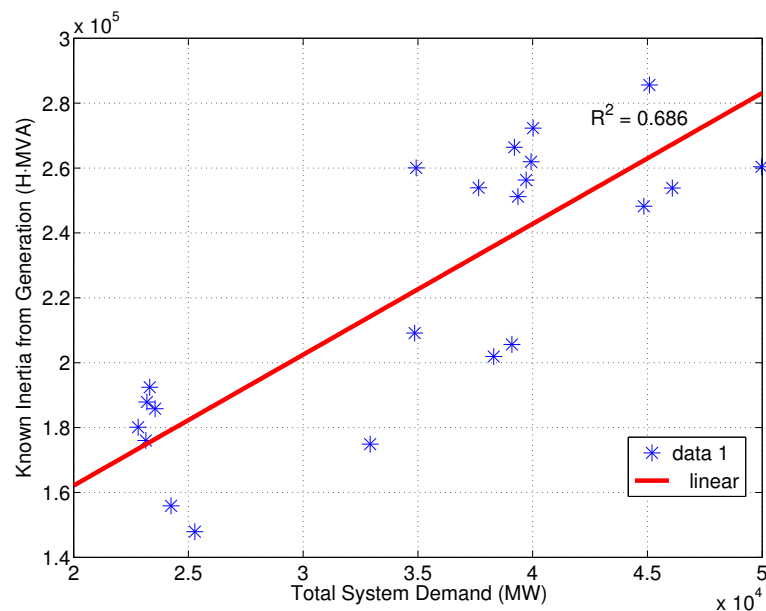


FIGURE 6.9: Known inertia from generation compared with total GB system demand for 22 separate generation loss events

It is currently assumed that system inertia varies linearly with system demand, as shown in Figure 6.9, this is becoming increasingly invalid on the GB system. The figure shows the ratio of system demand against the known value of inertia from generation, it can be clearly seen from the correlation coefficient,  $R^2$  value of 0.686 that this is definitely not a perfect linear relationship, system inertia does not increase exactly in line with demand. As the amount of renewable generation is continuing to increase and European market integration is continually developing, the percentage of non-synchronous generation on the GB system is rising and so

this assumption will become increasingly invalid.

TABLE 6.7: Inertia estimation based on 22 generation loss events from the GB transmission system with 3 monitoring nodes

Event	$\Delta P$	$\Delta \hat{P}$	$H_{Gen} \cdot \text{MVA}$	$H_{Tot} \cdot \text{MVA}$	$H_{Res} \cdot \text{MVA}$	% $H_{Res}$
1	380	284.96	253,932.63	338,621.50	84,688.87	25.01
2	360	272.23	209,139.06	276,569.90	67,430.84	24.38
3	354	270.84	155,858.45	203,712.60	47,854.15	23.49
4	240	189.44	251,204.53	318,248.96	67,044.43	21.07
5	590	449.24	180,125.10	236,564.12	56,439.02	23.86
6	300	229.75	272,310.84	355,567.95	83,257.11	23.42
7	212	191.1	260,056.55	288,504.10	28,447.55	9.86
8	316	262.21	192,428.56	231,907.36	39,478.80	17.02
9	320	266.17	176,032.93	211,636.24	35,603.31	16.82
10	312	244.14	248,224.95	317,216.74	68,991.79	21.75
11	324	269.33	253,840.30	305,365.74	51,525.44	16.87
12	328	270.39	285,612.67	346,470.76	60,858.09	17.57
13	312	285.69	261,934.93	286,062.18	24,127.25	8.43
14	228	205.99	266,418.37	294,883.64	28,465.27	9.65
15	999	852.74	187,890.67	220,061.86	32,171.19	14.62
16	996	784.07	256,306.14	325,667.29	69,361.15	21.30
17	263	213.37	185,821.70	229,039.84	43,218.14	18.87
18	998	879.88	147,920.44	167,693.40	19,772.96	11.79
19	996	845.71	174,881.98	206,011.84	31,129.86	15.11
20	999	762.45	260,402.39	341,105.12	80,702.73	23.66
21	980	840.4	201,902.08	235,321.44	33,419.36	14.20
22	530	417.03	205,614.39	261,163.76	55,549.37	21.27
Average					50,433.49	18.18

The total inertia of the system was estimated based on the ratio of the estimate of the loss  $\Delta \hat{P}$  to the known loss  $\Delta P$ , from Equation 6.17, using the regional inertia estimation method based on the 3 available PMUs

The results of total system inertia estimation are displayed in Table 6.7 and with this an estimate for the percentage of inertia provided by residual sources. The residual sources estimate is seen to vary from around 8% to 25% of total system inertia, with an average of 18.18% over the 22 events. When comparing these

estimates to the results of Section 6.5, it can be seen that there is far less variation, as the regional approach has much greater visibility of the network dynamics.

To further validate the regional approach data from the University PMUs was added. Applicable data was only captured for 3 of the events, namely 18, 19 and 20, as the University system transmits the PMU data to a remote server and currently operates on 2 weeks worth of rolling storage.

The network was divided into the 7 aforementioned regions, with the improvement to total inertia estimation and hence the estimate for the residual contribution now provided in Table 6.8.

TABLE 6.8: Inertia estimation based on 3 generation loss events from the GB transmission system with 7 monitoring nodes

Event	$\Delta P$	$\Delta \hat{P}$	$H_{Gen} \cdot \text{MVA}$	$H_{Tot} \cdot \text{MVA}$	% $H_{Res}$
18	998	894.48	147,920.44	164,956.89	10.33
19	996	847.22	174,881.98	205,644.55	14.96
20	999	765.28	260,402.39	339,845.40	23.38

The inclusion of the data from the additional PMUs provides a marginal adjustment to the inertia estimates. It should be noted that the 3 events were all from the loss of the BiPole to France in the South East of England, and so for this event the existing 3 NG PMUs can be considered to provide relatively good coverage over the impact to the whole network.

Applying continuous analysis of transmission events is likely to yield a more accurate estimate for the residual contribution to system inertia, this will also be continually improved as additional PMUs are added to the network and the reliability and accuracy of the existing devices is improved. This will lead to an increased coverage of the regional variations in the network. Further work is thus proposed to investigate the PMU placement requirements for full visibility of all system events, so that a robust monitoring solution can be developed to capture the true inertial frequency response of the whole GB system.

## 6.7 Concluding Remarks

In this chapter a method was demonstrated for estimating the total inertia of the GB power system, by dividing the network into groups or regions of generation based around the constraint boundaries of the GB network. The inertia was first estimated at a regional level before a summation is provided to give a total estimate for the whole network. This estimate is then compared with the known contribution to inertia from generation, to provide an estimate for the currently unknown contribution to inertia from residual sources; namely synchronously connected demand and embedded generation.

The accuracy of the approach was first demonstrated on the full dynamic model of the GB power system before results were presented from analysing the impact of a number of instantaneous transmission in-feed loss events, using phase-angle data provided by the 3 PMUs from the GB transmission network and also the devices installed at the domestic supply at 4 GB Universities.

The method was shown to be considerably more reliable than the approach based on a single monitoring node of the system, with the estimate for the contribution of inertia from residual sources coming out to between 8% and 25%.



# Chapter 7

## Conclusions and Further Work

### 7.1 Thesis Summary and Conclusions

The motivations for the research presented in this thesis were outlined in the first chapter, stemming from the massive amount of changes due to impact the GB electricity system as a result of the binding climate change targets enforced from UK Government and European Parliaments [1–3].

The GB system is required to accommodate an increasing volume of renewable energy, predominantly in the form of offshore wind, asynchronously connecting to the periphery of the transmission system. This displacement of traditional thermal generation is leading to a significant reduction in system inertia, thus making the task of system operation more challenging. The inevitable shift towards a more dynamic system compounds the existing issues of calculating generator response and reserve requirements, which traditionally assume that system inertia varies linearly with demand. With demand being met by a growing percentage of asynchronous generation, such as renewables and HVDC interconnectors, this assumption is becoming increasingly invalid [29, 30]. Frequency services are becoming more complicated and less predictable throughout the day, forcing reassessment of generation patterns and limitations on single circuit risks, making it more difficult to maintain security for all credible contingencies.

It is therefore necessary to gain an improved understanding of both the inertial frequency response of the power system and the security of the system in near to real-time. This will ensure the impact of incidents to specific areas of the network is understood, facilitating a more economically efficient operation of the power system. Importance is therefore placed on the provision of high resolution, time-synchronised measurements that are now vital for this analysis [29, 30].

In Chapter 2 an introduction to the concepts behind phasor measurement technology was provided, from the history behind PMUs to their growing use in electric power systems today. A summary of the global PMU deployment approaches, outlined that a large amount of investment is being provided to utilities and system operators for the continued extension of WAMS networks, in a major effort to provide an increased awareness of the evolving power system conditions. In the case of the US system current funding sits at over \$300 million [64].

The motivations behind the global PMU deployments are similar and stem from large challenges due to the integration of growing volumes of renewable generation and increased levels of interconnection with neighbouring TSOs. With power being transported over ever increasing distances at higher levels PMU data is being made available to improve situational awareness for system operators by furthering the wide area visibility of the power system.

The predominant application of synchrophasor technology is the monitoring of intra-area oscillation damping, as growing transmission distances and increased power flow variances are exciting existing modes. There is also growing concern over the presence of new modes of oscillation as a result of the rapidly developing systems.

One of the challenges identified in WAMS deployment are the supporting infrastructures in the communication systems and data storage requirements, as they are very different from those of existing power systems operations. Taking the example of the Chinese system where 10,000 phasors are already being stored at 100Hz in some PDCs, a phenomenal amount of data is being created [63], importance is firmly placed around understanding the long term storage requirements

of WAMS networks. An understanding is also required as to the application intentions of the PMU deployment, taking the example of the Nordic system where PMUs have been installed primarily for inter-area damping estimation and the PMU data is actually down-sampled to 10Hz [73] saving hugely on the storage of data, without compromising the accuracy of the applications. It is important to note however, that the downsampling of PMU data may not be suitable for the GB system as this could reduce the accuracy for other applications, such as inertia estimation or the monitoring or SSR, as is the intention in the VISOR project [59].

The other TSOs also already have experience with a lot of the new technology challenges set to face the GB system, with TCSC and intra-network HVDC already part of some of the networks. The most apparent example of this being the progression of the Nordic system from WAMS to WACS over a 5-10 year period [77], as it outlines the experience and knowledge required from the monitoring applications to be able to progress to wide-area control. The coordination between the involved TSOs of the network is also vital and this compares with the future requirements for WAMS on the GB system, in the necessity to acquire synchrophasor data from all of the TO's.

In order to understand the scale of the future monitoring challenges a review was provided of the existing SM practices at NG in Chapter 3. The current approaches, some of which having been in place for up to 20-years, were not deemed suitable to meet the requirements of the evolving network [79]. With growing levels of system variability and complexity, the traditional network assessment approach is deemed to be conducted too far in advance of live operations and as such is becoming increasingly unreliable. Greater accuracy is proposed with real-time system monitoring through the installation of PMUs or similar synchrophasor capable devices. The PMUs will also permit massive improvements to offline studies, through the relative ease of collating and time-aligning the data [87].

However, until recently [59], no direct funding had been made available for the wide scale deployment of PMUs. By contrast with the experience of other TSOs, the newly approved GB project (December 2013) has a more specific focus on

applications, and is not intended to fund a widespread rollout of PMUs. The GB project will facilitate data sharing between the three TOs, as recommended in this thesis, and trial new applications for risk mitigation and constraint management. Infrastructure requirements will also be addressed, but the actual widespread deployment is expected by the regulator to be justified as business as usual expense.

All of the previous installations of PMUs on the network has been part of business as usual practices. PMUs have predominantly been provided to the network through the upgrading of DFRs, as part of a bottom-up approach whereby the provision of synchronised data and how it can benefit areas of planning, operations and eventually control actions, is expected to develop business cases. It has been suggested that PMUs could provide improvements to a number of existing monitoring practices, through increased data resolution and the added benefit of time-synchronised measurements [79]. The installation of PMUs would offer a means to combine the SM requirements of DSM, PQ and FATE and may also provide visibility for ASBMON requirements [79].

This could result in a potentially large quantity of PMUs, the following would therefore need to be confirmed:

- The data resolution requirements for individual SM applications.
- Identification of communication system requirements for each different SM function.
- The need for and capacity of data storage, either locally, remotely or both, for all SM equipment.

With the increasing connection of HVDC interconnectors and non-synchronous wind farms to the network, concern is growing around power quality through increased interactions with the AC system and displacement of system inertia. To that extent much greater knowledge is required over the systems dynamics [29].

The provision of data from the Scottish TOs is also becoming vitally important to securing such future networks, as a large amount of the new generation and

technology is being installed in the Scottish part of the network, increasing the amount of uncertainty around system performance. It is also suggested that, as European market integration continues to develop, shared PMU data with the neighbouring TSOs of Ireland Central Europe and the Nordic countries may also be required, as the relative security of one system will have an increasing impact on the others.

In Chapter 4 the existing WAMS of the GB transmission system was analysed. Comparisons were made between the voltage magnitude and phase angle values of the PMUs with the output values from the SE. This served to both validate the data from the PMUs and also further highlighted some measurement errors with one of the devices [40]. The comparison was confirmed as being straightforward during steady-state operation and it was outlined that the presence of a system event should be used as a trigger to re-run the SE so that the most up to date view of the network could be provided [40].

An analysis was also provided of the communications infrastructure of the WAMS network in the configuration within NG's BLAN, it was concluded that this would only be suitable going forward if a dedicated proportion of the LAN could be reserved for SM. Monitoring nodes that are identified as vital to the operation of the transmission system should potentially be equipped with localised storage so that in the absence of sufficient communications the data is not lost. Alternatively, as PMUs become more critical to the planning and operation of the transmission system, they should be installed within a robust and reliable communications network [40]. The requirements for the future volumes of data storage were also considered along with the necessity for fast acting event detection algorithms capable of analysing massive datasets.

The ability of a University based WAMS network to monitor the transmission network was discussed and demonstrated to provide greater visibility for applications concerned with post-event analysis. The data was shown to provide greater insight into the response of the network to system events, through the provision of frequency and voltage phase angle data [29].

Having outlined the requirements for event detection algorithms, Chapter 5 presented a novel methodology based on Detrended Fluctuation Analysis [40]. The method was demonstrated as a basic means of event source location through the identification of the closest PMU to an event, and also the determination of the exact event start time ( $t = t_0$ ), deemed vital to inertia estimation methodologies.

This work led on to determining the suitability of a transmission system event to provide an estimate for the total inertia of the power system, the key requirement being the identification of the instantaneous nature of a loss. The identification of such events were demonstrated, again using the DFA algorithm [29, 30]. Understanding the future requirements for fast acting algorithms and the implications of large datasets, the approach was then further expanded to be parallellised for use on massive volumes of PMU data. With this, an introduction to Big Data analytics was provided and the implementation of the Parallel DFA (PDFA) approach was presented in the MapReduce programming model [109].

Experimental results proved the speedup capabilities of PDFA in computation whilst maintaining relative accuracy in comparison with the sequential DFA. This analysis into the speedup of computation, led to an improvement to Amdahls law being proposed, this work introduced the ratio of communication to computation to enhance the capability to analyse the performance gain in computation when parallelizing data intensive applications in a cluster computing environment [109].

In Chapter 6 a method was presented for estimating the total inertia of the GB power system. Following a demonstration of the issues associated with the existing literature based methods of inertia estimation, a method was proposed based on the summation of inertia estimates at a regional level [29]. The method divides the network into groups or regions of generation based around the constraint boundaries of the GB network, before calculating an accurate value of localised inertia. The summation of these regional estimates is then considered to represent the total inertia of the power system. The value is then compared with the known contribution to inertia from generation, to provide an estimate for the currently

unknown contribution to inertia from residual sources; namely synchronously connected demand and embedded generation.

The accuracy and reliability of the regional methodology was initially demonstrated on the full dynamic model of the GB power system before results were presented from analysing the impact of a number of genuine instantaneous transmission in-feed loss events, using phase angle data provided by the 3 PMUs from the GB transmission network, specifically devices from the England and Wales network. The approach was further qualified using the devices installed at the domestic supply from 4 GB Universities. The method was shown to be considerably more reliable than an approach based on a single monitoring node of the system, which presents comparably unusable results. The estimate for the contribution of inertia from residual sources was estimated to be between 8% and 25% [29], which confirms a reluctance to work with the previous assumed value of 20%.

### 7.1.1 Thesis Contributions

The research that has been presented in this thesis was concerned with three specific areas:

- The identification of disturbances on the transmission network.
- Determining the suitability of a disturbance to provide an estimate of the total inertia available in the power system
- The development of a method to determine the inertia available in the power system, more specifically to estimate the percentage of inertia provided by residual sources.

The first area led to the development of a novel event detection algorithm based on Detrended Fluctuation Analysis [40]. This method was initially suggested to form a trigger for the activation of the steady-state estimator, prompting it to be rerun to provide the most up to date view of the network. The method also

provides a basic method of event source location by identifying the PMU closest electrically to a disturbance [40].

The algorithm was then developed for the specific identification of frequency disturbances for the purpose of inertia estimation, from an understanding that these events provide the only means of analysing the true response of the power system [29, 30]. The impending future requirements for fast acting algorithms and the implications of large datasets, led to the approach being expanded and parallellised for the use on massive volumes of PMU data [109].

The second area identified the specific requirements for a generation loss event suitable for inertia estimation. The inertia estimation approaches are based on the swing equation and as such require a loss to the system prompting the system frequency to fall. It is required that the loss is instantaneous from a breaker action and must not be staggered such as a loss from multiple gensets, so that the value of the loss can be determined through SCADA measurements [29, 30].

This can be determined with the DFA method, which also identifies the exact start of the event, also deemed to be key to maintaining the accuracy of the inertia estimation methodology [29, 30].

The third area recognised the requirements for a greater understanding of the inertial frequency response of the GB power system, and with this greater knowledge was required over the variations in terms of frequency stability around the system. This should enable a more accurate approach to the calculation of generator response and reserve requirements, facilitating a more economic operation of the power system.

On this basis a method was demonstrated for estimating the total inertia of the GB power system. Based on the summation of separate estimates of inertia from a regional level. The method divides the network into groups or regions of generation based around the constraint boundaries of the GB network. This estimate is then compared with the known contribution to inertia from generation, to provide an



estimate for the currently unknown contribution to inertia from residual sources; namely synchronously connected demand and embedded generation [29].

## 7.2 Further Work

In the following section further work is proposed as a continuation of the work presented in this thesis.

### 7.2.1 Modelling and Analysis of WAMS Information and Communication Technology Infrastructures

In order to understand the minimum requirements in terms of bandwidth for a WAMS communications network, a simple model has been developed using the network simulation tool OPNET.

The model consists of 6 substations, configured to have different distances from the PDC, based on the known geographical distances at this stage, as the true length of the communications link will be unknown. The connectivity in terms of network link bandwidth is the same as for the real case shown in Figure 4.3, with substation 4 having a 2Mbps link and the rest having a 256Kbps link. In addition substations 5 and 6 have been equipped with two PMUs.

At this stage, to tailor the performance to be comparable with the measured results of Figure 4.4 different levels of background traffic have been factored into the model. Background traffic is introduced by adding additional workstations into the substations. All substations have one local server and several workstations. Substations 1 to 3 are assumed to have a similar structure and each of them has five workstations such that one of them is defined to operate as a PMU, this is equivalent to having 50% background traffic. Substation 4 was modelled to have 13 workstations with one of the workstations as a PMU, equivalent to 70%

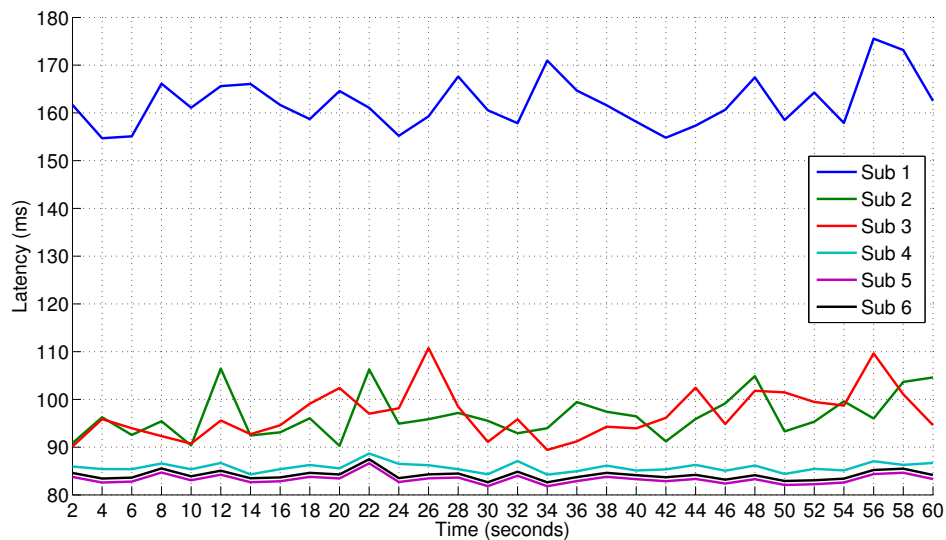


FIGURE 7.1: Network latencies for 6 modelled PMUs using the OPNET model

background traffic. Finally, substations 5 and 6 have been configured with 0% background traffic.

To account for the different PMUs internal processing latencies a delay of 95ms was introduced into the node model for substation 1 to be consistent with the parameters of the Arbiter PMU and a 30ms delay was introduced into all the other substations through the packet stream connected to the application layer.

The initial results are as displayed in Figure 7.1 and are comparable with the original analysis carried out on the wireshark data in Chapter 4.

The model has been used to analyse the minimum amount of dedicated bandwidth required to achieve suitable performance from 256Kbps and 2Mbps links, it can be seen that the 256Kbps link starts to show unsatisfactory performance when the background traffic exceeds 40%. The sudden rise in latency is considered to either be due to 100% utilisation of the bandwidth or as a result of collisions from the retransmission of TCP packets.

It is proposed that this model be improved with the provision of additional data on the performance of the real WAMS network at NG. More specific details will also be added to the model to cater for the different internal delays for all PMUs in use on the GB system. It is also proposed to develop the model to consider the

TABLE 7.1: Network latencies for variable background traffic

Background Traffic (%)	Number of PMUs	Bandwidth 256Kbps Latency (ms)	Bandwidth 2Mbps Latency (ms)
0	1	82.3	80.0
	2	83.8	80.7
	3	84.8	82.1
	4	86.3	82.3
20	1	87.3	80.3
	2	88.8	81.3
	3	91.3	82.3
	4	101.1	82.7
40	1	92.4	81.6
	2	97.4	82.2
	3	133.6	82.7
	4	3512.9	84.0
60	1	107.4	83.7
	2	176.3	84.1
	3	3603.8	84.9
	4	-	85.0

future WAMS network that will contain multiple PDCs and a SPDC to determine the requirements in terms of network connectivity at the various levels.

## 7.2.2 Development of an Ambient Inertia Estimation Methodology

Existing methods for the estimation of power system inertia are based on analysis following a disturbance such as a generation trip, these do not occur frequently enough on the GB system to provide network operators with up to date enough information, a method is required to determine the relative stability of the system in near to real-time.

The following section details some initial work analysing the ambient data of the power system to investigate any potentially detectable correlation between the inertia of the power system and the dominant inter-area mode of oscillation.

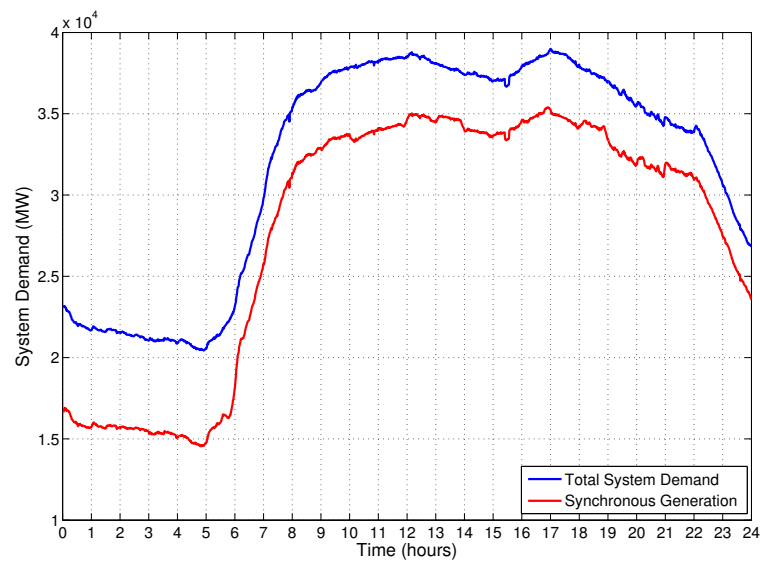


FIGURE 7.2: Total system demand with contribution from synchronous generation.

Inter-area oscillations are a common feature in interconnected power grids. They occur where two or more groups of generators connected through a relatively weak interconnection swing against each other. The frequencies of the oscillations are specific for each power system, and may also depend on the current operational conditions of the system. The modes are continually excited as a result of variations in generation and demand, system faults, and standard switching operations. However, the overriding influence over the oscillations is known to be the relative strength or the impedance of the network, and the inertia of the interconnected areas of the power system. The damping ratio and frequency of the inter-area mode will both decrease as system inertia and tie line impedance increase [146, 147]. It is important to note that the dominant inter-area mode present in the GB system [13, 148] is typically well damped, due to power system stabilizers (PSS) installed at generators throughout the GB network. The damping of inter-area modes can also be influenced by voltage control devices such as SVCs that do not contain an inertia component.

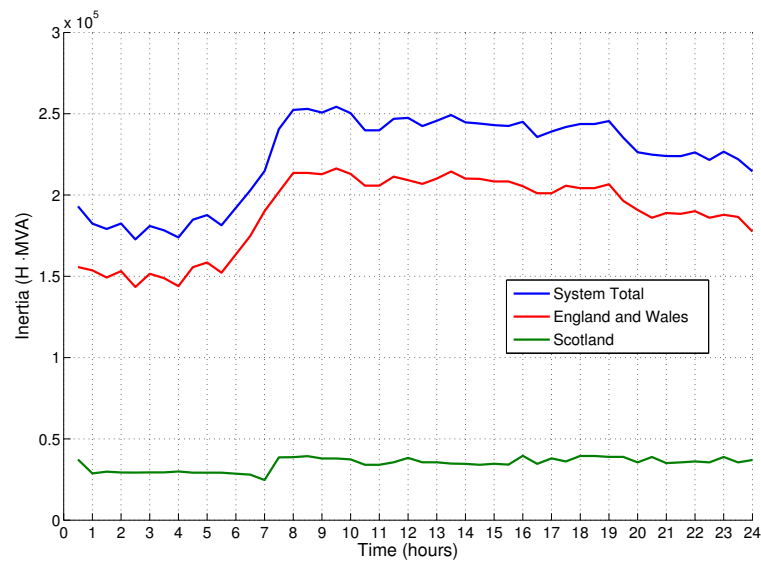


FIGURE 7.3: Total inertia from generation ( $H \cdot MVA$ ), including a split between Scotland and the network of England & Wales.

### 7.2.2.1 System Studies

To identify the inter-area mode of the GB system the voltage phase angle difference between the PMU closest to the Scotland-England border at Blyth and a reference node was analysed. The PMU located nearest to the electrical center of the network at Staythorpe provided the reference phasor. The analysis was carried out on data sampled at 50Hz for a day representing the summer minimum demand of 2013, where the configuration of the boundary circuits and the hence the impedance remained constant. The system demand for the day is displayed in Figure 7.2, separated in terms of the total demand and the amount of that demand that is met with synchronous generation.

The amount of synchronous generation online is shown in Figure 7.3, with the contribution from the Scottish system separated from that of the England & Wales portion of the network. For this specific day, the synchronous inertia of the Scottish system is less than one-third that of the system of England & Wales. The quantity of synchronous inertia in the Scottish portion of the system is seen to remain relatively constant, whereas the England & Wales portion of the network has an inertia which is observed to vary throughout the day.

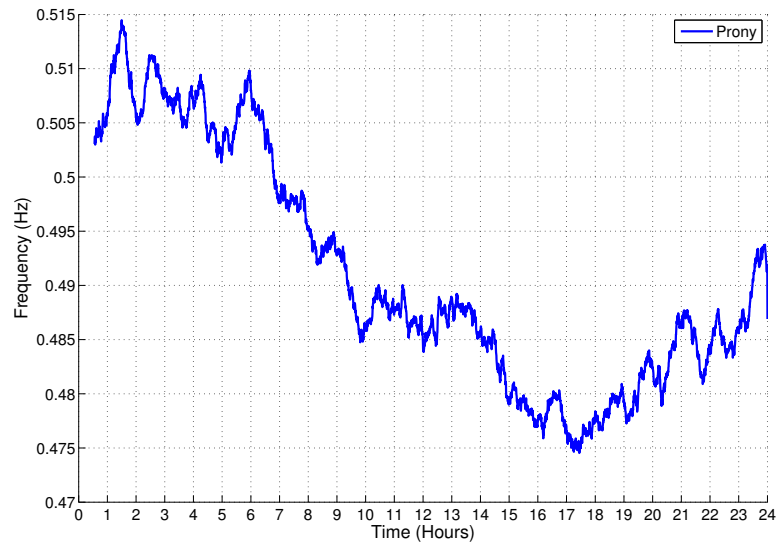


FIGURE 7.4: Analysis of the inter-area oscillation frequency using Prony’s method.

### 7.2.2.2 Inter-Area Oscillation Analysis

The Prony algorithm was run in the Matlab environment using a 20 second (1000 samples) sliding window with a 50% overlap. The results for the frequency estimation are displayed in Figure 7.4.

The modal frequency can be seen to reduce beginning at 06:00, which correlates to the increase in inertia from generation as shown in Figure 7.3. The modal frequency then begins to increase again at around 18:00-19:00 as the system inertia begins to decrease due to reduced system generation. From these results it can be seen that the varying inertia of the system in England & Wales is the dominant factor affecting the frequency of the inter-area oscillation.

### 7.2.2.3 System Impedance Analysis

In order to further investigate the effect of the tie line impedance on the modal frequency, an analysis was carried out over two separate days where all of the

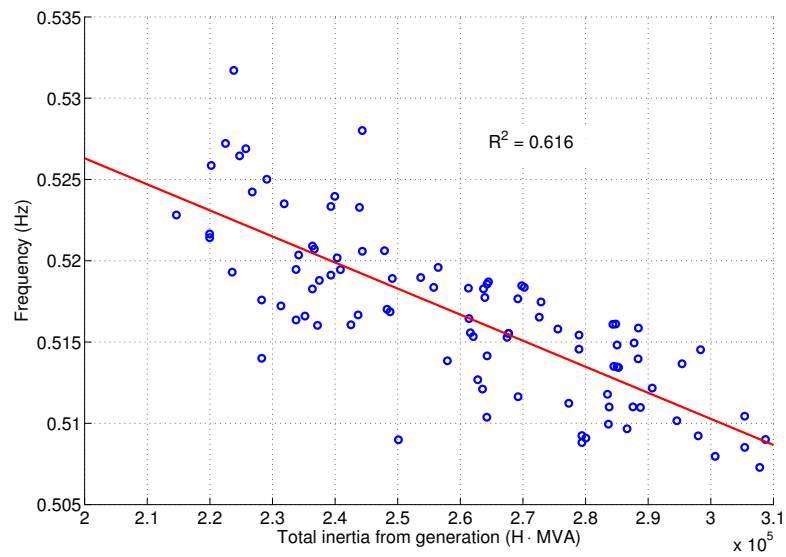


FIGURE 7.5: Frequency of inter-area mode plotted against inertia from generation, with all tie line circuits in service.

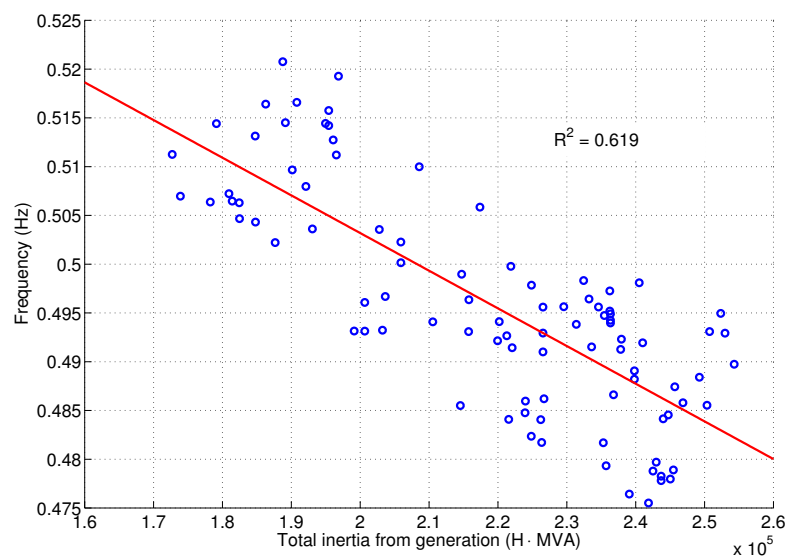


FIGURE 7.6: Frequency of inter-area mode plotted against inertia from generation, with one of the tie line circuits out of service.

boundary circuits were connected and therefore the impedance maintained constant value. The known inertia from generation was compared against the average frequency over half-hour windows. The results in Figure 7.5 show a good correlation over a wide range of inertial values, with modal frequency reduction corresponding to the increase of inertia.

The same study was applied with one of the double circuits of the Anglo-Scottish tie line running as a single circuit, thus increasing the impedance of the link. The results displayed in Figure 7.6 again show good correlation, but the overall modal frequency is reduced relative to the previous case for similar values of inertia, as a result of the impedance increase.

It is proposed that this analysis be carried out for a wider range of scenarios, potentially combining data from the Scottish network to provide a more accurate picture of the inter-area mode. The amount of powerflow down the interconnection also needs to be taken into consideration.



# Appendix A

## Generation Boundaries and Location of PMUs

This section serves to illustrate the location of the PMUs used in the analysis presented in this thesis. It also depicts the generation boundaries of the GB transmission system, as utilised in Chapter 6.

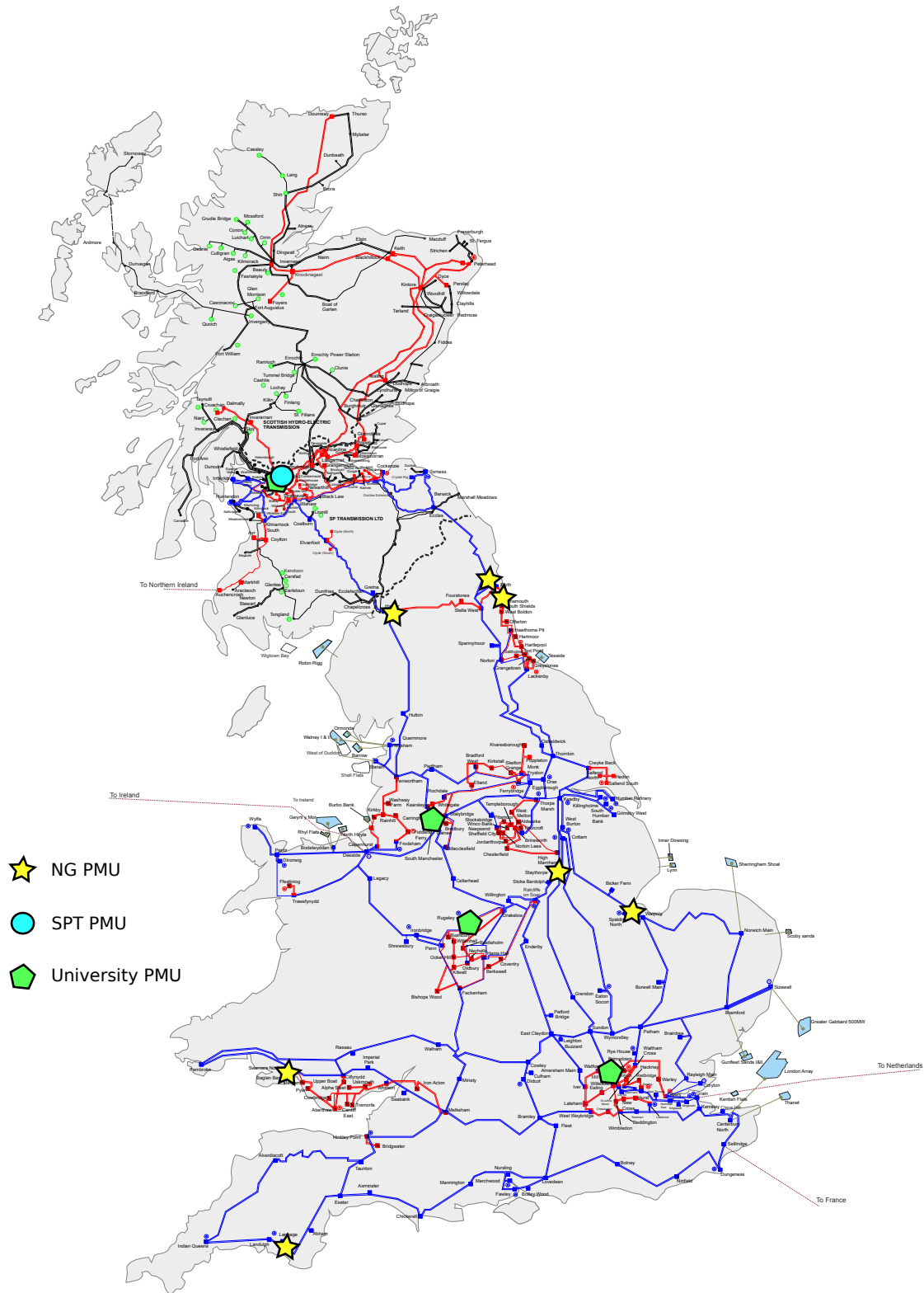


FIGURE A.1: Location of installed PMUs used in this thesis

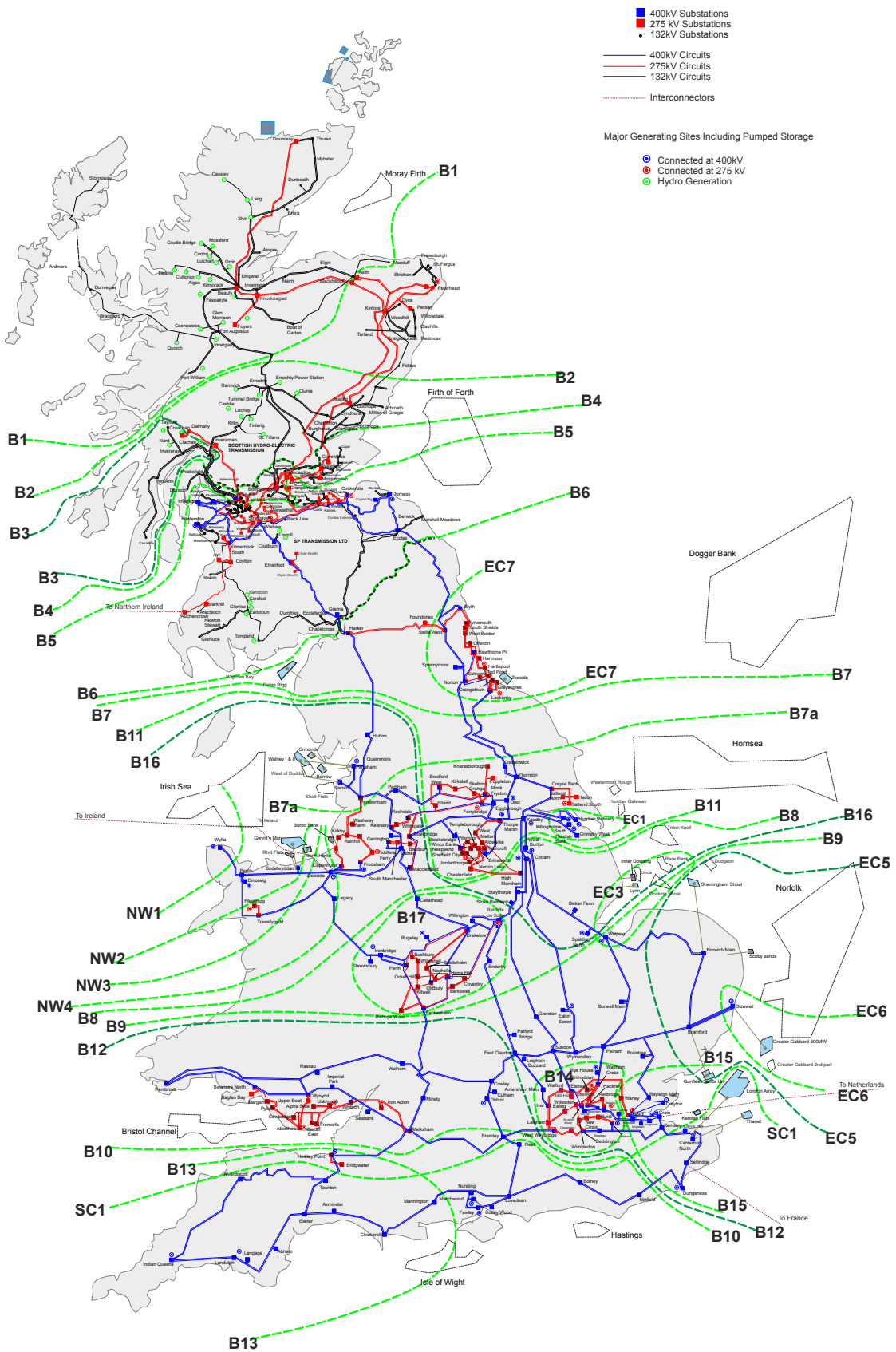


FIGURE A.2: Generation boundaries of the GB transmission system

# Appendix B

## Location of DSM Units in England and Wales

This section serves to illustrate the location of the DSM units on the transmission system of England and Wales, all of these devices have the potential to provide PMU functionality.

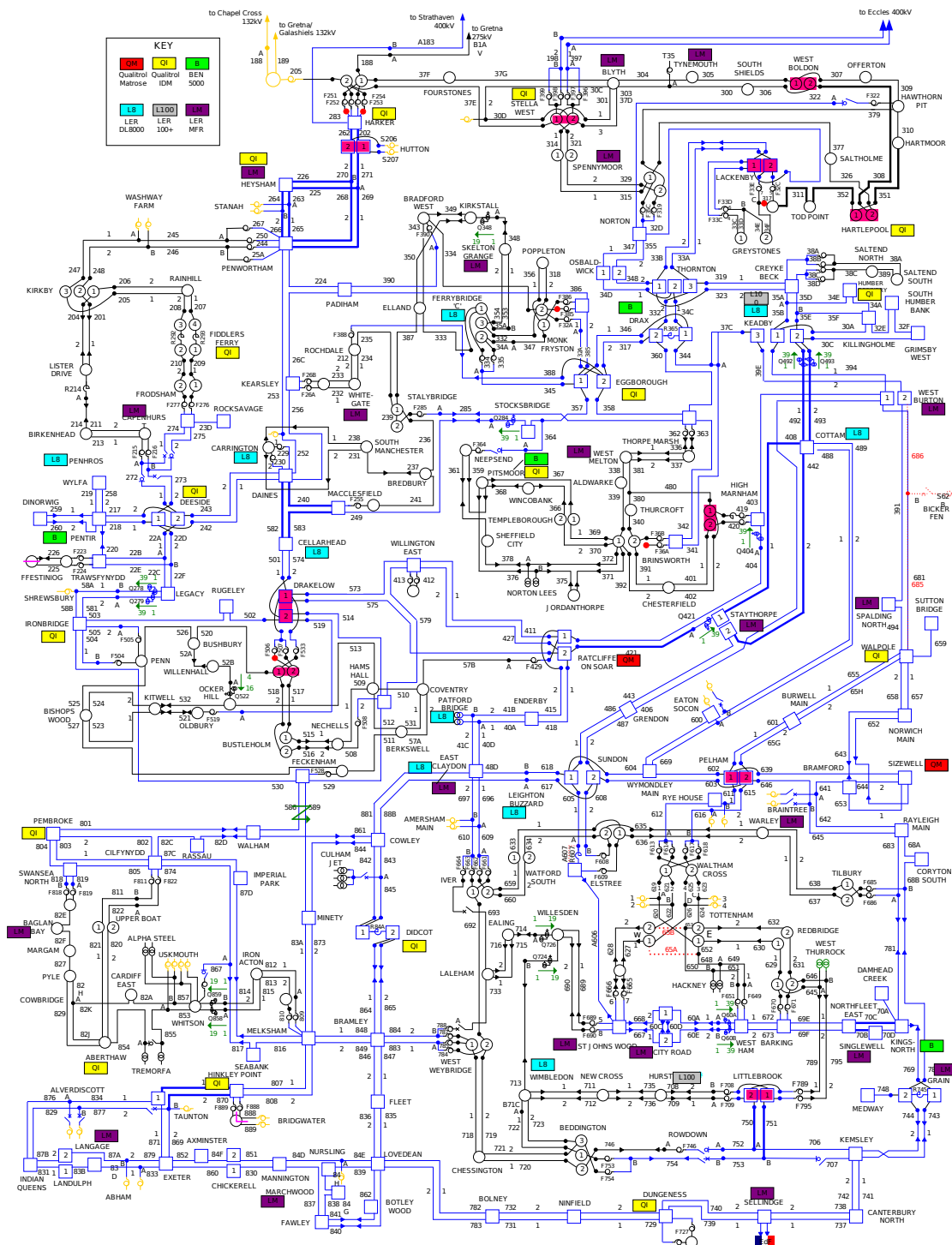


FIGURE B.1: Location of DSM units on the transmission system of England and Wales

# References

- [1] *Meeting the Energy Challenge A White Paper on Energy*. UK Departement of Trade and Industry, 2007.
- [2] *The Climate Change Act 2008*. HM Government United Kingdom, 2008.
- [3] The European Commission. *A Roadmap for moving to a competitive low carbon economy in 2050*. European Commission, Belgium, 2011.
- [4] *Our Electricity Transmission Network: A Vision for 2020*. Electricity Networks Strategy Group (ENSG), 2009.
- [5] *Our Electricity Transmission Network: A Vision for 2020*. Electricity Networks Strategy Group (ENSG), 2012.
- [6] *The Low Carbon Transition Plan, National Strategy for Climate and Energy*. The Department of Energy and Climate Change (DECC), 2009.
- [7] *The UK Renewable Energy Roadmap*. The Department of Energy and Climate Change, 2011.
- [8] *UK Future Energy Scenarios, July 2013*. Energy and Strategy Policy, National Grid UK, 2013.
- [9] *Winter Outlook Report 2013/2014*. National Grid, UK, October 2013.
- [10] *Summer Outlook Report 2014*. National Grid, UK, April 2014.
- [11] *Electricity Ten Year Statement*. National Grid, UK, 2013.

- 
- [12] *Grid Code Review Panel (GCRP) meeting report, frequency changes working group*. National Grid, UK, July 2013.
- [13] A. Myles. Application of power system stabilisers on the anglo-scottish interconnection, british system operation experience. *IEE Proc. Generation, Transmission, and Distribution*, 135(3), May 1988.
- [14] UK Ofgem. *Project Discovery - Energy Market Scenarios*. 2009.
- [15] Food Department for Environment and Rural Affairs (Defra). *Large Combustion Plant Directive (LCPD) - Update No. 7 to the final UK National Plan*. [www.defra.gov.uk](http://www.defra.gov.uk), October 2012.
- [16] UK Ofgem. *RHIO - A new way to regulate energy networks*. 2010.
- [17] European Network of Transmission System Operators for Electricity (ENTSO-E). *Ten Year Development Plan*. ENTSO-E, 2012.
- [18] e Highway 2050. *Modular Development Plan of the Pan-European Transmission System 2050*. Online, <http://www.e-highway2050.eu/e-highway2050/>, 2013.
- [19] Cordination of Electricity System Operators (Coreso). *Company Overview*. Online [www.coreso.eu](http://www.coreso.eu), 2014.
- [20] TSC. *Transmission System Operator Security Cooperation*. <http://www.tso-security-cooperation.net>, 2014.
- [21] UK Ofgem. *RHIO Factsheet - Price Controls Explained*. 2013.
- [22] A. G. Phadke and J. S. Thorpe. *Synchronised Phasor Measurements and Their Applications*. Springer, USA, 2008.
- [23] A. G. Phadke, J. S. Thorp, and K. J. Karimi. State estimation with phasor measurements. *IEEE Transactions on Power Systems*, 1:233–238, 1986.
- [24] M. B. Boisen T. L. Baldwin, L. Mili and R. Adapa. Power system observability with minimal phasor measurement placement. *IEEE Transactions on Power Systems*, 8(2):707–715, May 1993.

- 
- [25] V. Terzija, G. Valverde, D. Cai, P. Regulski, V. Madani, J. Fitch, S. Skok, M. Begovic, and A. Phadke. Wide area monitoring protection and control of future electric power networks. In *Proceedings of the IEEE*, pages 80–93, 2011.
- [26] Toshio Inoue, Haruhito Taniguchi, Yasuyuki Ikeguchi, and Kiyoshi Yoshida. Estimation of power system inertia constant and capacity of spinning-reserve support generators using measured frequency transients. *IEEE Transactions on Power Systems*, 12(1):136–143, Feb. 1997.
- [27] D. P. Chassin, Z. Huang, M. K. Donnelly, C. Hassler, E. Ramirez, and C. Ray. Estimation of WECC system inertia using observed frequency transients. *IEEE Transactions on Power Systems*, 20(2):1190–1192, May 2005.
- [28] P. Wall and V. Terzija. Simultaneous estimation of the time of disturbance and inertia in power systems. *IEEE Transactions on Power Delivery*, PP: 1–14.
- [29] P. M. Ashton, C. S. Saudners, G. A. Taylor, A. M. Carter, and M. E. Bradley. Inertia estimation of the gb power system using synchrophasor measurements. *IEEE Transactions on Power Systems*, 2014.
- [30] P. M. Ashton, G. A. Taylor, A. M. Carter, and W. Hung. Application of phasor measurement units to estimate power system inertial frequency response. In *Proc. of IEEE Power Engineering Society General Meeting*, July 2013.
- [31] *EngD Environmental Technology - Engineering Doctorate Handbook*. Brunel University London, May 2010.
- [32] North American Synchrophasor Initiative (NASPI). *Phasor Technology Overview*. Naspi.org, 2008.
- [33] A. G. Phadke. Synchronized phasor measurements a historical overview. In *Proc. IEEE Transmission and Distribution Conference and Exhibition*, volume 1, pages 476–479, 2002.



- 
- [34] M. Ibrahim A. G. Phadke and T. Hlibka. Fundamental basis for distance relaying with symmetrical components. *IEEE Transactions on Power Apparatus and Systems*, PAS. 96(2):635–646, March/April 1977.
- [35] C. L. Fortescue. Method of symmetrical co-ordinates applied to the solution of polyphase networks. *Published in AIEE Transactions*, pages 1027–1140, 1918.
- [36] A. G. Phadke, J. S. Thorp, and M. G. Adamiak. A new measurement technique for tracking voltage phasors, local system frequency, and rate of change of frequency. *IEEE Transactions on Power Apparatus and Systems*, PAS-102(5):1025–1038, May 1983.
- [37] A. G. Phadke. Synchronized phasor measurements in power systems. *Computer Applications in Power, IEEE*, 6(2):10–15, April 1993.
- [38] *IEEE Standard for Synchrophasor Measurements for Power Systems*. IEEE Power Engineering Society, IEEE C37.118.1-2011.
- [39] *IEEE Standard for Synchrophasor Data Transfer for Power Systems*. IEEE Power Engineering Society, IEEE C37.118.2-2011.
- [40] P. M. Ashton, G. A. Taylor, M. R. Irving, I. Pisica, A. Carter, and M. E. Bradley. Novel application of detrended fluctuation analysis for state estimation using synchrophasor measurements. *IEEE Transactions on Power Systems*, 28(2):1930–1938, May 2013.
- [41] *IEEE Standard for Synchrophasor for Power Systems*. IEEE Power Engineering Society, Power System Relaying Committee, IEEE 1344-1995.
- [42] A. G. Phadke J. Depablos, V. Centeno and M. Ingram. Comparative testing of synchronised phasor measurement units. In *Proc. IEEE Power and Energy Society General Meeting*, volume 1, pages 948–954, 6-10 June 2004.
- [43] *IEEE Standard for Synchrophasor for Power Systems*. IEEE Power Engineering Society, Power System Relaying Committee, IEEE C37.118-2005.

- 
- [44] *Joint IEC/IEEE taskforce integration of synchrophasor data based on IEEE C37.118 into IEC 61850*. NIST PAP 13, 2009-2012.
- [45] K. E. Martin. Synchrophasor standards and guides for the smart grid. In *Proc. IEEE Power and Energy Society General Meeting*, volume 1, pages 1–5, 2013.
- [46] North American Synchrophasor Initiative (NASPI). *Performance and Standards Task Team Announcement Regarding IEEE Standard C37.118.1-2011*. NASPI, June 2013.
- [47] *NASPI Standards Update, Standards and Guides in Process*. NASPI, October 2013.
- [48] *IEEE Standard for Synchrophasor Measurements for Power Systems*. IEEE Power Engineering Society, IEEE C37.118.1a-2011.
- [49] J. De La Ree, V. Centeno, J. S. Thorp, and A. G. Phadke. Synchronized phasor measurement applications in power systems. *Smart Grid, IEEE Transactions on*, 1(1):20–27, June 2010.
- [50] D. Faulk and R. J. Murphy. Comanche peak unit no 2 100 percent load rejection test - underfrequency and voltage phasors measured across tu electric system. In *Proc. of Protective Relay Conference Texas*, March 1994.
- [51] *Power Plant Model Validation and Performance Monitoring*. NASPI workshop, October 2013.
- [52] J. Bialek P. McNabb, D. Wilson and K. Hay. Dynamic model validation of the icelandic power system using wams-based measurement of oscillatory stability. In *Proc. PSCC Glasgow*, 2008.
- [53] S. Guo and J. Bialek. Synchronous machine inertia constants updating using wide area measurements. In *Proc. Innovative Smart Grid Technologies (ISGT Europe), 2012 3rd IEEE PES International Conference and Exhibition on*, Oct 2012.

- [54] Z. Huang, P. Du, D. Kosterev, and S. Yang. Generator dynamic model validation and parameter calibration using phasor measurements at the point of connection. *IEEE Transactions on Power Systems*, 28(2):1939–1949, May. 2013.
- [55] T.J. Overbye and J.D. Weber. Visualization of power system data. In *System Sciences, 2000. Proceedings of the 33rd Annual Hawaii International Conference on*, pages 7 pp.–, Jan 2000.
- [56] Power System Outage Task Force. *Final Report on the August 14, 2003 Blackout in the United States and Canada: Causes and Recommendations*. April 2004.
- [57] Z. Zhong, C. Xu, B. J. Billian, L. Zhang, S. J. S. Tsai, R. W. Conners, R. W. Centeno, A. G. Phadke, and Y. Liu. Power system frequency monitoring network (fnet) implementation. *IEEE Transactions on Power Systems*, 20(4):1914–1921, Nov. 2005.
- [58] P. Kundur. *Power System Stability and Control*. McGraw-Hill, 1994.
- [59] Scottish Power. *Visualisation of Real Time System Dynamics using Enhanced Monitoring (VISOR)*. OFGEM - Electricity Network Innovation Competition submission from SP Transmission, December 2013.
- [60] G. Valverde, D. Cai, and V. Fitch, J. Terzija. Enhanced state estimation with real-time updated network parameters using smt. In *IEEE Power and Energy Society General Meeting, 26-30 July 2009*, 2009.
- [61] G. Valverde, S Chakrabarti, E. Kyriakides, and V. Terzija. A constrained formulation for hybrid state estimation. *IEEE Transactions on Power Systems*, 26(3):1102–1109, Aug 2011.
- [62] G. Valverde and V. Terzija. Unscented kalman filter for power system dynamic state estimation. *IET Generation, Transmission and Distribution*, 5(1):29–37, 2011.

- 
- [63] A. G. Phadke and R. M. de Moraes. The wide world of wide-area measurement. *Power and Energy Magazine, IEEE*, 6(5):52–65, September 2008.
- [64] LLC ESTA International. *Executive Report on the State of Synchrophasors in the USA*. New Energy and Industrial Technology Development Organisation (NEDO), November 2011.
- [65] J. Ma, P. Zhang, H Fu, B Bo, and Z Dong. Application of phasor measurement unit on locating disturbance source for low-frequency oscillation. *IEEE Transactions on Smart Grids*, 1(3):340–346, Dec. 2010.
- [66] North American Synchrophasor Initiative (NASPI). *WAMS Implementation in China, NASPI Meeting Vancouver, BC*. North China Electric Power University, June 2010.
- [67] J. Interrante and K. S Aggour. Applying cluster computing to enable a large-scale smart grid stability monitoring application. In *Proc. of IEEE 14th International Conference on High Performance Computing and Communication*, 2012.
- [68] W. Sattinger. Application of pmu measurements in europe tso approach and experience. In *PowerTech, 2011 IEEE Trondheim*, pages 1–4, June 2011.
- [69] C. Carnal P. Reinhardt and W. Sattinger. *Reconnecting Europe*. Power Engineering International, January 2005.
- [70] A. Metsiou C. D. Vournas and B. M. Nomikos. Analysis of intra-area and interarea oscillations in south-eastern ucte interconnection. In *Proc. of IEEE Power and Energy Society General Meeting, Calgary*, 2009.
- [71] M. Larsson, L.-F. Santos, A. Suranyi, W. Sattinger, and R. Notter. Monitoring of oscillations in the continental european transmission grid. In *Industrial Electronics Society, IECON 2013 - 39th Annual Conference of the IEEE*, pages 4774–4778, Nov 2013.
- [72] The TWENTIES project 2010-2013. *TWENTIES Project - Final Report*. October 2013.

- [73] T. Rauhala, K. Saarinen, M. Latvala, M. Laasonen, and M. Uusitalo. Applications of phasor measurement units and wide-area measurement system in finland. In *PowerTech, 2011 IEEE Trondheim*, pages 1–8, June 2011.
- [74] A.B. Leirbukt, J.O. Gjerde, P. Korba, K. Uhlen, L. K. Vormedal, and L. Warland. Wide area monitoring experiences in norway. In *Power Systems Conference and Exposition, 2006. PSCE '06. 2006 IEEE PES*, pages 353–360, Oct 2006.
- [75] T. Rauhala, M. Lahtinen, H. Kuisti, J. Peltola, and P. Halonen. Static var compensator enhancing the operational reliability of finnish transmission network. In *Paper B4-206, Cigre Session 2010, Paris, France.*, 2010.
- [76] J. Rasmussen and P. Jorgensen. Synchronized phasor measurements of a power system event in eastern denmark. *Power Systems, IEEE Transactions on*, 21(1):278–284, Feb 2006.
- [77] K. Uhlen, L. Vanfretti, M. M. De Oliveira, A.B. Leirbukt, V. H. Aarstrand, and J. O. Gjerde. Wide-area power oscillation damper implementation and testing in the norwegian transmission network. In *Power and Energy Society General Meeting, 2012 IEEE*, pages 1–7, July 2012.
- [78] D. H. Wilson. Wide area monitoring systems in the uk: Operational experience and systems development. In *Proc. of Cigre session S1-9: Monitoring and system operation control based on synchronized phasor measurements, Monitoring of Power System Dynamics Performance 28-30 April 2008, Saint Petersburg, Russia*, 2008.
- [79] P. M. Ashton, G. A. Taylor, A. M. Carter, and H. Renner. Opportunities to exploit phasor measurement units and synchrophasor measurements on the gb transmission network. In *Universities' Power Engineering Conference (UPEC), Proceedings of 2011 46th International*, pages 1–6, Sept 2011.
- [80] R. Zhang and G. Bryan. *Architecture of Substation Secondary Systems, National Grid UK*. PACWorld, <http://www.pacw.org/no-cache/issue/>, September 2010.

- [81] *NETS Security and Quality of Supply Standard - Issue 2.2*. National Grid, UK, March 2012.
- [82] *The Grid Code*. National Grid, UK, January 2013.
- [83] *The Balancing and Settlements Code (BSC)*. [Accessed online] <http://www.elexon.co.uk/bsc-related-documents/balancing-settlement-code>, November 2013.
- [84] *Code of Practice One, Code of Practice for the Metering of Circuits with a Rated Capacity Exceeding 100MVA for Settlement Purposes, Issue 2 Version 9.0*. ELEXON, 23<sup>rd</sup>.
- [85] *System Monitoring Policy Document Draft, V1.0*. National Grid, UK, 2014.
- [86] I Hall, P. G. Beaumont, G. P. Baber, I Shuto, M. Saga, K. Okuno, and H. Ito. New line current differential relay using gps synchronization. In *Proc. IEEE Power Tech Conference, Bologna Italy*, Jun 2003.
- [87] P. M. Ashton, G. A. Taylor, M. R. Irving, A. M. Carter, and M. E. Bradley. Prospective wide area monitoring of the great britain transmission system using phasor measurement units. In *Proc. of IEEE Power Engineering Society General Meeting*, July 2012.
- [88] A. G. Phadke, J. S. Thorp, and K. J. Karimi. Real time voltage-phasor measurements for static state estimation. *Power Apparatus and Systems, IEEE Transactions on*, PAS-104(11):3098–3107, Nov 1985.
- [89] B. Fardanesh. *Use of Phasor Measurements in a Commercial (or Industrial) State Estimator*. EPRI, Palo Alto, CA, USA, Final Report 1011002, July 2004.
- [90] M. Parashar et al. *Implementation of Phasor Measurements in SDG & E State Estimator, Technical Report*. California Energy Commission, PIER Program Energy Commission-500-02-04 MR053, 2008.

- 
- [91] A. Ghassemian and B. Fardanesh. Cphasor assisted state estimation for nys transmission system implementation & testing. In *Proc. IEEE/PES Power Systems Conf. Expo*, number 1-8, March 2009.
- [92] R. Avila-Rosales, M. J. Rice, J. Giri, L. Beard, and F. Galvan. Recent experience with a hybrid scada/pmu on-line state estimator. In *in Proc. IEEE Power and Energy Society General Meeting*, pages 1–6, July 2009.
- [93] *Remote Access for Metering and Monitoring (RAMM) project*. National Grid, UK.
- [94] W. Fairne, A. Myles, T. M. Whitelegg, and N. S. Murray. Low frequency oscillations on the 275kv interconnected system between scotland and england. Sept 1982.
- [95] K. M. Trantor. Application of power system stabilisers on the anglo-scottish interconnection, installation of power system stabilisers and the evaluation of settings. *IEE Proc. Generation, Transmission, and Distribution*, 135(3), May 1988.
- [96] *PhasorPoint*. Psymetrix, UK, 2014.
- [97] V. Terzija, D. Cai, and J. Fitch. Monitoring of inter-area oscillations in power systems with renewable energy resources using prony method. In *20th International Conference and Exhibition on Electricity Distribution (CIRED 2009)*, *IET Conf. Pub., Volume 2009, Issue CP550*, p.746, 2009.
- [98] D. Cai, P. Regulski, M. Osborne, and V. Terzija. Wide area inter-area oscillation monitoring using fast nonlinear estimation algorithm. *IEEE Transactions on Smart Grid*, 4(3):1721–1731, 2013.
- [99] J. Turunen, H. Renner, W. Hung, A. M. Carter, P. M. Ashton, and L. C. Haarla. Simulated and measured inter-area mode shapes and frequencies in the electrical power system of great britain. *IEEE Transactions on Power systems (Submitted)*, 2014.

- 
- [100] Market Operation National Grid. *Market Operations Business Procedures, BP1612 - Power System Oscillation Identification*. National Grid, UK internal, May 2011.
- [101] *TCPDUMP*. [www.tcpdump.org](http://www.tcpdump.org), 2010-2014.
- [102] [www.arbiter.com](http://www.arbiter.com) Arbiter Systems. *Model 1133A Power Sentinel Power Quality, Operation Manual*. June 2012.
- [103] [www.ametekpower.com](http://www.ametekpower.com) Ametek. *Ametek TR2000 Multifunction Recorder, Operation Manual*. 2005.
- [104] EPSRC FLEXNET. *SUPERGEN 1 Renewal Core - FlexNet: Renewal of the Supergen consortium on Future Network Technologies*. <http://gow.epsrc.ac.uk/NGBOViewGrant.aspx?GrantRef=EP/E04011X/11>, 2007.
- [105] [www.elpros.si](http://www.elpros.si) ELPROS. *WAProtector*. 2001.
- [106] Deyu Cai. *Wide Area Monitoring Protection and Control in the Future Great Britain Power System*. PhD Thesis, The University of Manchester, May 2011.
- [107] V. Terzija, D. Cai, A. Vaccaro, and J. Fitch. Wide area monitoring, protection and control practices in the united kingdom. In *Cigre Study Committee B5 Colloquium, Jeju Island, Korea, October 19-24*, 2009.
- [108] V. Terzija, D. Cai, A. Vaccaro, and J. Fitch. Architecture of wide area monitoring systems and their communication requirements. In *Paris Cigre Session 2010*, 2010.
- [109] M. Khan, P. M. Ashton, M. Li, G. A. Taylor, and J. Liu. Parallel detrended fluctuation analysis for fast event detection on massive pmu data. *IEEE Transactions on Power Systems (Submitted 2013)*.
- [110] C-K Peng, Sergey V Buldyrev, Shlomo Havlin, M Simons, H Eugene Stanley, and Ary L Goldberger. Mosaic organization of DNA nucleotides. *Physical Review E*, 49(2):1685–1689, Feb. 1994.



- [111] A. R. Messina, V. Vittal, G. T. Heydt, and T. J. Browne. Nonstationary approaches to trend identification and denoising of measured power system oscillations. *IEEE Transactions on Power Systems*, 24(4):1798–1807, Nov 2009.
- [112] N. Zhou, D. Trudnowski, J. W. Pierre, S. Sarawgi, and N. Bhatt. An algorithm for removing trends from power-system oscillation data. In *in Proc. IEEE Power and Energy Society General Meeting, Conversion and Delivery of Electrical Energy in the 21st Century*, 2008.
- [113] W. Xingzhi, Y. Zhen, and L. Li. A grid computing based approach for the power system dynamic security assessment. *Journal of Computer and Electrical Engineering, Elsevier*, 36(3):553–564, May 2010.
- [114] G. A. Ezhilarasi and K. S. Swarup. Parallel contingency analysis in a high performance computing environment. In *Proc. International Conference Power System (ICPS)*, pages 1–6, July 2009.
- [115] I. Gorton, Z. Huang, Y. Chen, B. Kalahar, S. Jin, D. Chavarra-Miranda, and J. Baxter. A high-performance hybrid computing approach to massive contingency analysis in the power grid. In *Proc. the 2009 Fifth IEEE International Conference on e-Science, IEEE Computer Society*, pages 277–283, July 2009.
- [116] W. Gao and X. Chen. Distributed generation placement design and contingency analysis with parallel computing technology. *Journal of Computer and Electrical Engineering, Elsevier*, 4(4):347–354, April 2009.
- [117] J. C H Peng, A. Mead, and N. K C Nair. Exploring parallel processing for wide area measurement data applications. In *Power and Energy Society General Meeting, 2011 IEEE*, pages 1–8, July 2011.
- [118] L. Wang and C. Singh. Multi-deme parallel genetic algorithm in reliability analysis of composite power systems. In *Proc. of the 2009 IEEE Bucharest PowerTech Conference, Bucharest Romania*, July 2009.

- 
- [119] K. Maheshwari, M. Lim, L. Wang, K. Birman, and R. Renesse. Toward a reliable, secure and fault tolerant smart grid state estimation in the cloud. In *Proc. of the IEEE PES Innovative Smart Grid Technologies (ISGT)*, pages 1–6, Feb 2013.
- [120] P. Trachian. Machine learning and windowed subsecond event detection on pmu data via hadoop and the openpdc. In *Proc. of IEEE Power and Energy Society General Meeting, TVA, USA*, 2010.
- [121] M. Edwards, A. Rambani, Y. Zhu, and M. T. Musavi. Design of hadoop-based framework for analytics of large synchrophasor datasets. *Procedia Computer Science, Complex Adaptive Systems, Elsevier*, 12:254–258, 2012.
- [122] H. Mass, H. K. Camak, F. Bach, and U. G. Kuhnappel. One year high rate low voltage recording device, method and results. In *Proc. of the IEEE International Workshop on Applied Measurements for Power Systems (AMPS)*, pages 68–72, Sept 2013.
- [123] F. Bach, H. K. Cakmak, H. Mass, and U. Kuehnappel. Power grid time series data analysis with pig on a hadoop cluster compared to multi core system. In *Proc. of IEEE 21st Euromicro International Conference on Parallel, Distributed and Network-Based Processing (PDP)*, pages 208–212, Feb 2013.
- [124] J. Dean and S. Ghemawat. Mapreduce: simplified data processing on large cluster. *Communication of the ACM*, 51(1):107–133, Jan 2008.
- [125] R. Lammel. Googles mapreduce programming model revisited. *Science of Computer Programming*, 70(1):1–30, 2008.
- [126] M. Isard, V. Prabhakaran, J. Currey, U. Wieder, K. Talwar, and A. Goldberg. Quincy: fair scheduling for distributed computing clusters. In *Proc. of the 22nd Symposium on Operating Systems Principles (ACM SIGOPS)*, 2009.

- [127] B. He, W. Fang, Q. Luo, Govindaraju N. K., and T. Wang. Mars: Mapreduce framework on graphics processors. In *Proc. of ACM 17th Int. Conference on Parallel Architectures and Compilation Techniques*, 2008.
- [128] C. Ranger, R. Raghuraman, A. Penmetsa, G. Bradski, and C. Kozyrakis. Evaluating mapreduce for multi-core and multiprocessor systems. In *Proc. of the IEEE 13th Int. Symposium on High Performance Computer Architecture*, Feb 2007.
- [129] M. Isard, M. Budiu, Y. Yu, A. Birrell, and D. Fetterly. Dryad: distributed data-parallel programs from sequential building blocks. In *Proc. of the European Conference on Computer Systems (EuroSys)*, 2007.
- [130] *Apache Hadoop*. <http://hadoop.apache.org>, Accessed on 14 August 2013.
- [131] Yahoo! *Yahoo! Launches Worlds Largest Hadoop Production Application*. <http://developer.yahoo.com/blogs/hadoop>, Accessed April 2013.
- [132] *Amazon Elastic Computer Cloud*. <http://aws.amazon.com/ec2>, Accessed April 2013.
- [133] K. Shvachko, H. Kuang, S. Radia, and R. Chansler. The hadoop distributed file system. In *Proc. of 26th IEEE Symposium on Massive Storage Systems and Technologies (MSST)*, 2010.
- [134] *An Introduction to HDFS High Availability*. [Available online] [http://www.cloudera.com/content/cloudera-content/cloudera-docs/CDH4/latest/CDH4-High-Availability-Guide/cdh4hag\\_topic\\_2\\_1.html](http://www.cloudera.com/content/cloudera-content/cloudera-docs/CDH4/latest/CDH4-High-Availability-Guide/cdh4hag_topic_2_1.html), Accessed March 2014.
- [135] K. Kambatla, A. Pathak, and H. Pucha. Towards optimizing hadoop provisioning in the cloud. In *Proc. of the Workshop on Hot Topics in Cloud Computing, held in conjunction with the USENIX Annual Technical Conference*, 2009.
- [136] S. Babu. Towards automatic optimization of mapreduce programs. In *Proc. of the 1st ACM Symposium on Cloud Computing (SoCC)*, 2010.

- 
- [137] *OpenPDC*. <http://openpdc.codeplex.com>, Accessed April 2013.
- [138] *Hadoop Streaming*. <http://hadoop.apache.org/docs/r1.2.1/streaming.html>, April 2013.
- [139] G. M. Amdahl. Validity of the single processor approach to achieving large scale computing capabilities. In *Proc. of AFIPS Spring Joint Computer Conference*, 1967.
- [140] UK National Grid. *The Grid Code, Balancing Code No. 3 (BC3), Frequency Control Process*. March .
- [141] *Frequency Response Technical Sub-Group Report, Stage 01 Working Group Report*. National Grid, UK, November 2011.
- [142] *Firm Frequency Response Review, Outline Change Proposals Documnet 13*. National Grid, UK, November 2013.
- [143] J. D. Glover, M. S. Sarma, and T. J. Overbye. *Power System Analysis and Design*. Thomsonl, 2008.
- [144] P. Wall, F. Gonzlez-Longatt, and V. Terzija. Demonstration of an inertia constant estimation method through simulation. In *Universities Power Engineering Conference (UPEC), 2010 45th International*, pages 1–6, Aug 2010.
- [145] V. V. Terzija. Adaptive underfrequency load shedding based on the magnitude of the disturbance estimation. *Power Systems, IEEE Transactions on*, 21(3):1260–1266, Aug 2006.
- [146] Chen Xiangyi, Li Chunyan, and Wang Yunli. Analysis of the inter-area low frequency oscillations in large scale power systems. In *2011 6th IEEE Conference on Industrial Electronics and Applications (ICIEA)*, pages 1627–1631, 2011.
- [147] M. Klein, G.J. Rogers, and P. Kundur. A fundamental study of inter-area oscillations in power systems. *IEEE Transactions on Power Systems*, 6(3): 914–921, Aug. 1991.

- 
- [148] D. H. Wilson, K. Hay, and J. Toal. Probability of oscillatory instability and its implications. In *Proc. of Bulk Power System Dynamic and Control VI, Cortina dAmpezzo, Italy*, 2004.